A. I. Alikhanian National Science Laboratory

(Yerevan Physics Institute)

Elena Apresyan

Some aspects of quantum Hall effect

Thesis for acquiring the degree of candidate of physical-mathematical sciences

in division 01.04.02 (Theoretical Physics)

Scientific supervisor

Doctor of phys.-math. sciences

Prof. A. Sedrakyan

YEREVAN 2019

Contents

List of Figures

Introduction

Let us take a bunch of electrons, confine them in a two-dimensional plane and turn on a strong magnetic field. This simple step provides the setting for some of the unexpected and surprising results in physics. These phenomena are known as the quantum Hall effect. The name comes from experimental results. The Hall conductivity takes quantised values

$$\sigma_{xy} = \frac{e^2}{2\pi\hbar}\nu. \tag{1}$$

From the beginning it was found that ν takes integer valued. Certainly,we are used to see things being quantised at the microscopic, atomic level. But here the picture is different : it's the quantisation of a macroscopic property in a messy system involving many particles and its explanation requires new approach. It comes out that this new approach is related to the role that topology can play in quantum many-body systems. Later, it was found that the conductivity not only takes integer values, but can also take specific rational values. The most known experimentally found fractions are $\nu = 1/3$ and $\nu = 2/5$ but there are some other fractions that have been observed. In this case the interaction between electrons was observed which is now known as a new state of matter.The charged particles that wander around these system, transport a fraction of the charge of the electron, as though the electron has break itself into several pieces. It is not just the charge of the electron that fractionalises: this occurs to the "statistics" of the electron also.Yet this happens in spite of the fact that the electron is an indivisible component of matter. Recollect that the electron is a fermion, which is governed by the Fermi-Dirac distribution function. Because of fermionic nature electron

splits.But the individual components are no longer fermions, but neither are they bosons. They are new objects known as anyons which lie somewhere between bosons and fermions. In more general cases, even this description breaks down: the resulting objects are called non-Abelian anyons and provide physical manifestation of the kind of non-local entanglement famous in quantum mechanics.

Because of this fact, the quantum Hall effect has been a constant source of new ideas, most of them related to the ways in which the topology invades the quantum physics. Attractive examples include the subject of topological insulators, topological order and topological quantum computing. Basically, all of these phenomena are impressive theoretical constructions, which include a journey through some of the most fascinating and important developments in theoretical and mathematical physics over the past decades. The first attack on the problem focused on the microscopic details of the electron wave functions. Subsequent approaches looked at the system from a more coarse-grained, field-theoretic perspective where a subtle construction known as Chern-Simons theory plays a key role. Yet another perspective comes from the edge of the sample where certain excitation live that know more about what is happening inside the system than you might think. Graphene is now attracting scientists with its peculiar material characteristics.Electrons in graphene strongly interact and therefore exhibit fractional quantum Hall effect(FQHE).But remarkably,the evidence for collective behaviour of electrons in graphene still is absent.The integer quantum Hall effect (IQHE) can be described only in terms of individual electrons in a magnetic field while the (FQHE)can be understood by studying the collective behaviour of all the electrons [1].The quantum Hall effect is also studied in context of conform field theory (CFT). In this [2] paper is examined the application of Quantum Fractional Hall effect. It is shown that the Gaussian model together with appropriate boundary conditions for the order parameter provides an effective theory for the Laughlin type (FQHE). The plateau forming condition corresponds to the taking the chiral portion of the theory $c = 1$ conformal field theory to the description of the (FQHE).

The first example of a topological quantum state [3–7] is the integer quantum Hall effect (QHE) in a $2D$ electron system in the presence of a perpendicular magnetic field. For conductivity, the distinction between localised and extended states is an important.Only the

extended states can transport charge from one side of the sample to the other. So only these states can contribute to the conductivity. Suppose that we have filled all the extended states in a given Landau level and consider what happens when we decrease B with fixed n. Each Landau level can contain fewer electrons, so the Fermi energy will increase. Before jumping up to the next Landau level, we now begin to settle the localised states. As long as these states can not contribute to the current, the conductivity stays constant. This brings to exactly the kind of plateaux that are observed, with constant conductivities over a range of magnetic field. The presence of disorder explains the presence of plateaux.In result the resistivities take specific quantised values. These were computed assuming that all states in the Landau level contribute to the current.Many of these states are localised by impurities and don't transport charge.We expect that the value of the resistivity should be different. Uncommonly, current carried by the extended states increases to compensate for the lack of current transported by localised states,because of that the resistivity remains quantised in presence of disorder. When a one-dimensional world is observed we have two basic motions forward and backward. The random scattering can mingle them, which brings to resistance.The QH effect is possible when a strong magnetic field is applied to a $2D$ gas of electrons in a semiconductor. When we have low temperature and high magnetic field, the electrons transport only along the edge of the semiconductor.In $1D$ system the electrons are propagating in both directions, the top edge of a QH bar contains only half the degrees of freedom.When an edge-state electron meets an impurity, it just rounds and still keeps going in the same direction, as there is no option for it to turn back. This dissipationless transport mechanism could be extremely useful for semiconductor devices. The fact that we should have a large magnetic field strongly confines the application potential of the QH effect. The quantum Hall (QH) systems now is a major paradigm in condensed matter physics, with important applications such as resistance metrology and measurements of fundamental constants. In the recent years,it has been shown that the QHE is just one member of a much larger family of topologically specific quantum states,some instances of which contain the quantum spin Hall (QSH) effect which is famous also as the $2D$ topological insulator and $3D$ TIs [8]. Current time there are a large number of materials,TIs with their characteristic spin-helical Dirac fermion TSS

brings forth intense interests. In a real $1-D$ system, there are four channels for the forward and backward moving paths with spin-up or spin-down electrons. The traffic lanes for the electrons can be split without any magnetic field.It's possible to leave the spin-up forward mover and the spin-down backward mover on the top edge and go the other two channels to the bottom edge.The similar system with such edge states is in a QSH (quantum Spin Hall) state, because it has a net transport of spin forward along the top edge and backward along the bottom edge,as the separated transport of charge in the QH state. Charles Kane and Eugene Mele from the University of Pennsylvania [9, 10], and Andrei Bernevig [11] from Stanford University, independently offered in 2005 and 2006 that such a divided, and therefore the QSH state, can basicaly be real in some theoretical models with spin-orbit coupling. The fractional QSH state should be experimentally observed. Actually QSH edge consists of both backward and forward movers, but back-scattering by nonmagnetic impurities is forbidden. Most eye-glasses and camera lenses have a so-called anti-reflection coating.The reflected light from the top and the bottom surfaces interfere with each other, bringing to the zero net reflection and thereby perfect transmission. However, such an effect is not strong, as it depends on the matching between the optical wavelength and the thickness of the coating [12–14]. A large part of the unique quantum-mechanical properties of TIs come from the peculiar characteristics of the surface states. Currently, the TI research is concentrated basically on time-reversal (TR) invariant systems, where the nontrivial topology is preserved by time-reversal symmetry (TRS). In those systems, the surface states present Dirac dispersion therefore the physics of relativistic Dirac fermions becomes pertinent. Furthermore, spin degeneracy is appeared in the Dirac fermions staying in the surface states of TR-invariant TIs and their spin is blocked to the momentum. In similar cases we say that a spin states have helical spin polarization and it brings chance to realize Majorana fermions in the presence of proximity-induced superconductivity. The first $3D$ TI material $Bi_{1-x}Sb_x$, whose topological surface state contains $2D$ massless Dirac fermions, has unique band structure which brings $3D$ massive Dirac fermions in the bulk. This situation is like to the Kane-Mele model where $1D$ massless Dirac fermions come out of $2D$ massive Dirac fermions. Since Dirac fermions play significant roles in TIs, it is necessary to mention the history of Dirac physics in con-

densed matter. The semi-metal Bi has played an important role in quantum mechanichs , this is significant because the extremely low carrier density and the very long mean free path easily set the system in the quantum limit at relatively low magnetic fields [15] In the mid 20-th century, one of the long-standing puzzles in Bi was its large diamagnetism, which defies the common wisdom for magnetism in metals involving Pauli paramagnetism and Landau diamagnetism [16]. Entertainingly, in $Bi_{1-x}Sb_x$ at low Sb concentration, the carrier density becomes even lower than in Bi, in same time the diamagnetic susceptibility increases, which is also opposite to the expectation from Landau diamagnetism. The peculiar electronic properties of Bi, an effective two-band model was formed by Cohen and Blount in 1960. In 1964, Wolff acknowledged that this two-band model can be transformed into the four-component massive Dirac Hamiltonian, and he expressed delicate analysis of the selection rules using the Dirac theory. This was the start of the concept of Dirac fermions in solid states, though some of the special physics of massless Dirac fermions were established in as early as 1956 by McClure in the scope of graphite. Speaking of graphite, the mapping of the Hamiltonian of its $2D$ sheet to the massless Dirac Hamiltonian was first used by Semenoff in 1984 [17]. With the experimental realization of graphene, this system has become a prototypical Dirac material. One of the distinguishing properties of massless Dirac fermions is the Berry phase of, a special effect of the Berry phase in the condensed matter setting is the absence of backscattering, which was indicated first by Ando, Nakanishi, and Saito in 1998 [18]. The substantial aspect of the Dirac physics is that magnetic fields surely cause interactions between upper and lower Dirac cones. In fact, the Dirac formalism allows one to easily involve such interband effects of magnetic fields into calculations [19]. Expending the range of topological materials is an important subject.So far as superconductors have a superconducting gap at the Fermi level, they are in a way similar to insulators and one can comprehend topological superconductors described by a topological invariant that is covered by the existence of a gap [20]. So far, topological classifications of insulators and superconductors based on three discrete symmetries (TR, particle-hole and chiral) have been established [21].The new topological classifications based on point group symmetry of the crystal lattice is attracting significant interest [22–24], particularly after the new type of topological materials called topological crystalline insula-

tors [25–27] have been experimentally discovered [28, 29]. Also, although it was considered necessary to have topological materials fully-gapped energy energy spectrum for topological invariant be clearly defined, it becomes possible to present a non-trivial topology for gapless systems [30–33]. The experimental innovations of several materials that are nontrivial with respect to the new topologies will continue be mainly considered. Whereas the concept of topological insulators became popular when the discovery of the Z_2 topology by Kane and Mele, there had been theoretical attempts to comprehend topological states of matter beyond the range of the quantum Hall system. In this regard, an important development was made in 2001 by Zhang and Hu, who extended the $2D$ quantum Hall state to a four-dimensional ($4D$) TR-invariant state possessing an integer topological invariant. The effective field theory for this $4D$ topological system was constructed by Bernevig.After the Z_2 topology was discovered for TR-invariant systems in $2D$ and $3D$, it was shown by Qi, Hughes, and Zhang that the framework of topological field theory is useful for describing those systems as well, and they further demonstrated that the Z_2 TIs in $2D$ and $3D$ can actually be deduced from the $4D$ effective field theory by using the dimensional reduction. The topological field theory is appropriate for describing the electromagnetic response of TIs and has been used for foretelling new topological magnetoelectric effects. Two-dimensional conformal field theories describe statistical systems at critical points and provide the classical solutions of string theory. Recently, it has been proposed that the order parameter of the fractional quantum Hall effect (FQHE) is related to the vertex operator, and the ground state wavefunction of a certain fractional filling factor can be expressed in terms of the N-point correlation function of vertex operators [34, 35]. The application of conformal field theory has thus been expended into a rather specific condensed matter phenomenon. In [36] the Laughlin states for N interacting electrons at the plateaus of the fractional Hall effect are examined in the thermodynamic limit of large N. It was shown that this limit related to the semiclassical regime for these states, thus connecting their stability to their semiclassical nature. The analogous problem of two-dimensional plasmas is studied analytically, to leading order for $N \to \infty$, by the saddle-point approximation - a two-dimensional extension of the method used in random matrix models of quantum gravity and gauge theories. The Laughlin states describe classical droplets of

fluids with uniform density and sharp boundaries, as expected from the Laughlin plasma analogy [37–45]. In this limit, the dynamical W_∞-symmetry of the quantum Hall states represents the kinematics of the area-preserving deformations of incondensable liquid droplets. The main idea of this theory is the existence of incompressible quantum fluids at specific rational values of the electron density. These values are very stable, macroscopical quantum states with uniform density $\rho(x) = \nu eB/hc = const$, $\nu = 1/m$,$m = 1, 3, 5, ...$, which has an energy gap where B is the external magnetic field. Incompressibility accounts for the lack of low-lying conduction modes, which arises the longitudinal conductivity σ_{xx} to vanish, while the generally strict motion of the uniform droplet of fluid gives the rational values of the Hall conductivity $\sigma_{xy} = \nu e^2/h$ [46–49].

The topological phases of matter [50–53] have been examined by some models , such as wave function modeling , band theory and effective field theory of boundary excitations. In [54], is investigated $(3 + 1)$-dimensional time-reversal invariant topological insulators applying field theory methods. The main idea of exploring such a system is the success of the field theory approach for $(2 + 1)$ dimensional topological states [55, 56] . The comprehensive modeling of quantum Hall states has been used to the definition of the quantum spin Hall effect and then to time-reversal invariant topological insulators [57]. In some cases,the Z_2 characterization of stability of topological insulators, initially deduced within band theory by Fu, Kane and Mele , has been redefined in field-theory language and expanded to interacting fermion models with Abelian and non-Abelian fractional statics of excitations. The Z_2 stability also expends to $(3 + 1)$ dimensional band insulators and it is important to find the corresponding field theory argument for exploring the interacting systems [58, 59]. The quantization of the compactified boson in $(2 + 1)$ dimension produces eight sectors that correspond to the spin sectors of the fermionic theory on the torus. The partition functions in two theories are modified under flux insertions and modular transformations;in fact , they become equal due to dimensional reduction to $(1 + 1)$ dimensions. This thesis is composed ofintroduction,three chapters,conclusion and bibliography. In introduction are presented the general view of the problem. In the first chapter we studied $3D$ massive Dirac fermions in the presence of chemical potential,where we have used Feynman diagrams for the calculations.The

response of fermionic system to external gauge fields is defined by current-current correlation function $\Pi_{\mu\nu}(q, q_0)$. The transport properties of various physical quantities are determined by the zero limit of the energy-momentum. As it is known, the close to half-filling the physics of graphene is described by $2+1$ dimensional Dirac theory.We calculate current-current correlation function in Dirac theory in a presence of chemical potential η and gap m. The fermionic system to external gauge fields in presence of non-quantized magnetic field is determined by current-current correlation function $\Pi_{\mu\nu}(\mathbf{B})$. We study $2+1$ dimensional Dirac electron system and calculate current-current correlation function in a presence of magnetic field B,gap m and chimical potential η. In the second chapter we present polarization operator of non-relativistic fermions with spin-orbit (SO) Rashba interaction. The spectrum of this fermions is moat type having minimum on a circle. Contrary to Dirac or non-relativistic fermions Fermi sea here has a geometry of Corbino disk which reflects in a transport properties of excitation's.

In the third chapter we study mini-superspace semiclassical limit of the boundary three-point function in the Liouville field theory. We compute also matrix elements for the Morse potential quantum mechanics. An exact agreement between the former and the latter is found. We show that both of them are given by the generalized hypergeometric functions. In this chapter chapter also are constructed topological defects in the Liouville field theory producing jump in the value of cosmological constant. We construct them using the Cardy-Lewellen equation for the two-point function with defect. We show that there are continuous and discrete families of such kind of defects. For the continuous family of defects we also find the Lagrangian description and check its agreement with the solution of the Cardy-Lewellen equation using the heavy asymptotic semiclasscial limit.

The equation of motion in a magnetic Field

The fact that a magnetic field causes charged particles to move in circles arises the Hall effect. The equation of motion for a particle which has mass m and charge e in a magnetic

field has the following form

$$m\frac{d\mathbf{v}}{dt} = -e\mathbf{E} - e\mathbf{v} \times \mathbf{B} - \frac{m\mathbf{v}}{\tau}, \tag{2}$$

τ is called scattering time, which is the average time between collisions.This (2) equation describes the most simple model of charge transport. It is the Drude model.The velocity of the particle when $\frac{d\mathbf{v}}{dt} = 0$ will be

$$\mathbf{v} + \frac{e\tau}{m}\mathbf{v} \times \mathbf{B} = \frac{e\tau}{m}\mathbf{E}. \tag{3}$$

The current density $\mathbf{J}$ is related to velocity by following form

$$\mathbf{J} = -\mathbf{nev}, \tag{4}$$

where n is the density of charge carriers.In matrix form from (3) for ω_B is received

$$\begin{pmatrix} 1 & \omega_B\tau \\ -\omega_B\tau & 1 \end{pmatrix} \tag{5}$$

$$\mathbf{J} = \frac{e^2 n\tau}{m}\mathbf{E} \tag{6}$$

This equation is known as Ohm's law,where σ is conductivity.In the presence of a magnetic field σ is a matrix

$$\mathbf{J} = \sigma\mathbf{E} \tag{7}$$

We can write it as

$$\sigma = \begin{pmatrix} \sigma_{xx} & \sigma_{xy} \\ -\sigma_{xy} & \sigma_{xx} \end{pmatrix} \tag{8}$$

From the Drude model,we obtain the accurate expression for the conductivity

$$\sigma = \frac{\sigma_{DC}}{1 + \omega_B^2\tau^2} \begin{pmatrix} 1 & -\omega_B\tau \\ \omega_B\tau & 1, \end{pmatrix} \tag{9}$$

where $\sigma_{DC} = \frac{ne^2\tau}{m}$ is the conductivity in the absence of a magnetic field. The resistivity is defined as the inverse of the conductivity

$$\rho = \sigma^{-1} = \begin{pmatrix} \rho_{xx} & \rho_{xy} \\ -\rho_{yx} & \rho_{yy} \end{pmatrix} \tag{10}$$

From the Drude model we get

$$\rho = \frac{1}{\sigma_{DC}} \begin{pmatrix} 1 & \omega_B\tau \\ -\omega_B\tau & 1 \end{pmatrix} \tag{11}$$

When me measure the resistance R it differs from the resistivity ρ by geometrical factor

Landau Levels

It won't come as a unexpected to study that the physics of the quantum Hall effect includes quantum mechanics [60]. In this subsection, we will observe the quantum mechanics of free particles which are moving in a background of magnetic field and the creation of Landau levels.When we have a nonzero magnetic field B, there is a Zeeman splitting between the energies of up and down spins. The Lagrangian for a particle of charge e and mass m which is moving in a background magnetic field $\mathbf{B} = \bigtriangledown \times \mathbf{A}$

$$L = \frac{1}{2}m\dot{\mathbf{x}}^2 - e\dot{\mathbf{x}}\mathbf{A} \tag{12}$$

When $\mathbf{A} \to \mathbf{A} + \bigtriangledown\alpha$ the Lagrangian changes $L \to L - e\dot{\alpha}$ From here we see that the equations of motion remain unchanged under a gauge transformation. For canonical momentum of this Lagrangian we can write

$$\mathbf{p} = \frac{\partial L}{\partial \dot{\mathbf{x}}} = m\dot{\mathbf{x}} - e\mathbf{A} \tag{13}$$

In this case Hamiltonian will have the following form

$$H = \dot{\mathbf{x}}\mathbf{p} - L = \frac{1}{2m}(\mathbf{p} + e\mathbf{A})^2 \tag{14}$$

We should notice that $\mathbf{p}$ is not gauge invariant,in contrast,the mechanical momentum $m\dot{\mathbf{x}}$ is gauge invariant. $\mathbf{x}$ and $\mathbf{p}$ are canonical,it means that

$$\{x_i, p_j\} = \delta_{ij}, \quad \{x_i, x_j\} = \{p_i, p_j\} = 0 \tag{15}$$

For the Poisson bracket of the mechanical momentum we will have

$$\{m\dot{x_i}, m\dot{x_j}\} = \{p_i + eA_i, p_j + eA_j\} = -e\left(\frac{\partial A_j}{\partial x_i} - \frac{\partial A_i}{\partial x_j}\right) = -e\epsilon_{ijk}B_k \tag{16}$$

Now our problem is to find for the spectrum and wave functions of the quantum Hamiltonian,

$$H = \frac{1}{2}\left(\mathbf{p} + e\mathbf{A}\right)^2 \tag{17}$$

The fact, that particle is restricted in the plane,it means that $x = (x, y)$.The magnetic field we will take constant and perpendicular to this plane,$\bigtriangledown \times \mathbf{A} = B\hat{z}$. From (15) for canonical commutation relations we will have

$$[x_i, p_j] = i\hbar\delta_{ij}, \quad [x_i, x_j] = [p_i, p_j] = 0 \tag{18}$$

We will denote $\pi = \mathbf{p} + e\mathbf{A} = m\dot{\mathbf{x}}$, then for commutation relations we can write

$$[\pi_x, \pi_y] = -ie\hbar B \tag{19}$$

For convenience we will introduce new variables

$$a = \frac{1}{\sqrt{2e\hbar B}}(\pi_x - i\pi_y) \quad a^+ = \frac{1}{\sqrt{2e\hbar B}}(\pi_x + i\pi_y) \tag{20}$$

The new commutation relations is

$$[a, a^+] = 1 \tag{21}$$

Then the Hamiltonian gets the following form

$$H = \frac{1}{2}\bar{\pi}\bar{\pi} = \hbar\omega_B \left(a^+ a + \frac{1}{2}\right) \tag{22}$$

where $\omega_B = \frac{eB}{m}$ is the cyclotron frequency. The state $|n>$ has energy

$$E = \hbar\omega_B = \left(n + \frac{1}{2}\right) \quad n \in \mathbf{N} \tag{23}$$

In the presence of a magnetic field the energy levels of a particle become equally spaced, where the gap between each level is proportional to the magnetic field B. These energy levels are called Landau levels. It's important to notice that the spectrum looks very different in the absence of a magnetic field.The splitting between Landau levels is $\Delta = \hbar\omega_B = \frac{e\hbar B}{m}$. In case of free electrons, this level coincides with the Zeeman splitting $\Delta = g\mu_B B$ between spins, where $\mu_B = \frac{e\hbar}{2m}$ is the Bohr magneton. It looks as though the spin up particles in Landau level n have the same energy as the spin down particles in the level $n+1$. Actually, in real materials, the situation is different. The real value of the cyclotron frequency is $\omega_B = \frac{eB}{m_{eff}}$, where m_{eff} is the effective mass of the electron moving in its environment.The g factor can also change due to effects of band structure.

The Lowest Landau Level

Now we will frame the wave functions in symmetric gauge. We are going to discuss the lowest Landau level $n = 0$. The states in the lowest Landau are annihilated by a,meaning $a|0, m >= 0$.The problem is to interpret this into a differential equation. For the lowering operator we can write

$$a = \frac{1}{\sqrt{2e\hbar B}}(\pi_x - i\pi_y) = \frac{1}{\sqrt{2e\hbar B}}(p_x - ip_y + e(A_x - iA_y)) =$$

In the complex coordinates we introduce

$$z = x - iy \quad \bar{z} = x + iy \tag{24}$$

For holomorphic and anti-holomorphic derivatives we can write

$$\partial = \frac{1}{2}\left(\frac{\partial}{\partial x} + i\frac{\partial}{\partial y}\right) \quad \bar{\partial} = \frac{1}{2}\left(\frac{\partial}{\partial x} - i\frac{\partial}{\partial y}\right) \tag{25}$$

where $\partial z = \bar{\partial}\bar{z} = 1$ and $\bar{\partial} z = \partial \bar{z} = 0$. Using holomorphic coordinates for a we get

$$a = -i\sqrt{2}\left(l_B\bar{\partial} + \frac{z}{4l_B}\right) \tag{26}$$

$$a^+ = -i\sqrt{2}\left(l_B\partial - \frac{\bar{z}}{4l_B}\right) \tag{27}$$

where $l_B = \sqrt{\frac{\hbar}{eB}}$.The lowest Landau level wave function has the following form

$$\psi_{LLL}(z,\bar{z}) = f(z)e^{\frac{-|z|^2}{4l_B^2}} \tag{28}$$

In the lowest Landau level we can form the states $|0,m>$ and write

$$b = -i\sqrt{2}\left(l_B\partial - \frac{\bar{z}}{4l_B}\right) \tag{29}$$

$$b^+ = -i\sqrt{2}\left(l_B\bar{\partial} - \frac{\bar{z}}{4l_B}\right) \tag{30}$$

There is state given by

$$\psi_{LLL,m=0} \sim e^{\frac{-|z|^2}{4l_B^2}} \tag{31}$$

For the lowest Landau level wave function in terms of holomorphic polynomials we can write

$$\psi_{LLL,m=0} \sim \left(\frac{z}{l_B}\right)^m e^{\frac{-|z|^2}{4l_B^2}} \tag{32}$$

These states are the eigenstates of angular momentum.The angular momentum operator is

the following

$$J = i\hbar\left(x\frac{\partial}{\partial y} - y\frac{\partial}{\partial x}\right) = \hbar(z\partial - \bar{z}\bar{\partial}) \tag{33}$$

Acting on these lowest Landau level states, we get

$$J\psi_{LLL,m} = \hbar m\psi_{LLL,m} \tag{34}$$

Landau Gauge

In order to find wave functions we should specify a gauge potential corresponding to the energy eigenstates in following way

$$\bigtriangledown \times \mathbf{A} = B\hat{\mathbf{z}} \tag{35}$$

Here we work with the choice

$$\mathbf{A} = xB\hat{\mathbf{y}} \tag{36}$$

This is called Landau gauge.We should note that the magnetic field B is invariant under translational symmetry and rotational symmetry in the (x, y)-plane.The choice of A breaks the translational symmetry in the x direction and rotational symmetry.While the physics will stay invariant under all symmetries, the intermediate calculations will not be manifestly invariant. This sort of situation is typical when dealing with magnetic field. For Hamiltonian we can write

$$H = \frac{1}{2m}(p_x^2 + (p_y + eBx)^2) \tag{37}$$

Because we have obvious translational invariance in the y direction, we can seek energy eigenstates which are also eigenstates of p_y.Using the separation of variables we get

$$\psi_k(x, y) = e^{iky} f_k(x) \tag{38}$$

Acting on this wavefunction with the Hamiltonian we obtain

$$H\psi_k(x,y) = \frac{1}{2m}(p_x^2 + (\hbar k + eBx)^2)psi_x(x,y) \equiv H_k\psi_k(x,y) \tag{39}$$

We should note that it's the Hamiltonian for a harmonic oscillator in the x direction

$$H_k = \frac{1}{2m}p_x^2 + \frac{m\omega_B^2}{2}(x + kl_B^2)^2 \tag{40}$$

The frequency of the harmonic oscillator is equal to the cyclotron frequency $\omega_B = \frac{eB}{m}$, where l_B is a length scale. This is a peculiar length scale which manages any quantum phenomena when exists magnetic field. It is called a magnetic length.

$$l_B = \sqrt{\frac{\hbar}{eB}} \tag{41}$$

The energy eigenvalues are represented in (23).

The explicit wavefunctions depend on two quantum numbers $k \in R$ and $n \in N$

$$\psi_{n,k}(x,y) \sim e^{iky}H_n(x + kl_B^2)e^{-\frac{(x+kl_B^2)^2}{2l_B^2}} \tag{42}$$

where H_n is the usual Hermite polynomial wavefunctions of the harmonic oscillator. The $\sim$ means that we have made no attempt to normalize these wavefunction. One privilege of this approach is that we can instantly find the degeneracy in each Landau level. The wavefunction (42) depends on two quantum numbers, the energy levels depend only on n.At first we need to confine a finite region of the (x,y)-plane. We choose a rectangle with sides of lengths L_x and L_y.Our purpose is to know how many states we have inside this rectangle. The side of rectangle L_y has a finite size,it means that we can put the system in a box in the y-direction. Note that the effect of this is to quantise the momentum k in units of $2\pi/L_y$. The finite size of L_x is something more subtle,than L_y.That is the result of fact that the gauge choice (36) does not include translational invariance in the x-direction. The reason is that,the wavefunctions (42) are exponentially localized around $x = -kl_B^2$, for a finite sample confined to $0 \leq x \leq L_x$

we would expect the allowed k values to range between$-L_x/l_B^2 \leq k \leq 0$. The number of states is

$$N = \frac{L_y}{2\pi}\int_{-L_x/l_B^2}^{0} dk = \frac{L_x L_y}{2\pi l_B^2} = \frac{eBA}{2\pi\hbar} \tag{43}$$

where $A = L_x L_y$.In spite of the small approximation used above,this is the accurate answer for the number of states on a torus. The degeneracy in (43) is significant.We have a macroscopic number of states in each Landau level. The resulting spectrum looks like the figure on the right, with $n \in N$ labelling the Landau levels and the energy independent of k.

In order to describe the degeneracy it is convenient to input some new notation in (43).We write

$$N = \frac{AB}{\Phi_0} with \quad \Phi_0 = \frac{2\pi\hbar}{e} \tag{44}$$

Φ_0 is called the quantum of flux. We can consider that the magnetic flux falls within the area $2\pi l_B^2$.It is an important in a number of quantum phenomena in the presence of magnetic fields. The Landau gauge is helpful when we work in rectangular geometries.In this gauge it is easy to add an electric field E in the x direction. That is possible to realize by the addition of an electric potential $\phi = -Ex$.In result we get

$$H = \frac{1}{2m}(p_x^2 + (p_y + eBx)^2) + eEx \tag{45}$$

For wave function we can write

$$\psi(x,y) = \psi_{n,k}\left(x - \frac{mE}{eB^2}, y\right) \tag{46}$$

The energies are given by

$$E_{n,k} = \hbar\omega_B\left(n + \frac{1}{2}\right) + eE\left(kl_B^2 - \frac{eE}{m\omega_B^2}\right) + \frac{mE^2}{2B^2} \tag{47}$$

Now the degeneracy in each Landau level rises,as a result, the energy in each level depends linearly on k .

We see that the energy depends on the momentum,therefore the states drift in the y

direction. For the group velocity we can write

$$v_y = \frac{1}{\hbar}\frac{\partial E_{n,k}}{\partial k} = e\hbar E l_b^2 = \frac{E}{B} \tag{48}$$

If we try to put an electric field E perpendicular to a magnetic field B then we will see that the cyclotron orbits of the electron drift in the direction $E \times B$, they don't drift in the direction of the electric field.

Chapter 1

Current-current correlation function

1.1 The Kubo Formula

Our problem in this subsection will be to get a formula for the Hall conductivity σ_{xy}. At first our aim is to derive the Kubo formula. We'll derive the Kubo formula for a general case, multi-particle Hamiltonian H_0 where the index 0 indicates that this is the unperturbed Hamiltonian before we switch on an electric field.Here H_0 could be the single e-particle Hamiltonian. We represent the energy eigenstates of H_0 as $|m>$,with $H_0|m>= E_m|m>$ When we have background electric field and also gauge $A_t = 0$ for electric filed we can write $\mathbf{E} = -\partial_\mathbf{t}\mathbf{A}$.The Hamiltonian gets the form $H = H_0 + \Delta H$ with

$$\Delta H = -\mathbf{JA} \tag{1.1}$$

where J is the quantum operator associated with the electric current. Our purpose is to calculate the current $<\mathbf{J}>$ that flows because of the perturbation ΔH. We will suppose that the electric field is small and continue using standard perturbation theory.We are using interaction representation,it means that operators expand as $O(t) = V^{-1}OV$ with $V = e^{-iH_0t/\hbar}$.For $|\psi(t)>$ we can write

$$|\psi(t)>_I= U(t, t_0)\psi(t_0)>_I \tag{1.2}$$

where the unitary operator

$$U(t,t_0) = T\exp\left(-\frac{i}{\hbar}\int_{t_0}^{t}\Delta H(t')dt'\right) \tag{1.3}$$

Here T means time ordering, it assures that U obeys the equation $i\hbar dU/dt = \Delta HU$.

We investigate the system at time $t \to -\infty$in a specific many-body state $|0>$. The expectation value of the current is given by

$$< \mathbf{J} >=< 0(t)|\mathbf{J}|0(t) >=< 0|U^{-1}(t)\mathbf{J}(t)U(t)|0 > \approx< \left(\mathbf{J}(t) + \frac{i}{\hbar}\int_{-\infty}^{t} dt^{'}\Delta H(t^{'})\mathbf{J}(t) >\right) \tag{1.4}$$

Because of electric field the current will have the following form

$$< J_i(t) >= \frac{1}{\hbar\omega}\int_{-\infty}^{t} dt^{'} < 0|[J_j(t^{'})J_i(t)]|0 > E_j e^{-i\omega t^{'}} \tag{1.5}$$

Due to the fact that the system is invariant under time translations,the correlation function above will depend on $t^{"} = t - t^{'}$.Therefore (1.5) we can write

$$< J_i(t) >= \frac{1}{\hbar\omega}\left(\int_0^{\infty} dt^{"}e^{i\omega t"} < 0|[J_j(0), J_i(t^{"}]|0 >\right) E_j e^{i\omega t} \tag{1.6}$$

t dependence in the formula (1.6) means that if we apply an electric field at frequency ω, the current will oscillate at the same frequency ω.This is the essence of linear response. The Hall conductivity has the following form

$$\sigma_{xy}(\omega) = \frac{1}{\hbar\omega}\int_0^{\infty} dt e^{i\omega t} < 0|[J_y(0), J_x(t)]|0 > \tag{1.7}$$

This is the Kubo formula for the Hall conductivity. For current operator $\mathbf{J}(t) = V^{-1}\mathbf{J}(0)V$ with $V = e^{-iH_0 t/\hbar}$.Then for σ_{xy} we get

$$\sigma_{xy}(\omega) = \frac{1}{\hbar\omega}\int_0^{\infty} dt e^{i\omega t}\sum_n [< 0|J_y|n >< n|J_x|0 >]e^{i(E_n - E_0)t/\hbar} - < 0|J_x|n >< n|J_y|0 > e^{i(E_0 - E_n)t/\hbar} \tag{1.8}$$

In order to provide convergence we should substitute $\omega \to \omega + i\epsilon$,in result we obtain

$$\sigma_{xy}(\omega) = -\frac{i}{\omega}\sum_{n\neq 0}\left[\frac{<0|J_y|n><n|J_x|0>}{\hbar\omega + E_n - E_0} - \frac{<0|J_x|n><n|J_y|0>}{\hbar\omega + E_0 - E_n}\right] \tag{1.9}$$

When $\omega \to 0$ we expand the denominators

$$\frac{1}{\hbar\omega + E_n - E_0} \approx \frac{1}{E_n - E_0} - \frac{\hbar\omega}{(E_n - E_0)^2} + O(\omega^2)... \tag{1.10}$$

Finite contribution in the limit $\omega \to 0$ is given by

$$\sigma_{xy} = i\hbar\sum_{n\neq 0}\frac{<0|J_y|n><0|J_x|n> - <0|J_x|n><0|J_y|n>}{(E_n - E_0)^2} \tag{1.11}$$

1.2 Current-current correlation function $\Pi_{\mu\nu}(\mathbf{q}, q_0)$

The electrical conductivity of graphene, a two-dimensional hexagonal lattice of carbon atoms,has a great deal of qualities needed for prospective applications in both fundamental physics and nanotechnology. At energies below a few electron volts the electronic properties of graphene are perfectly reported by the Dirac model [61, 62, 64]. In the scope of this model graphene quasiparticles submit a linear dispersion relation, where the speed of light c is susbstituted with the Fermi velocity $vFc/300$. The electrical properties of graphene are substantially associated with an existence of the so-called universal conductivity σ_0 discribed via the electron charge e and Planck constant.A few specific values for σ_0 have been received by different authors [65–68]. Ultimately was obtained the expression $\sigma_0 = e^2/4\hbar$. Generally, the conductivity of graphene is nonlocal,depends on both the frequency and the magnitude of the wave vector, and also on the temperature. It was explored by many authors applying the phenomenological two-dimensional Drude model, the current-current correlation function in the random phase approximation, the Kubo response formalism, and the Boltzmann transport equation [69–73].Moreover, the electrical conductivity of graphene is susceptible to weather the mass of quasiparticles m is accurately equal to zero or it is rather small but nonzero.In case when we have real graphene models a nonzero mass gap $\delta = 2mc^2$ in the energy spectrum

of quasiparticles appears under the impact of electron-electron interactions, substrates and impurities [74, 75]. Some partial results for the conductivity of gapped graphene have been gotten using the two-band model [76] and the static polarization function [77]. In the local approximation at zero temperature the conductivity of gapped graphene was also examined in [78, 79]. The real graphene models have some peculiarites,they are always doped and can be describe by some nonzero chemical potential μ.Particularly the electrical conductivity of doped graphene was investigated by using some approximate methods [80, 81]. The question emerges of whether there are spacial differences in influences of the nonzero mass-gap parameter and chemical potential on the conductivity of graphene. It was examined [82] that at zero temperature in the local approximation the response function for undoped but gapped graphene is similar to the case of doped but ungapped graphene if to identify the gap parameter Δ, with twice the Fermi energy $2E_F$.

A comprehensive investigation of the conductivity of graphene can be performed using the exact expression for its polarization tensor at any temperature, mass gap and chemical potential. Although in some specific cases the polarization tensor in (2+1)-dimensional space-time has been calculated by many authors, the complete results needed for a fundamental understanding of the conductivity were obtained only recently.The exact polarization tensor of graphene with any mass-gap parameter has been found at zero temperature. The extension of this tensor to the case of nonzero temperature was made in [83], but only at the pure imaginary Matsubara frequencies. The results of have been extensively used to calculate the Casimir force in graphene systems [84], but they are not directly applicable in the studies of conductivity which is defined along the real frequency axis. Another representation for the polarization tensor of gapped graphene, allowing an analytic continuation to the real frequency axis, was derived in [85]. It was applied in calculations of the Casimir force, on the one hand, and of the reflectivity properties of graphene and graphene-coated substrates, on the other hand. For the latter purposes, explicit expressions for the polarization tensor at real frequencies have been obtained for a gapless and gapped graphene. This has opened up opportunities for a detailed study of the conductivity of graphene on the basis of first principles of quantum electrodynamics at nonzero temperature. The conductivity of pure

(gapless) graphene was investigated using the continuation of the polarization tensor to real frequencies.The previously known partial results for the conductivity of graphene have been reproduced and their generalizations to the case of any temperature with taken into account effects of nonlocality have been obtained. In this chapter, we develop the complete theory for the electrical conductivity of graphene in the framework of the Dirac model at arbitrary values of the mass gap, temperature and chemical potential. For this purpose, the results are used, where the polarization tensor of graphene of Ref. was generalized to the case of graphene with nonzero chemical potential. We perform an analytic continuation of the polarization tensor to the real frequency axis and express both the longitudinal (in-plane) and transverse (perpendicular to the plane of graphene) conductivities in terms of its component.

The fermions on honeycomb lattice, as an effectively three dimensional Dirac theory around K-point with high mobility, graphene, is interesting with transport and magnetic properties and provides unique opportunity to introduce and analyze set of parameters, which control their behavior [86, 87]. Most intriguing property, which first attracted tremendous interest continuing up to our days, is unusual quantum Hall effect (QHE), expressing itself in absence of zero conductivity at zero magnetic field [88]. This effect comes from Z_2-anomaly first observed by Jackiw in a seminal paper [89, 90]. The set of parameters, which affects the physical properties of the fermions are gap(mass, m), chemical potential (η), applied magnetic field (B) and the scattering rate (Γ), which phenomenologically reflects the presence of impurities.

The presence of Dirac points with different chiralities is the main characteristic of 2D topological insulators. Transport properties of this systems contain huge potential for their practical application in various environment. Therefore the importance of the study of response functions in 3D Dirac theory is hard to overestimate. In the papers [91–95] the polarization of media in graphene was studied, namely, the density-density correlators were calculated.

The conductivity of fermions in graphene in most general situation was investigated in a large amount of papers (see [96] for complete set of references). In a series of papers authors had calculated conductivity with non-zero gap, chemical potential, scattering rate

and magnetic field.

However, as it appears, current response functions were not studied properly in a mentioned above literature, namely, the precise expression for the current-current correlation function $\Pi_{\mu\nu}(q_0, \mathbf{q}) = \langle j_\mu(q_0, \mathbf{q}) j_\nu(-q_0, -\mathbf{q})\rangle$, $\mu, \nu = 0, 1, 2$ for most general case is not presented there. One of our goals in this chapter is the calculation of current-current correlation function in one loop approximation and in a presence of non-zero chemical potential η and a gap m, which appears to have simple expression. The extension of the result to RPA series is straightforward.

The action which describes the graphene in the Effective Field Theory (EFT) framework via N_f four-component massive Dirac fermions with instantaneous three-dimensional Coulomb interactions is the following (in Eucliean space time) [97, 98]

$$S_g = -\sum_{i=1}^{N_f} \int d^2x dt \bar{\psi}_i \left(\gamma^0\partial_0 + v\gamma^k\partial_k + iA_0\gamma^0 + i\gamma^0\eta) + m\right)\psi_i + \frac{1}{2g^2}\int d^2x dt (\partial_k A_0)^2. \quad (1.12)$$

Here v is the velocity, which can be taken as 1 in the calculations and then restore in the resulting formulas. In real graphene $N_f = 2$, γ-matrices satisfy to Euclidean Clifford algebra and can be chosen as

$$\gamma^0 = \sigma^3 \otimes \sigma^3, \quad \gamma^i = \sigma^i \otimes 1, \quad \{\gamma^\mu\gamma^\nu\} = 2\delta^{\mu\nu}. \quad (1.13)$$

The four-component fermionic structure is conditioned by the existence of the quasi-particle excitations in two sublattices in the graphene around two Dirac points.

Since each Dirac point contributes to response function additively, below, for simplicity, we will be concentrated on calculation of current-current correlation function only for single Dirac point. Therefore we start from Dirac action in three dimensional space-time with chemical potential η and gap m, which after Wick rotation to complex time/energy acquires the form

$$S = \int \frac{d\mathbf{k}d\omega}{(2\pi)^3}\bar{\psi}_{\mathbf{k},\omega}[\sigma\mathbf{k} + \sigma_3(\omega + i\eta) + m]\psi_{\mathbf{k},\omega}, \quad (1.14)$$

where the Fourier transformation is done ($\mathbf{k} = \{k_1, k_2\}$) and in the role of γ functions

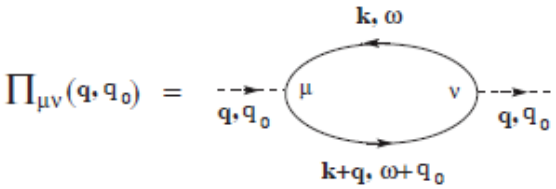

Figure 1.1: One-loop Feynman's diagram .

Pauli matrices are taken.

Here we intend to calculate the current-current correlation function for the three-dimensional theory with the kinetic part for the fermions presented above and the interaction term with $U(1)$ gauge field A_μ in the one-loop approximation.

The current-current correlation function $\Pi_{\mu\nu}(\mathbf{r}-\mathbf{r}') = \langle j_\mu(\mathbf{r}) j_\nu(\mathbf{r}')\rangle$ is defined by Feynman diagram Fig.1.1 and in momentum space it reads

$$\begin{aligned}\Pi_{\mu\nu} &= \int_{-\infty}^{\infty} \frac{d^3k}{(2\pi)^3} Tr\Big[\sigma_\mu G(k)\sigma_\nu G(k+q)\Big] \\ &= \int_{-\infty}^{\infty} \frac{d^3k}{(2\pi)^3} \frac{Tr\big[\sigma_\mu(k_\rho\sigma_\rho - m)\sigma_\nu(k_\lambda\sigma_\lambda - m)\big]}{\big[k^2+m^2\big]\big[(k+q)^2+m^2\big]}.\end{aligned} \tag{1.15}$$

where $G(k)$ is the Green function of the fermion and and we have used the notation $k^2 = |\mathbf{k}|^2 + (\omega + i\eta)^2$, $(k+q)^2 = \mathbf{k}+\mathbf{q}|^2 + (\omega + i\eta + q_0)^2$. The calculation of Trace gives

$$\begin{aligned}&Tr\big[\sigma_\mu(k_\rho\sigma_\rho - m)\sigma_\nu(k_\lambda\sigma_\lambda - m)\big] = \\ &2\Big[k_\mu(k+q)_\nu + k_\nu(k+q)_\mu - \delta_{\mu\nu}k_\lambda(k+q)_\lambda + \delta_{\mu\nu}m^2 - i\frac{m}{2}\epsilon_{\mu\nu\rho}q_\rho\Big].\end{aligned} \tag{1.16}$$

Note, that for the graphene model's case with four-component fermions, the last term linear by m must be annihilated, due to the contributions of two different two-dimensional fermions with opposite parities. The expression (1.16) combined with the formula of Feynman parametrization

$$\frac{1}{AB} = \int_0^1 dx \frac{1}{[xA + (1-x)B]^2} \tag{1.17}$$

applied to denominator of (1.15), and the shift of integration energy/momenta $k \to k-(1-x)q$ gives

$$\begin{aligned}\Pi_{\mu\nu} &= 2\int_{\infty}^{\infty}\frac{d^3k}{(2\pi)^3}\int_0^1 dx\frac{2k^\rho k^\nu-\delta^{\rho\nu}\Big(k^2+m^2+q^2x(1-x)\Big)+2x(1-x)(\delta^{\rho\nu}q^2-q^\rho q^\nu)}{\Big(k^2+m^2+q^2x(1-x)\Big)^2}\\ &- im\,\epsilon_{\mu\nu\rho}\,q_\rho\int_{\infty}^{\infty}\frac{d^3k}{(2\pi)^3}\int_0^1 dx\frac{1}{\Big(k^2+m^2+q^2x(1-x)\Big)^2}=\Pi^{(1)}_{\mu\nu}+\Pi^{(2)}_{\mu\nu}+\Pi^{(3)}_{\mu\nu}. \quad (1.18)\end{aligned}$$

Three summands in (1.18) are chosen in this way. The first one is the part, which does not satisfy the condition of conservation of charge - $\partial_\mu\Pi_{\mu\nu}=0$. The third summand is the Z_2-anomaly part.

We will prove now that the first, non-transversal part $\Pi^{(1)}_{\mu\nu}$ in the integral (1.18) is zero. Indeed, it is clear, that due to integration over angles and the presence of $\delta^{\mu\nu}$ the integral

$$\Pi^{(1)}_{\mu\nu} = 2\int_{-\infty}^{\infty}\frac{d^3k}{(2\pi)^3}\int_0^1 dx\frac{2k^\mu k^\nu-\delta^{\mu\nu}\Big(k^2+m^2+q^2x(1-x)\Big)}{\Big(k^2+m^2+q^2x(1-x)\Big)^2} \quad (1.19)$$

is zero for $\mu\neq\nu$. For $\mu=\nu$ we have (see Appendix)

$$\begin{aligned}\Pi^{(1)}_{\mu\mu} &= 2\int_0^1 dx\int\frac{d^2k}{(2\pi)^2}\int\frac{d\omega}{2\pi}\frac{2\Big(\delta^{\mu0}(\omega+i\mu)^2+\delta^{\mu a}|\mathbf{k}|^2/2\Big)-\Big(|\mathbf{k}|^2+(\omega+i\eta)^2+m^2+q^2x(1-x)\Big)}{\Big(|\mathbf{k}|^2+(\omega+i\eta)^2+m^2+q^2x(1-x)\Big)^2}\\ &= 2\int_0^1 dx\int\frac{d^2k}{(2\pi)^2}\left(\frac{\delta^{\mu a}|\mathbf{k}|^2}{4\Big(|\mathbf{k}|^2+m^2+q^2x(1-x)\Big)^{\frac{3}{2}}}-\frac{(1-\delta^{\mu0})}{2\Big(|\mathbf{k}|^2+m^2+q^2x(1-x)\Big)^{\frac{1}{2}}}\right) \quad (1.20\end{aligned}$$

Here $a=1,2$. For $\mu=0$ this expression vanishes immediately (because of $1-\delta^{00}$ and δ^{0a}), while for the case $\mu=a$ - after integration over momentum $\mathbf{k}^2$ with proper regularization. Regularized momentum integrals can be taken easily and reads

$$\int_{-\Lambda}^{-\Lambda}\frac{d^2k}{(2\pi)^2}(|\mathbf{k}|^2+z)^{-n/2}=\frac{1}{4\pi(1-n/2)}(|\mathbf{k}|^2+z)^{1-n/2}\Big|_0^\Lambda\to^{reg}-\frac{1}{2\pi(2-n)}z^{1-n/2} \quad (1.21)$$

By use of (1.21) one can easily check that $\Pi^{(1)}_{\mu\nu}=0$.

1.3 Calculation of $\Pi^{(2)}_{\mu\nu}$

Second, the main q-dependent transverse term is

$$\Pi^{(2)}_{\mu\nu} = 2(\delta^{\rho\nu}q^2 - q^\rho q^\nu)\int_{-\infty}^{\infty}\frac{d^3k}{(2\pi)^3}\int_0^1 dx\frac{2x(1-x)}{\Big(k^2+m^2+q^2x(1-x)\Big)^2} \tag{1.22}$$

Cauchy integration over ω (see formula (1.34) in Appendix) and subsequent integration over $\mathbf{k}$ by (1.21) gives

$$\begin{aligned}\Pi^{(2)}_{\mu\nu} &= 2(\delta^{\mu\nu}q^2 - q^\mu q^\nu)\int_0^1 dx\int\frac{d^2k}{(2\pi)^2}\int\frac{d\omega}{2\pi}\frac{2x(1-x)}{\Big(|\mathbf{k}|^2+m^2+(\omega+i\eta)^2+q^2x(1-x)\Big)^2} \qquad (1.23\\ &= 2(\delta^{\mu\nu}q^2 - q^\mu q^\nu)\int_0^1 dx\int\frac{d^2k}{(2\pi)^2}\frac{2x(1-x)}{4\Big(|\mathbf{k}|^2+m^2+q^2x(1-x)\Big)^{3/2}}\Theta\Big[|\mathbf{k}|^2+m^2+q^2x(1-x)-\eta^2\\ &= \frac{(\delta^{\mu\nu}q^2 - q^\mu q^\nu)}{\pi}\Big(\int_{x_1}^{x_2}dx\frac{(x(1-x))}{2q\left(x(1-x)+m^2/q^2\right)^{\frac{1}{2}}}+\int_0^{x_1}dx\frac{x(1-x)}{2\eta}+\int_{x_2}^1 dx\frac{x(1-x)}{2\eta}\Big)\end{aligned}$$

where $x_{1,2}=\frac{1}{2}(1\pm\sqrt{1-\frac{4(\eta^2-m^2)}{q^2}})$ obtained from $m^2+q^2x(1-x)-\eta^2=0$.

Then, for $q^2\geq 4(\eta^2-m^2)\geq 0$, when the square root in the expression of $x_{1,2}$ is real, the integral over x gives

$$\begin{aligned}\Pi^{(2)}_{\mu\nu} &= \frac{(\delta^{\mu\nu}q^2 - q^\mu q^\nu)}{\pi} \qquad (1.24)\\ \times\ &\left[\frac{1}{12\eta}\left(1+\left(\frac{\eta^2+2m^2}{q^2}-1\right)\sqrt{1-\frac{4(\eta^2-m^2)}{q^2}}\right)+\frac{1-\frac{4m^2}{q^2}}{8q}\arctan\frac{q\sqrt{1-\frac{4(\eta^2-m^2)}{q^2}}}{2\eta}\right]\end{aligned}$$

In the opposite region $4(\eta^2-m^2)\geq q^2$ we should take $x_{1,2}=1/2$ and the integral becomes

$$\Pi^{(2)}_{\mu\nu} = \frac{(\delta^{\mu\nu}q^2 - q^\nu q^\nu)}{12\pi\eta}. \tag{1.25}$$

For the case $(\eta^2-m^2)\leq 0$ the expressions for $x_{1,2}$ define larger than segment $[0,1]$ region

and we have to put $x_1 = 0,\ x_2 = 1$. In a result

$$\Pi^{(2)}_{\mu\nu} = \frac{(\delta^{\mu\nu}q^2 - q^\mu q^\nu)}{\pi}\frac{1}{8q}\Big(\frac{2m}{q} + (1 - \frac{4m^2}{q^2})\arctan\frac{q}{2m}\Big). \tag{1.26}$$

where $q = \sqrt{|\mathbf{q}|^2 + q_0^2}$.

1.4 Calculation of $\Pi^{(3)}_{\mu\nu}$

Last term gives

$$\Pi^{(3)}_{\mu\nu} = -imq_\rho\epsilon_{\mu\nu\rho}\int_\infty^\infty \frac{d^3k}{(2\pi)^3}\int_0^1 dx \frac{1}{\Big(k^2 + m^2 + q^2x(1-x)\Big)^2}. \tag{1.27}$$

Using formula (1.34) for the integration over ω and (1.21) for $\mathbf{k}$ we obtain

$$\Pi^{(3)}_{\mu\nu} = -imq_\rho\epsilon_{\mu\nu\rho}\int_\infty^\infty \frac{d^2k}{(2\pi)^2}\int_0^1 dx \frac{1}{4\Big(\sqrt{|\mathbf{k}|^2 + m^2 + q^2x(1-x)}\Big)^3}\Theta\Big[|\mathbf{k}|^2 + m^2 + q^2x(1-x) - \eta^2\Big]$$

$$= \frac{-imq_\rho\epsilon_{\mu\nu\rho}}{2\pi}\Big(\int_{x_1}^{x_2} dx \frac{1}{2q\left(x(1-x) + m^2/q^2\right)^{\frac{1}{2}}} + \int_0^{x_1} dx\frac{1}{2\eta} + \int_{x_2}^1 dx\frac{1}{2\eta}\Big). \tag{1.28}$$

Again, as above, for the region $q^2 \geq 4(\eta^2 - m^2) \geq 0$ the integral gives

$$\Pi^{(3)}_{\mu\nu} = \frac{-imq_\rho\epsilon_{\mu\nu\rho}}{2\pi}\Big[\frac{1}{q}\arctan\frac{q\sqrt{1 - \frac{4(\mu^2-m^2)}{q^2}}}{2\eta} + \frac{1 - \sqrt{1 - \frac{4(\eta^2-m^2)}{q^2}}}{2\eta}\Big]. \tag{1.29}$$

For the case $4(\eta^2 - m^2) \geq q^2$ we have $x_{1,2} = 1/2$ and the integral becomes

$$\Pi^{(3)}_{\mu\nu} = \frac{-imq_\rho\epsilon_{\mu\nu\rho}}{4\pi\eta}. \tag{1.30}$$

In the interesting region $(\eta^2 - m^2) \leq 0$, when $x_1 = 0,\ x_2 = 1$, the calculation brings to

the formula

$$\Pi^{(3)}_{\mu\nu} = -\frac{im\ q_\rho\ \epsilon_{\mu\nu\rho}}{2\pi q}\ \arctan[\frac{q}{2|m|}] = -\frac{i}{4\pi} sign[m]\ q_\rho\ \epsilon_{\mu\nu\rho} + \mathcal{O}(\frac{q^2}{m^2}), \tag{1.31}$$

in full accordance with the Z_2 anomaly, first observed by Jackiw and further by Semenoff.

1.5 Summary

Finally the result for $\Pi_{\mu\nu}$ is

$$\Pi_{\mu\nu} = \Pi^{(2)}_{\mu\nu} + \Pi^{(3)}_{\mu\nu}, \tag{1.32}$$

where $\Pi^{(2)}_{\mu\nu}$ is presented in formulas (1.24,1.25,1.26), while $\Pi^{(3)}_{\mu\nu}$ in (1.29,1.30,1.31) . The result for the graphene with two Dirac fields of opposite chirality is

$$\Pi_{\mu\ nu_g} = 2\Pi^{(2)}_{\mu\nu} \tag{1.33}$$

cause the anomaly term will be cancelled.

It is interesting to mention about the dependence of the polarization operator (1.33) over the mass m (or chemical potential η) for the fixed values of q. At the region $m^2 \leq \eta^2 - q^2/4$ ($\eta^2 \leq m^2$) the function is constant in respect of the variable m (η), then the function is monotonic decreasing in respect of m (η) via two different laws at the regions $\eta^2 - q^2/4 \leq m^2 \leq \eta^2$ and $m^2 \geq \eta^2$ ($m^2 \leq \eta^2 \leq m^2 + q^2/4$ and $\eta^2 \geq m^2 + q^2/4$). In the case of $m = 0,\ \eta = 0$ and with $A^\nu = \{A^0, 0, 0\}$ the obtained result coincides with the one presented in a paper [93].

1.6 Appendix:

Here we present integration formulas over the energy ω, used in the calculations above. Integration is taken in the complex plane (the upper half-plane) by use of Cauchy formulas.

First integral is

$$\int \frac{d\omega}{2\pi} \frac{1}{\Big(|\mathbf{k}|^2 + (\omega + i\eta)^2 + m^2 + q^2 x(1-x)\Big)^2} \tag{1.34}$$
$$= \frac{1}{4\Big(\sqrt{|\mathbf{k}|^2 + m^2 + q^2 x(1-x)}\Big)^3} \Theta\big[|\mathbf{k}|^2 + m^2 + q^2 x(1-x) - \eta^2\big],$$

Second integral has the same poles and reads

$$\int \frac{d\omega}{2\pi} \frac{(\omega + i\eta)^2}{\Big(|\mathbf{k}|^2 + (\omega + i\eta)^2 + m^2 + q^2 x(1-x)\Big)^2} \tag{1.35}$$
$$= \frac{1}{4\sqrt{|\mathbf{k}|^2 + m^2 + q^2 x(1-x)}} \Theta\big[|\mathbf{k}|^2 + m^2 + q^2 x(1-x) - \eta^2\big],$$

The last integral gives

$$\int \frac{d\omega}{2\pi} \frac{1}{\Big(|\mathbf{k}|^2 + (\omega + i\eta)^2 + m^2 + q^2 x(1-x)\Big)} \tag{1.36}$$
$$= \frac{1}{2\sqrt{|\mathbf{k}|^2 + m^2 + q^2 x(1-x)}} \Theta\big[|\mathbf{k}|^2 + m^2 + q^2 x(1-x) - \eta^2\big].$$

In this formulas Θ-functions ensures, that integrals are non-zero when the poles $\omega = \Big(-i\eta \pm i\sqrt{|\mathbf{k}|^2 + m^2 + q^2 x(1-x)}\Big)$ are on different sides of real axes. The range of the integration of the parameter x is defined as in the formulas (1.24,1.25,1.26).

1.7 The culculation of $\Pi_{\mu 3}$

Experimental and theoretical investigations of graphene form an extremely fast growing area of the present-day field of condensed matter research. The diversity of chemical and physical properties of graphene is due to the crystal structure and π-electrons of carbon atoms making up the graphene. The graphene is a semiconductor with zero energy gap because the band and the conduction band converge in the Dirac point. Owing to the linear dispersion law the effective mass of electrons and holes in graphene is zero. The electronic properties of graphene are sensitive to conditions of environment and, hence, change in the

presence of other layers. The band structure of graphene is singular, as a result of which the electron at Fermi energies is described by means of the effective invariant Lorentz theory. The graphene is notable for the highest heat conduction, electric conductivity and an ability to change these properties depending on modifications of structure and on the nature of external influences. Recently, theoretical and experimental studies of the influence of external fields on the transport characteristics of graphene are carried out [94–98]. A constant magnetic field acts as a strong catalyst of dynamic symmetry by leading to generation of fermion masses in $(2+1)$ dimension. As is well known from quantum-mechanical calculations, an application of magnetic field to a conductor causes the conduction electrons to move (within the framework of semiclassical approximation) in a limited area of space with a discrete and uniformly distributed set of energies. Such quantized orbits are termed as the Landau levels. In graphene these levels are nonuniform, since the conduction electrons behave in it as massless fermions, the velocity of which is independent of their energy. In particular, the Landau levels in graphene were first experimentally fixed recently. The aim of this chapter is the calculation of the correlation function of the density of current via third order Feynman diagram, in the presence of gap m , the chemical potential η and magnetic field B.

The result obtained may be used for the investigation of the transport and magnetic properties of graphene. In the frameworks of efficient field theory the graphene is described by means of four-component massive Dirac fermions with instantaneous three-dimensional Coulomb interaction. In the frameworks of efficient field theory the graphene is described by means of four-component massive Dirac fermions with instantaneous three-dimensional Coulomb interaction. For such a system the action has the following form (in the Euclidean space-time)

$$S_g = -\sum_{i=1}^{N_f} \int d^2x dt \bar{\psi}_i \left(\gamma^0\partial_0 + v\gamma^k\partial_k + iA_0\gamma^0 + i\gamma^0\eta + m\right)\psi_i + \frac{1}{2g^2}\int d^2x dt (\partial_k A_\mu)^2. \quad (1.37)$$

Here v is the velocity, which can be taken as 1 in the calculations and then restore in the resulting formulas. In real graphene $N_f = 2$, γ-matrices satisfy to Euclidean Clifford algebra

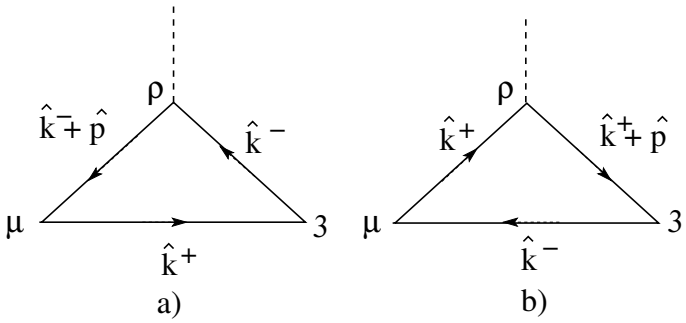

Figure 1.2: Third order Feynman diagram for current-current correlation function .

and can be chosen as

$$\gamma^0 = \sigma^3 \otimes \sigma^3, \quad \gamma^i = \sigma^i \otimes 1, \quad \{\gamma^\mu \gamma^\nu\} = 2\delta^{\mu\nu}. \tag{1.38}$$

The four-component fermionic structure is conditioned by the existence of the quasi-particle excitations in two sublattices in the graphene around two Dirac points.

The four-component fermion structure is due to the presence of quasi-excitation of particles in two sublattices of graphene around two Dirac points. As the contribution of each Dirac point to the response function is additive, we shall concentrate for simplicity on the calculation of current-current correlation function only for one Dirac point. Therefore, we start from the free Dirac action in three-dimensional space-time with chemical potential η , gap m and magnetic field B, that acquires the following form after the Wick rotation:

$$S = \int \frac{d\mathbf{k}d\omega}{(2\pi)^3} \bar{\psi}_{\mathbf{k},\omega}[\sigma\mathbf{k} + \sigma_3(\omega + i\eta) + m]\psi_{\mathbf{k},\omega}, \tag{1.39}$$

where the Fourier transformation is done ($\mathbf{k} = \{k_1, k_2\}$) and in the role of γ functions Pauli matrices are taken. Here we intend to calculate the current-current correlation function for the three-dimensional theory with the kinetic part for the fermions presented above and the interaction term with $U(1)$ gauge field A_μ in the third order approximation.

The magnetic field dependence of the current-current correlation function is defined by third order Feynman diagrams in Fig.1.1 [99, 100], where the vector potential A_ρ couples to vertex ρ. After some transformations diagram a) reads

$$\Pi_{\mu 3} = Ng^2 \int_{-\infty}^{+\infty} \frac{d^3k}{(2\pi)^3} \mathrm{Tr}[\sigma_\mu G(\hat{k}^+) A_\rho \sigma_\rho G(\hat{k}^+ + \hat{p}) \sigma_3 G(\hat{k}^-)]$$
$$= Ng^2 \int_{-\infty}^{+\infty} \frac{d^3k}{(2\pi)^3} \mathrm{Tr}[\sigma_\mu G(\hat{k}^+) A_\rho \sigma_\rho \frac{\hat{p}}{p^2+m^2} \sigma_3 G(\hat{k}^-)] \quad (1.40)$$

where $G(\hat{k}) = \frac{\hat{k}-m}{k^2+m^2}$ is the Green function of the fermion and we have used the notation $k^\pm = (\vec{k} \pm \frac{\vec{q}}{2}, \Omega \pm \frac{\omega}{2})$. By using identity $A_\rho \sigma_\rho \hat{p} = \vec{A}\vec{p} + i\epsilon_{\nu\rho} A_\nu p_\rho \sigma_3 = iB\sigma_3$ in second row of the expression (1.40), where we have dropped $\vec{A}\vec{p}$ term since it gives zero, we come to following Trace in the nominator

$$B\mathrm{Tr}[\sigma_\mu(\hat{k}^+ - m)\sigma_3\sigma_3(\hat{k}^- - m)] = 2B(\epsilon_{\mu\nu\sigma} k^+_\nu k^-_\sigma - m(k^+ + k^-)_\mu) \quad (1.41)$$
$$= 2B[\epsilon_{\mu\nu}(q_\nu\Omega - k_\nu\omega) - 2mk_\mu]$$

In the same way one can find corresponding expression for Trace for diagram of Fig.1(b), which coincides with (1.41).

We see, that in three dimensional space the third order Feynman's diagrams are not vanish, therefore, summarizing Trace results we obtain $4B[\epsilon_{\mu\nu}(q_\nu\Omega - k_\nu\omega) - 2mk_\mu]$.

1.8 Calculation of $\Pi_{\mu 3}$

Using the trace result $\Pi_{\mu 3}$ is acquired following form

$$\Pi_{\mu 3}(B) = Ng^2 \int_{-\infty}^{+\infty} \frac{d^3k}{(2\pi)^3} \Big(\frac{4B[\epsilon_{\mu\nu}(q_\nu\Omega - k_\nu\omega) - 2mk_\mu]}{(k^{+2}+m^2)(k^{-2}+m^2)^2} + \frac{4B[\epsilon_{\mu\nu}(q_\nu\Omega - k_\nu\omega) - 2mk_\mu]}{(k^{-2}+m^2)(k^{+2}+m^2)^2} \Big) \quad (1.42)$$

where $k^2 = \vec{k^2} + (\Omega + \Gamma + i\eta)$. Generally $\Pi_{\mu\nu}$ must satisfy the condition of conservation of charge $\partial_\mu \Pi_{\mu\nu} = 0$. The evaluation of such integrals is performed with the method of Feynman parametrization. These method gives opportunity to squeeze the three denominator factors into single quadratic as polynomial of k. After we shift k by a constant. It is easy to begin

with trivial case when in denominator we have two factors

$$\frac{1}{AB} = 2\int_0^1 dx_1 dx_2 \frac{\delta(x_1+x_2-1)}{[x_1A+x_2B]^2} \tag{1.43}$$

When we have three factors then

$$\frac{1}{ABC} = 2\int_0^1 dx_1 dx_2 dx_3 \frac{\delta(x_1+x_2+x_3-1)}{[x_1A+x_2B+x_3C]^3} \tag{1.44}$$

Our integral (1.42) has three factors in the denominator, therefore by using (1.44) we obtain

$$\frac{1}{AB^2} = \frac{\Gamma(1+2)}{\Gamma(1)\Gamma(2)}\int_0^1 du_1 du_2 \frac{\delta(u_1+u_2-1)u_2}{(u_1A+u_2B)^3} = 2!\int_0^1 du \frac{1-u}{(uA+(1-u)B)^3} \tag{1.45}$$

where $A = k^{-2}+m^2$, $B = k^{+2}+m^2$. Easy to find out, that making shift $k^{\pm} = k'^{\pm}+(1/2-u)q$ we come to very simple expressions

$$\begin{aligned} \frac{1}{AB^2} &= 2!\int_0^1 du \frac{1-u}{[k'^2+u(1-u)q^2+m^2]^3} \\ \frac{1}{A^2B} &= 2!\int_0^1 du \frac{u}{[k'^2+u(1-u)q^2+m^2]^3}. \end{aligned} \tag{1.46}$$

Then the polarization operator $\Pi_{\mu 3}$ defined by (1.42) acquires the form

$$\begin{aligned} &\Pi_{\mu 3}(B) \\ =\ & 8B\int_0^1 du \frac{d^3k'}{(2\pi)^3} \frac{[\epsilon_{\mu\nu}q_\nu(\Omega'+(\frac{1}{2}-u)\omega)-(k'+(\frac{1}{2}-u)q)_\nu\omega-2m(k'+(\frac{1}{2}-u)q)_\nu]}{(k'^2+m^2+u(1-u)q^2)^3} \\ =\ & 8B\int_0^1 du \frac{d^3k}{(2\pi)^3} \frac{\epsilon_{\mu\nu}[q_\nu(\frac{1}{2}-u)(\Gamma+i\eta)-(\frac{1}{2}-u)q_{\nu\omega}]-2m(\frac{1}{2}-u)q_\mu}{(k^2+m^2+u(1-u)q^2)^3} \\ =\ & 8B\int_0^1 du \frac{d^2k}{(2\pi)^2}\frac{d\Omega}{2\pi} \frac{\epsilon_{\mu\nu}q_\nu(\Gamma+i\eta)-m(1-2u)q_\mu}{\left[(\Omega+\Gamma+i\eta)-\sqrt{\vec{k}^2+m^2+u(1-u)q^2}\right]^3} \\ & \times\frac{1}{\left[(\Omega+\Gamma+i\eta)+\sqrt{\vec{k}^2+m^2+u(1-u)q^2}\right]^3} \end{aligned} \tag{1.47}$$

In (1.47) we see, that have a pole of third order, therefore, applying Cauchy integration

formula and differentiating twice integrand of (1.47) over Ω we obtain

$$\begin{aligned}\Pi_{\mu 3}(B) &= 8iB\int_0^1 du\frac{d\vec{k}}{(2\pi)^2}\frac{\partial^2}{\partial\Omega^2}\frac{\epsilon_{\mu\nu}q_\nu(\Gamma+i\eta)-m(1-2u)q_\mu}{[(\Omega+\Gamma+i\eta)-\sqrt{\vec{k}^2+m^2+u(1-u)q^2}]^3} \\ &\times\frac{1}{[(\Omega+\Gamma+i\eta)+\sqrt{\vec{k}^2+m^2+u(1-u)q^2}]^3} \\ &= \frac{3iB}{2}\int_0^1 du\frac{d\vec{k}}{(2\pi)^2}\frac{\epsilon_{\mu\nu}q_\nu(\Gamma+i\eta)-m(1-2u)q_\mu}{(\vec{k}+m^2+u(1-u)q^2)^{5/2}}\end{aligned} \tag{1.48}$$

Now, by performing integration over $\vec{k}$ using standard formula of dimensional regularization

$$\int\frac{d^2k}{(2\pi)^d}\frac{1}{(k^2+\Delta)^n}=\frac{1}{(4\pi)^{\frac{d}{2}}}\frac{\Gamma(n-\frac{d}{2})}{\Gamma(n)}\frac{1}{\Delta^{n-\frac{d}{2}}} \tag{1.49}$$

and dividing the range of integration $[0,1]$ in three part we obtain

$$\begin{aligned}&\Pi_{\mu 3}(B)= \\ =\;& \frac{iB}{4\pi}\Bigg\{\int_{u_1}^{u_2}du\frac{\epsilon_{\mu\nu}q_\nu(\Gamma+i\eta)-m(1-2u)q_\mu}{(m^2+u(1-u)q^2)^{3/2}}-\int_0^{u^1}du\frac{\epsilon_{\mu\nu}q_\nu(\Gamma+i\eta)-m(1-2u)q_\mu}{\eta^3} \\ &\int_{u_2}^1 du\frac{\epsilon_{\mu\nu}q_\nu(\Gamma+i\eta)-m(1-2u)q_\mu}{\eta^3}\Bigg\}=-\frac{iB}{4\pi}\Bigg[\Bigg(-2\frac{\frac{1-2u}{4m^2+q^2}\epsilon_{\mu\nu}q_\nu(\Gamma+i\eta)+2m\frac{q_\mu}{q^2}}{(m^2+u(1-u)q^2)^{1/2}}|_{u_1}^{u_2}\Bigg) \\ +\;& \frac{1}{\eta^3}\epsilon_{\mu\nu}q_\mu(\Gamma+i\eta)(1+u_1-u_2)+\frac{m}{\eta^3}q_\mu(u_1-u_2)(u_1+u_2-1)\Bigg] \\ =\;& -\frac{Bi}{\pi}\frac{\epsilon_{\mu\nu}q_\nu(\Gamma+i\eta)}{(4m^2+q^2)|\eta|}\sqrt{1-\frac{4(\eta^2-m^2)}{q^2}}-\frac{Bi}{4\pi|\eta|}\frac{\epsilon_{\mu\nu}q_\nu}{\eta^3}(\Gamma+i\eta)\Bigg[1-\sqrt{1-\frac{4(\eta^2-m^2)}{q^2}}\Bigg]\end{aligned} \tag{1.50}$$

where expressions $u_1=\frac{1}{2}\Big(1-\sqrt{1-\frac{4(\eta^2-m^2)}{q^2}}\Big)$, $u_2=\frac{1}{2}\Big(1+\sqrt{1-\frac{4(\eta^2-m^2)}{q^2}}\Big)$ are obtained from the equation $m^2+u(1-u)q^2=\eta^2$.

1.9 Results

Finally, in case of $\frac{q^2}{4} \geq (\eta^2 - m^2) \geq 0$, when the square root in the expression of $u_{1,2}$ is real, the integral over u gives

$$\Pi_{\mu 3}(B) = -\frac{iB}{4\pi|\eta|}\epsilon_{\mu\nu}q_\nu(\Gamma + i\eta)\Big(\frac{1}{m^2 + \frac{q^2}{4}}\sqrt{1 - \frac{4(\eta^2 - m^2)}{q^2}} + \frac{1}{\eta^2}\Big(1 - \sqrt{1 - \frac{4(\eta^2 - m^2)}{q^2}}\Big)\Big) \quad (1.51)$$

Denote that for polarization operator take place the condition of conservation of charge. When $\eta^2 - m^2 \geq \frac{q^2}{4}$, then $u_1 = u_2 = \frac{1}{2}$ and for $\Pi_{\mu 3}(B)$ we obtain

$$\Pi_{\mu 3}(B) = -\frac{iB}{4\pi|\eta|^3}\epsilon_{\mu\nu}q_\nu(\Gamma + i\eta) \quad (1.52)$$

For $\eta^2 - m^2 \leq 0$ then $u_1 = 0, u_2 = 1$ and in a result we have following expression

$$\Pi_{\mu\nu}(B) = -\frac{iB}{\pi m}\epsilon_{\mu\nu}q_\nu(\Gamma + i\eta)\frac{1}{4m^2 + q^2} \quad (1.53)$$

The main results of this chapter are published in [99, 100].

Chapter 2

Topological Insulators

Topological insulators are electronic materials that have a bulk band gap and also have protected conducting states on their edge or surface. These states are possible because of the combination of spin-orbit interactions and time-reversal symmetry. The two-dimensional $2D$ topological insulator is a quantum spin Hall insulator. A three-dimensional $3D$ topological insulator contributes new spin-polarized $2D$ Dirac fermions on its surface. A magnetic gap drives to a novel quantum Hall state that brings forth to a topological magnetoelectric effect. A superconducting energy gap brings to a state that contributes Majorana fermions.The progress in condensed matter physics is particularly based on openings of new materials. In this respect, materials presenting exeptional quantum-mechanical properties are special importance. Topological insulators (TIs) are a materials which at the present time creating a blast of research activities [101–103]. The band insulators can be topologically classified by evaluating the Z_2 invariant from valence band Bloch wave functions. This classification is based on TRS of the system.It is also possible to classify band insulators based on topologies protected by point-group symmetries of the crystal lattice. Those insulators that have nontrivial topology protected by point-group symmetries are called topological crystalline insulators (TCIs).The most known property of a TI is the presence of a gapless surface state. The gapless nature is protected by TRS in Z_2 topological insulators. What makes this surface state distinct from ordinary surface states (including accumulation and inversion layers) is its

helical spin polarization, which is also called spin-momentum locking,specifically, the surface state is spin non-degenerate and the direction of the spin is perpendicular to the momentum vector and is primarily confined in the surface plane. In fact, if a band has such a peculiar spin polarization and the system preserves TRS, there must be a Kramers partner for each eigenstate and Kramers theorem says that the two eigenstates cross each other at TRIMs, which guarantees the gapless nature of the surface state. The helical spin polarization of the surface state means that a dissipationless spin current exists on the surface in equilibrium, because there is no net charge flow but the spin angular momentum flows in the direction perpendicular to the spin direction. The spin helicity of the surface state determines the spin current direction. [104–106].

An important consequence of a nontrivial topology associated with the wave functions of an insulator is that a gapless interface state necessarily shows up when the insulator is physically terminated and faces an ordinary insulator (including the vacuum). This is because the nontrivial topology is a discrete characteristic of gapped energy states, and as long as the energy gap remains open, the topology cannot change.In order to change the topology across the interface into a trivial one, the gap must close at the interface. Therefore, three-dimensional $3D$ TIs are always connected with gapless surface states, and so are two-dimensional (2D) TIs with gapless edge states [107–109]. This principle for the necessary occurrence of gapless interface states is called bulk-boundary correspondence in topological phases [110–112].

2.1 Berry's phase in Hall effects and topological insulators

It is not surprising that Berry's phase can be important in the Hall effect because there is analogs between Berry's phase and vector potentials.We will start think about adiabaticity by putting a Bloch electron in an electric field. Lets discuss that problem. We can look this problem in terms of adiabatic evolution by applying a gauge where the electric field arises from a time dependent vector potential:

$$H = \frac{1}{2m}(\mathbf{p} - e\mathbf{A}/c)^2 + V(\mathbf{r}) \tag{2.1}$$

where V is the potential of the ions.In case when we have a constant electric field we take

$$\mathbf{A} = -\mathbf{E}t \tag{2.2}$$

If this is changing slowly enough during time,the state at time t will simply be

$$|\psi(t)>= e^{-i\Phi(t)}|p_0 - eE/c>, \tag{2.3}$$

where p_0 is the momentum at time 0.The momentum only increases with time . The phase factor

$$\Pi(t) = \int^t \epsilon(t)dt + \int^t (\partial_t eA/c) < p|\partial_p|p > \tag{2.4}$$

where

$$p = p_0 - eA/c. \tag{2.5}$$

This extra phase factor gives an extra contribution to the group velocity of a wave packet.Therefore

$$\mathbf{v} = \partial_p \epsilon_p - \frac{e}{\hbar}\mathbf{E} \times \mathbf{\Omega}(\mathbf{p}) \tag{2.6}$$

where

$$\mathbf{\Omega}(\mathbf{p}) = i(\nabla_p < p|) \times (\nabla_p < p|). \tag{2.7}$$

Even in the absence of a magnetic field we can see a Hall effect: if we place a voltage across the $\hat{x}$ axis, and allow a current flowing along the $\hat{y}$ axis.This is famous as the "Anomalous Hall effect". A question arises: what materials have non-zero $\mathbf{\Omega}$ and thence a considerable Anomalous Hall effect? When $\mathbf{\Omega} = \mathbf{0}$ the system has both time reversal and inversion symmetry.Time reversal takes $v \to v$, $E \to E$ and $k \to -k$. Therefore, if the system has time reversal symmetry then$\Omega(-k) = -\Omega(-k)$, inversion symmetry will be $v \to -v$, $E \to -E$ and $k \to -k$. Thus if the system has inversion symmetry then $\Omega(-k) = \Omega(k)$. The coherent way to have both symmetry is to have $\Omega = 0$. Time reversal symmetry is broken in ferromagnets and antiferromagnets. Actually, it is generally the Hall effect in ferromagnets which is known to as the "Anomalous Hall Effect". An ordinary case would be a two-dimensional

tight binding model with a Rashba spin-orbit term $\hat{z}(S \times p)$ and an exchange splitting

$$H = \sum_{i,\sigma,\tau}[a^{+}_{i,\sigma}a_{i-\hat{x},\tau}(-t\delta_{\sigma\tau}+i\alpha(S_y)_{\sigma\tau}+a^{+}_{i,\sigma}a_{i-\hat{y},\tau}(-t\delta_{\sigma\tau}-i\alpha(S_x)_{\sigma\tau}]+HC+\epsilon\sum_{i}(a^{+}_{i\uparrow}-a_{i\uparrow}-a^{+}_{i\downarrow}-a_{i\downarrow}) \tag{2.8}$$

The importance of spin-orbit coupling is natural. Actually the idea is the following:when we adiabatically move through k-space, our spin rotates. This rotation in spin space produces a Berry phase.An exemplary model without inversion symmetry would be graphene with an extra superlattice potential.When we have a conductor with non-zero Ω,the Anomalous Hall conductivity will appear if we sum up all the velocities from all the occupied states:

$$\sigma_{xy} = \frac{e^2}{\hbar}\int \frac{d^dk}{(2\pi)^d} f(\epsilon_k)\Omega_{k_x,k_y}, \tag{2.9}$$

where f is a step function at the Fermi surface. Applying Stokes theorem we will have

$$\sigma_{xy} = \frac{e^2}{\hbar}\oint dk\dot{A}_k. \tag{2.10}$$

In this way the Hall conductivity can be considered as the Berry phase accumulated in moving around the Fermi surface.

2.2 Hall conductivity of an insulator

The Hall conductivity of an insulator arises easily from summing 2.6 over the filled bands. For two dimensions we can write

$$\sigma_{xy} = \frac{e^2}{\hbar}\int_{BZ}\frac{d^2k^2}{2\pi}\Omega_{kx,ky}. \tag{2.11}$$

This integral must be an integer,the idea is that the Berry phase accumulated in any closed loop in k-space is exceptional. Applying Stoke's theorem, for this phase we can write an integral of the Berry curvature. There are two cases the integral can be done over. These phases are just the same if the integral is a multiple of an integer. This integer is known

as the first Chern number. Any insulator which has a topological invariant is a "topological insulator". So far we have seen one invariant, the first Chern number. There are interesting varients of this invarient: for example, there is at least one model for which the up-spins have a Chern number of $+1$, and the down spins -1. This gives rise to a "Spin Hall Effect".

Graphene directed interest to Dirac fermions in crystals [113].The valence band and the conduction band linearly contact in the Brillouin zone on the honeycomb lattice, which provides massless Dirac fermions . This peculiarity is perfectly manifest under a strong magnetic field, in which unusual quantum Hall effect (QHE) for relativistic particles [114,115] has been exemined. Various topological aspects of graphene QHE for example disorder effects and the bulk-edge correspondence have been observed. In graphene,arise two Dirac fermions in the Brillouin zone because of the overlapping mechanism on lattice systems [116, 117].Thus,the Hall conductivity as the result of degenerate Dirac fermions is always observed. What concerns two-dimensional Dirac fermions they can also be observed on the surface of three dimensional $3D$ topological insulators [118].In spite of fact that they are doubled , it may be easier to control them, because they emerge on the opposite surfaces which are spatially separated.Some experimental and theoretical studies on the QHE of the surface states of topological insulators have been examined.Particularly in a magnetic topological insulator in presence of broken inversion symmetry nondegenerate surface states have been realized and the QHE for a single Dirac fermion has been observed [119]. An insulator is characterized as a material with an energy gap dividing filled and empty energy bands.There is also other a more complicated definition of an insulator,it's the following: the material for which all electronic phenomena are local [120]. This definition implies that such a material insensitive to boundary conditions, so that in a multiply connected model, such as a ring,also is important to notice that there is exponentially small sensitivity to magnetic flux threading the holes. In atomic insulator electrons are tightly bound to atoms in closed shells, obviously satisfies both properties. When we have ionic and covalent insulators the picture is the same.These band insulators are topologically equivalent,it means that the Hamiltonian can be adiabatically transformed into an atomic insulator without going through any phase transitions.From point of view their low-energy electronic behavior, conventional insulators are equivalent to atomic insulators.

The existence of a bulk energy gap does not provide the insensitivity to boundary conditions, and also there exist phases with bulk gaps, which are topologically special.In complement to strongly correlated phases [121,122] are appearing even for noninteracting electrons described within band theory. The simplest example is the integer quantum Hall effect (IQHE). In two dimensions, a magnetic field creats a cyclotron gap between Landau levels, which is possible to express as energy bands in the magnetic Brillouin zone. This phase can exist even without Landau levels in the absence of a uniform magnetic field [123].But there is a necessary condition according which time-reversal symmetry must be broken.What concerns to the band structure, it is not easy exactly to observe the difference between the IQHE state and a band insulator. The veriety between the two is expressed by a triad of Chern integers [124]. A hallmark of the (IQHE) phases, which is intimately related to their topology, is the existence of gapless chiral edge states which are strong in the presence of disorder [125, 126]. The surface states are provided by topologically nontrivial phase of the bulk which is famous as the bulk-edge correspondence.Consequently,it is not explicit whether the QHE of massless Dirac fermions are indeed observed in a strong magnetic field regime, since broken time reversal symmetry makes the bulk topological insulating phase instable. The stability of the surface Dirac fermions of a topological insulator under a strong magnetic field has been invaestigated. Recently, new topological insulating phases for systems with time-reversal symmetry have been observed [127–130]. The quantum spin-Hall phase is prominenet from a band insulator by a single Z_2 invariant.This phase demonstrates gapless spin-filtered edge states, which is important because that states allow for dissipationless transport of charge and spin at zero temperature and are protected from weak disorder and interactions by time-reversal symmetry. A timereversal invariant band structure is described by four Z_2 invariants . Three of the invariants depend on the translational symmetry of the lattice and are not strong in the presence of disorder, leading to "weak topological insulators". The fourth invariant is enough strong and discerns the "strong topological insulator" STI. Nontrivial Z_2 invariants assume the presence of gapless surface states.The surface states form a two-dimensional "topological metal", in the STI phase, encircles an odd number of Dirac points. This fact brings to a quantized Berry's phase of obtained by an electron circling the surface Fermi arc, which does not

change under continuous perturbations [131, 132]. It's important to notice that the Berry's phase also indicates that with disorder, the surface states are in the symplectic universality class and show antilocalization. Therefore,the metallic surface states mold a uncommon phase, which cannot be fulfilled in a conventional two-dimensional electron system for which Dirac points must be in pairs [133].

2.3 Time-reversal polarization

In [134] is represented the idea of the time-reversal polarization, in the same way as charge polarization. For description of the Z_2 invariants has been used a Laughlin-type gedanken experiment on a cylinder. For understanding the time-reversal polarization, we need at first begin with a discussion of the charge polarization.The charge polarization implies that the surface charges present in a finite system. After electrons may be added or removed from a surface, the charge polarization is determined only modulo an integer.In [135–138] ,the changing in the charge polarization caused by adiabatic changes in the Hamiltonian is accurately described. In Laughlin's gedanken experiment for the integer quantum Hall effect, a quantum of magnetic flux h/e is adiabatically input in a cylindrical quantum Hall sample at filling $\nu = N$. The resulting transfer of N electrons from one end of the cylinder to the other can be modified as a change in the charge polarization of the cylinder. What concerns to the Chern invariant, which distinguishes the integer quantum Hall state, accurately describes this quantized change in charge polarization [139–143]. The time-reversal polarization is a Z_2 quantity, which shows the presence or absence of a Kramers degeneracy related with a surface. As in case of the charge polarization, the value can be changed by adding an extra electron to the surface. Therefore, the time-reversal polarization is not significant.What concerns to changes in the time-reversal polarization because of adiabatic changes in the bulk Hamiltonian are correctly defined.Particularly, the change in the time-reversal polarization when half a flux quantum $h/2e$ is cut through a cylinder defines a Z_2 invariant, which is analogous to the Chern invariant, and differentiates topological insulators.

The topological invariant describing a two dimensional band structure may be formed by

imagining a long cylinder whose axis is parallel to a reciprocal-lattice vector $\mathbf{G}$ and which has a circumference of a single lattice constant. Then, the magnetic flux cutting the cylinder plays the role of the circumferential or "edge" crystal momentum k_x, with $\Phi = 0$ and $\Phi = h/2e$ corresponding to two edge time-reversal invariant momenta $k_x = \Lambda_1$ and $k_x = \Lambda_2$. The Z_2 invariant characterizes the change in the Kramers degeneracy at the boundariess of this one-dimensional system between $k_x = \Lambda_1$ and $k_x = \Lambda_2$. For a three-dimensional crystal, suppose a "generalized cylinder" which is long in one direction,parallel to $\mathbf{G}$ but, in the other two directions, has a width of one lattice constant with periodic boundary conditions.Though this structure is not possible represent as regular cylinder, a misrepresented(but topologically equivalent) version can be viewed as a torus with a finite thickness. This "Corbino donut" is similar to the generalized cylinder in same analogy the Corbino disk is like to the regular cylinder.The "long" direction corresponds to the thickness of the torus, and the two boundaries correspond to the inner and outer surfaces. This system can be divided by two independent magnetic fluxes,where they correspond to the two components of the momentum perpendicular to $\mathbf{G}$. In result we have four time-reversal invariant surface momenta Λ_a, corresponding to the two fluxes which can get either 0 or $h/2e$ values . The band structure can be described by the difference in the time-reversal polarization between any pair. The Z_2 invariants can be derived from the topological structure of the Bloch wave functions of the bulk crystal in the Brillouin zone. Some recent experimental results related to peculiar properties of (TI) are in this [144–149] works.

2.4 Transport properties of fermions with moat spectra

In modern physics there are materials, such as topological insulators (TI) (see for a review [150–153]) with edge states, Bose-Einstein condensates of Rb atoms with spin-orbit interactions (SOBEC) [154, 155] and honeycomb lattices with next to nearest neighbor (NNN) interactions [156], where the spectrum of non-relativistic particles combined with relativistic Dirac component. The analyze of transport properties of this type of systems is an important task which is necessary to carry out. The polarization operator is a variety which determines

both, longitudinal and Hall conductivity from one side and effective action of $U(1)$ gauge field, defined by quantum fluctuations of fermions, from the other. The goal of this paper is the calculation of the polarization operator of fermions with moat type spectrum. Similar type of investigations were carry earlier [157, 158].

Most general form of the basic Hamiltonian of such systems has a form

$$H(k) = \epsilon_k + \sum_{i=x,y,z} d_i(\vec{k})\sigma_i, \tag{2.12}$$

where $\epsilon_k = -\mu + D\vec{k}^2$, $\vec{d} = A\vec{k}$ and $d_z = \Delta - M\vec{k}^2$. For topological insulators $D < 0$, while for cold atom systems $D > 0$, because it defines positive non-relativistic kinetic energy of Rubidium atoms used in fabrication of artificial Rashba term by the system of lasers [159].

The edge states in TI or excitation's on honeycomb lattice whit NNN interaction come in pairs with states of opposite chirality defined by time reversal Hamiltonian

$$H^*(-\vec{k}) = \varepsilon_k + A(-k_x\sigma_x + k_y\sigma_y) + d_z\sigma_3^s \tag{2.13}$$

where $\sigma_z^s = s\sigma_z$, $s = \pm 1$ defines chirality. Without loss of generality we can take $\sigma_i^s = s\sigma_i$, $i = x, y, z$. The total Hamiltonian of such systems is

$$\mathcal{H} = \begin{pmatrix} H(k) & 0 \\ 0, & H^*(-k) \end{pmatrix} \tag{2.14}$$

The action of fermions with particular chirality is

$$S = \bar{\psi}^+[\Omega - \epsilon_k - v_F\vec{\sigma^s}\vec{k} - d_z\sigma_z^s]\psi \tag{2.15}$$

Causal/Feynman Green function can be written in a simple form

$$G(\Omega, \vec{k}) = \frac{1}{2}\left(\frac{1 + \sigma^i n^i}{\Omega - E_k^- + i\eta_k} + \frac{1 - \sigma^i n^i}{\Omega - E_k^+ + i\eta_k}\right) \tag{2.16}$$

where $n^i = k^i/k$ is the unit vector along momentum direction, $E^{\pm} = \varepsilon_k \pm \epsilon_k = D\vec{k}^2 \pm$

$\sqrt{{v_F}^2\vec{k}^2 + d_z^2}$, μ is the chemical potential and $\eta_k = \eta\ \mathrm{sign}(\Omega - \mu)$ with $\eta = 1/2\tau$, defined by scattering rate τ.

We will be concentrated on a problem of cold atoms with spin-orbit interacting [160]. For simplicity we take $M = 0$ and in that case the spectrum become

$$E_k^{\pm} = D\vec{k}^2 \pm \sqrt{v_F^2\vec{k}^2 + \Delta^2}. \tag{2.17}$$

Characteristics picture of two branches of this spectrum is presented on Fig.2.1, while only lower branch, which is forming ground state, on Fig.2.2a.

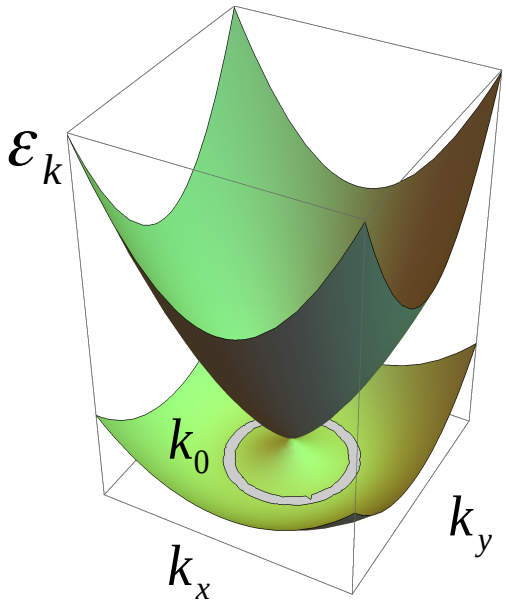

Figure 2.1: Two branches of spectra of moat type. k_0 denotes radius of circle of minimal energy.

Lowest energy located on a circle of radius $k_0 = \sqrt{m^2v_F^2 - \frac{\Delta^2}{v_F^2}}$ in E_k^- branch. Interesting for us region for chemical potential is $\Delta > \mu > -\Delta^2/2mv_F^2 - mv_F^2/2$ when Fermi sea has a form of Corbino disk with radius

$$k_{1/2,F}^2 = 2m\left[\mu + mv_F^2 \pm \sqrt{2m\mu v_F^2 + m^2v_F^4 + \Delta^2}\right]. \tag{2.18}$$

At $\mu^2 - \Delta^2 = 0$, Fermi momenta are $k_{F_2} = 0$ and $k_{F_1}^2 = 4m(\mu + mv_F^2)$. On Fig2.2a we present

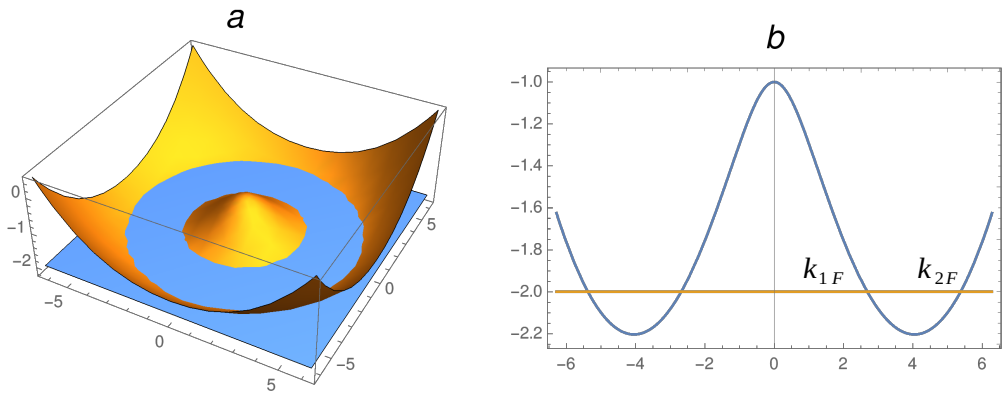

Figure 2.2: a) Lower branch of spectrum with filled Fermi sea. b) $k_y = 0$ projection of the spectrum. k_{1F} and k_{2F} denote Fermi momenta of inner and outer circles.

characteristic form of the Fermi sea. Fig.2.2b demonstrates projection of spectrum on $k_y = 0$ plane with notion of Fermi momenta $k_{F_{1,2}}$.

2.5 Transport property. The polarization operator

Study of transport properties in this systems, as usual, should start from calculation and analyze of polarization operator

$$\Pi_{\mu\nu} = \langle j_\mu j_\nu \rangle, , \quad \mu, \nu = x, y. \tag{2.19}$$

Here current $\vec{j}$ defined from the action (2.15) as

$$\vec{j} = \frac{\delta S}{\delta \vec{j}} = 2iD\psi^+ \vec{\partial}\psi + v_F \psi^+ \vec{\sigma}\psi - 2D\frac{e}{c}\vec{A}\psi^+\psi \tag{2.20}$$

which, due to gauge invariance and according to Neuter's theorem, fulfills conservation low $\vec{\partial}\vec{j} = \frac{1}{c}\partial_t(\psi^+\psi)$. Last term in the current (2.20) given by $\vec{A}$ just insures gauge invariance.

By taking $D = \frac{1}{2m}$, we get

$$\vec{j} = i\frac{1}{m}\psi^{+}\vec{\partial}\psi + v_F\psi^{+}\vec{\sigma}\psi - \frac{e}{mc}\vec{A}\psi^{+}\psi \tag{2.21}$$

Linear response of currents to external gauge field A_μ is given by

$$< j_\mu >= \int \Pi_{\mu\nu}A_\nu d\vec{r}dt + \frac{ne}{c}A_\mu,\ \mu,\nu = 1,2 \tag{2.22}$$

where

$$\Pi_{\mu\nu} =< \left(i\frac{\partial_\mu}{m} + v_F\sigma_\mu\right)\left(\frac{\partial_\nu}{m} + v_F\sigma_\nu\right) > . \tag{2.23}$$

Denoting matter field defined part of the current as $j^0_\mu = i\frac{\partial_\mu}{m} + v_F\sigma_\mu$ for gauge invariant full polarization operator $K_{\mu\nu}$ we have

$$K_{\mu\nu}(\vec{r}-\vec{r}') =< j^0_\mu(\vec{r})j^0_\nu(\vec{r}') > -\frac{ne}{c}\delta^{(2)}(\vec{r}-\vec{r}')\delta(t-t') \tag{2.24}$$

Therefore, for the analyze of the transport properties of cold atom systems with moat spectrum (2.17) we need to calculate

$$\Pi_{\mu\nu} = i\,\mathrm{Tr}\int \frac{d\Omega d^2k}{(2\pi)^3}\left[j^0_\mu G\left(\Omega - \frac{\omega}{2}, k - \frac{q}{2}\right)j^0_\nu G\left(\Omega + \frac{\omega}{2}, k + \frac{q}{2}\right)\right] \tag{2.25}$$

We consider only lower branch of the spectrum, therefore

$$\Pi_{\mu\nu} = \frac{i}{4}\int \frac{d\Omega d^2k}{(2\pi)^3}\frac{T_{\mu\nu}}{(\Omega - \frac{\omega}{2} - E^-_{k-\frac{q}{2}} + i\eta_{k-\frac{q}{2}})(\Omega + \frac{\omega}{2} - E^-_{k+\frac{q}{2}} + i\eta_{k+\frac{q}{2}})} \tag{2.26}$$

where

$$T_{\mu\nu} = \mathrm{Tr}\left[\left(\frac{(k-\frac{q}{2})_\mu}{m} + v_F\sigma_\mu\right)(1 + n^i_{k-\frac{q}{2}}\sigma^i))(m(k+\frac{q}{2})_\nu + v_F\sigma_\nu)(1 + n^j_{k+\frac{q}{2}}\sigma^j))\right] \tag{2.27}$$

Integration over Ω in (2.26) gives

$$\Pi_{\mu\nu} = \frac{i^2}{4}\int \frac{d^2k}{(2\pi)^2}\frac{T_{\mu\nu}(n(E_{k+\frac{q}{2}} - i\eta_{k+\frac{q}{2}} - \mu) - n(E_{k-\frac{q}{2}} - i\eta_{k-\frac{q}{2}} - \mu))}{\omega + E_{k-\frac{q}{2}} - E_{k+\frac{q}{2}} + i(\eta_{k+\frac{q}{2}} - \eta_{k-\frac{q}{2}})}. \tag{2.28}$$

Where $n(E_{k\pm\frac{q}{2}} - i\eta_{k\pm\frac{q}{2}} - \mu)$ are Fermi distribution functions of occupied/empty states. For small $\vec{q}$ and in linear approximation

$$E_{k-\frac{q}{2}} - E_{k+\frac{q}{2}} = -\left(\frac{\epsilon_k - v_F^2 m}{m\epsilon_k}\right)\vec{k}\vec{q} \tag{2.29}$$

Therefore the expression (2.28) become

$$\Pi_{\mu\nu} = -\frac{1}{4}\int \frac{d^2k}{(2\pi)^2}\frac{T_{\mu\nu}\left[n(E_{k+\frac{q}{2}} - i\eta_{k+\frac{q}{2}} - \mu) - n(E_{k-\frac{q}{2}} - i\eta_{k-\frac{q}{2}} - \mu)\right]}{\omega + 2i\eta - \left(\frac{1}{m} - \frac{v_F^2}{\epsilon_k}\right)kq\cos\phi + \theta(q^3)}. \tag{2.30}$$

Taking into account, that the terms $\epsilon^{ij}k_iq_j \sim k_xq_y - k_yq_x \sim k_y \sim \sin\phi$ and after integration over angles will give 0 and consequently $\left(k - \frac{q}{2}\right)_\mu \left(k + \frac{q}{2}\right)_\nu = k_\mu k_\nu - \frac{q_\mu q_\nu}{4} + \frac{k_\mu q_\nu}{2} - \frac{k_\nu q_\mu}{2} \to k_\mu k_\nu - \frac{q_\mu q_\nu}{4}$, we left with expression

$$\begin{aligned} T_{\mu\nu}(k) &= 2\left(k_\mu k_\nu - \frac{q_\mu q_\nu}{4}\right)\left[2\left(\frac{1}{m} + \frac{v_F^2}{\epsilon_k}\right)^2 - \frac{1}{m^2} + \frac{v_F^2}{m^2}\left(\frac{\vec{k}^2 - \frac{\vec{q}^2}{4}}{\epsilon_k^2}\right)\right] \\ &+ \delta_{\mu\nu}v_F^2\left[1 - \frac{v_F^2}{\epsilon_k^2}\left(\vec{k}^2 - \frac{\vec{q}^2}{4}\right)\right] + 2i\frac{v_F^3}{\epsilon_k}\epsilon^{\mu\nu j}q_j. \end{aligned} \tag{2.31}$$

Finally we obtain

$$\Pi_{\mu\nu} = -\frac{1}{4}\int_0^{2\pi} \frac{kdkd\phi}{(2\pi)^2}\frac{T_{\mu\nu}(k)[n(E_{k+\frac{q}{2}} - i\eta_{k+\frac{q}{2}} - \mu) - n(E_{k-\frac{q}{2}} - i\eta_{k-\frac{q}{2}} - \mu)]}{\omega + 2i\eta - \left(\frac{1}{m} - \frac{v_F^2}{\epsilon_k}\right)kq\cos\phi + O(q^3)}. \tag{2.32}$$

Integral over k is located on two Fermi surfaces $E_k - \mu = 0$ when $n(E_{k+\frac{q}{2}} - i\eta_{k+\frac{q}{2}} - \mu) - n(E_{k-\frac{q}{2}} - i\eta_{k-\frac{q}{2}} - \mu) \neq 0$. Because

$$E_k - \mu = \frac{k^2}{2m} - \sqrt{v_F^2k^2 + \Delta^2} - \frac{k_{1F}^2}{2m} - \sqrt{v_{1F}^2k^2 + \Delta^2} = \vec{k}_{1F}(\vec{k} - \vec{k}_{1F})\left[\frac{1}{m} - \frac{v_F^2}{\epsilon_{k_{1F}}}\right], \tag{2.33}$$

where $k - k_{1F} << \{\Delta^2, m^2\}$ and $k + k_{1F} \sim 2k_{1F}$, one can obtain

$$E_{\vec{k}_{1F}+\vec{q}/2} - \mu \approx \frac{\vec{k}_{1F}\vec{q}}{2}\left(\frac{1}{m} - \frac{v_F^2}{\epsilon_{k_{1F}}}\right) \tag{2.34}$$

$$E_{\vec{k}_{1F}-\vec{q}/2} - \mu \approx -\frac{\vec{k}_{1F}\vec{q}}{2}\left(\frac{1}{m} - \frac{v_F^2}{\epsilon_{k_F}}\right) \tag{2.35}$$

The function $n(E_{k+\frac{q}{2}} - i\eta_{k+\frac{q}{2}} - \mu) - n(E_{k-\frac{q}{2}} - i\eta_{k-\frac{q}{2}} - \mu)$ is not zero(correspondingly the integral (2.30) is not zero) only for momenta around Fermi surfaces obeying $\Delta k^2 \sim \vec{k}_{1/2,F}\vec{q} - 2i\eta\frac{m\epsilon_{k_{1/2,F}}}{\epsilon_{k_{1/2,F}} - mv_F^2}$. Therefore from the contribution of the inner Fermi surface to the integral (2.32) we receive

$$\begin{aligned}\Pi^{(1)}_{\mu\nu}(k_{1F}) &= \frac{1}{4}\int_0^{2\pi}\frac{d\phi}{(2\pi)^2}\frac{T_{\mu\nu}(k_{1F})\left[\vec{k}_{1F}\vec{q} - 2i\eta\frac{m\epsilon_{k_{1F}}}{\epsilon_{k_{1F}} - mv_F^2}\right]}{\omega + 2i\eta - \left(\frac{1}{m} - \frac{v_F^2}{\epsilon_k}\right)k_{1F}q\cos\phi} \\ &= -\frac{T_{\mu\nu}(k_{1F},q)}{8\pi}\frac{1}{\left(\frac{1}{m} - \frac{v_F^2}{\epsilon_{k_{1F}}}\right)}\left(1 - \frac{\omega}{\sqrt{(\omega+2i\eta)^2 - \left(\frac{1}{m} - \frac{v_F^2}{\epsilon_{k_{1F}}}\right)^2 k_{1F}^2 q^2}}\right) + \mathcal{O}(\frac{\omega^3}{\mu^3}, \frac{q^3}{k_{1F}^3})\end{aligned} \tag{2.36}$$

where

$$\begin{aligned}T_{\mu\nu}(k_{1F},q) &= 2\left(\frac{q_\mu q_\nu}{4} - \frac{k_{1F}^2}{2}\delta_{\mu\nu} + v_F^2 m^2\delta_{\mu\nu}\right)\frac{1}{m^2}\left(\frac{\Delta^2 + v_F^2\vec{q^2}/4}{\epsilon_{k_{1F}}^2}\right) \\ &+ 4\left(\frac{k_{1F}^2}{2}\delta_{\mu\nu} - \frac{q_\mu q_\nu}{4}\right)\left(\frac{1}{m} + \frac{v_F^2}{\epsilon_k}\right)^2 + 2i\frac{v_F^2}{\epsilon_{k_{1F}}}\epsilon^{\mu\nu}\omega\end{aligned} \tag{2.37}$$

We have used

$$< k_\mu k_\nu >= \frac{< \vec{k^2} >}{2} = \frac{k_{1F}^2}{2}\delta_{\mu\nu} \tag{2.38}$$

We see, that Z_2 chiral anomaly based term proportional to $v_F^2\epsilon_{\mu\nu}$ defined by Rashba term of the action (2.15), because it will disappear if $v_F = 0$.

At the point k_{2F} the answer is the same but will appear with opposite sign, because velocity at k_{2F} is negative. Finally, for total polarization operator we obtain

$$\Pi_{\mu\nu}(q,\omega) = \Pi^{(1)}_{\mu\nu}(k_{1F}) - \Pi^{(1)}_{\mu\nu}(k_{2F}) \tag{2.39}$$

where $\Pi^{(1)}_{\mu\nu}(k_{1,2F})$ are defined by formulas (2.36) and (2.37).

Longitudinal conductivity $\sigma_{xx}(\omega) = i(\Pi_{xx}(0,\omega) - \Pi_{xx}(0,0))/\omega$ as a coefficient of linear response to external electric field will give

$$\sigma_{xx}(\omega) = \frac{T_{xx}(k_{1F},0) - T_{xx}(k_{2F},0)}{8\pi\left(\frac{1}{m} - \frac{v_F^2}{\epsilon_k}\right)} \frac{i}{\omega + 2i\eta} \tag{2.40}$$

The expression shows, that at chemical potential $\mu = -\frac{m^2 v_F^4 + \Delta^2}{2mv_F^2}$, when it is at level of energy minima, the conductivity is zero. Furthermore, in the limit $v_F = 0,\ \Delta = 0$ Rashba term is disappearing in the action (2.15) and we have non-relativistic fermions. Then moat absent in the spectrum, we have only outer k_{2F} Fermi momentum and conductivity acquires Drude form

$$\sigma_{xx}(\omega) = \frac{k_{2F}^2}{4\pi m} \frac{i}{\omega + 2i\eta} \tag{2.41}$$

2.6 Conclusions

We have presented here the calculation of the polarization operator in the fermionic system, which have moat type spectrum. The answer has normal part, leading to Drude conductivity and Z_2 anomaly part, defined by Rashba SO-term in the Hamiltonian. The result presents correct, expected limits at $v_F = 0$, when Rashba term is zero, at $m = \infty$, when non-relativistic part of the Hamiltonian is zero and we have only Rashba term. At the minimal chemical potential the conductivity became zero.

The main results of this chapter is published in [160].

Chapter 3

Liouville field theory

3.1 Introduction to the conformal field theory

We define by $g_{\mu\nu}$ the metric tensor in a space-time of dimension d. By defnition a conformal transformation of the coordinates is an reverseable mapping $x \to x^{'}$ which leaves the metric tensor invariant up to a scale:

$$g^{'}_{\mu\nu}(x^{'}) = \Lambda(x) g_{\mu\nu}(x) \tag{3.1}$$

where

$$g^{'}_{\mu\nu}(x^{'}) = \frac{\partial x^{'\mu}}{\partial x^{\lambda}} \frac{\partial x^{'\nu}}{\partial x^{\rho}} = g_{\lambda\rho} \tag{3.2}$$

A conformal transformation is locally equivalent to the rotation and dilatation. For convenience, we assume that the conformal transformation is an infinitesimal deformation of the standard Cartesian metric $g_{\mu\nu=\eta_{\mu\nu}}$,where $\eta_{\mu\nu} = diag(1, ..., 1)$. The set of conformal transformations clearly forms a group, and it evidently has the Poincare group as a subgroup, since the latter corresponds to the special case $\Lambda(x) = 1$.Let us examine the outcomes of the definition (3.1)on an infinitesimal transformation

$$x^{\mu} \to x^{'\mu} = x^{\mu} + \epsilon^{\mu}(x) \tag{3.3}$$

it comes from (3.1)

$$\eta_{\mu\nu} = \frac{\partial x'^{\mu}}{\partial x^{\lambda}} \frac{\partial x'^{\nu}}{\partial x^{\rho}} = \Lambda^{-1} \eta_{\lambda\rho} \tag{3.4}$$

and inserting in (3.3) we get in the first order by epsilon

$$\eta_{\mu\nu} \left(\delta^{\lambda}_{\mu} + \frac{\partial \epsilon^{\mu}}{\partial x^{\lambda}} \right) \left(\delta^{\rho}_{\nu} + \frac{\partial \epsilon^{\nu}}{\partial x^{\rho}} \right) \tag{3.5}$$

Therefore, the requirement that the transformation be conformal means that

$$\partial_{\mu}\epsilon_{\nu} + \partial_{\nu}\epsilon_{\mu} = (\lambda^{-1} - 1)\eta_{\mu\nu} = f(x)\eta_{\mu\nu} \tag{3.6}$$

The factor $f(x)$ is defined by taking the trace on both sides:

$$f(x) = \frac{2}{d} \partial_{\rho}\epsilon^{\rho} \tag{3.7}$$

By using an additional derivative ∂_{ρ} on Eq.(3.6),inverting the indices and taking a linear combinations,we have

$$2\partial_{\mu}\partial\nu\epsilon_{\rho} = \eta_{\mu\rho}\partial_{\nu}f + \eta_{\nu\rho}\partial_{\mu}f - \eta_{\mu\nu}\partial_{\rho}f \tag{3.8}$$

Upon contracting with $\eta_{\mu\nu}$ = this gets following form

$$2\partial^{2}\epsilon_{\mu} = (2 - d)\partial_{\mu}f \tag{3.9}$$

From (3.6) we find

$$(2 - d)\partial_{\mu}\partial_{\nu}f = \eta_{\mu\nu}\partial^{2}f \tag{3.10}$$

In result we get

$$(d - 1)\partial^{2}f = 0 \tag{3.11}$$

Now we can extract the accurate form of conformal transformation in d dimensions.When $d = 1$ the above equations do not inflict any limitation on the function f, and thus any smooth transformation is conformal in one dimension.Condition (3.6) for $g_{\mu\nu} = \delta_{\mu\nu}$ becomes

the Cauchy-Riemann equation

$$\partial_1\epsilon_1 = \partial_2\epsilon_2 \quad \partial_1\epsilon_2 = -\partial_2\epsilon_1 \tag{3.12}$$

Then $\epsilon(z)\epsilon_1 - i\epsilon_2$ and $\bar{\epsilon}(\bar{z}) = \epsilon_1 + i\epsilon_2$ in the complex coordinates $z = x+iy$ and $\bar{z} = x-iy$.In case of two dimensional conformal transformations hereby coincide with the analytic coordinate transformations

$$z \to f(z), \bar{z} \to \bar{f}(\bar{z}) \tag{3.13}$$

In case of complex coordinates the metric is

$$ds^2 = dzd\bar{z} \tag{3.14}$$

Under the analytic coordinate transformations

$$z \to f(z), \bar{z} \to \bar{f}(\bar{z}) \quad ds^2 = dzd\bar{z} \to \left|\frac{\partial f}{\partial z}\right|^2 dzd\bar{z} \tag{3.15}$$

Any holomorphic infinitesimal transformation is possible expressed as:

$$z^{'} = z + \epsilon z, \quad \epsilon z = \sum_{\infty}^{\infty} c_n z^{n+1} \tag{3.16}$$

In this case

$$\delta\phi = -\epsilon(z)\partial\phi - \bar{\epsilon}(\bar{z})\bar{\partial}\phi = \sum_n c_n l_n \phi(z,\bar{z}) + \bar{c_n}\bar{l_n}\phi(z,\bar{z}) \tag{3.17}$$

where we have represented the generators

$$l_n = -z^{n+1}\partial_z \quad \bar{l_n} = -\bar{z}^{n+1}\partial_{\bar{z}} \tag{3.18}$$

For these generators are right the following commutation relations:

$$[l_n, l_m] = (n-m)l_{n+m} \tag{3.19}$$

$$[l_n, l_m] = (n-m)\bar{l}_{n+m} \tag{3.20}$$

$$[l_n, \bar{l}_m] = 0 \tag{3.21}$$

We see that the conformal algebra is the direct sum of two isomorphic algebras,which obey very simple commutation relations. The algebra (3.19) is famous as the de Witt algebra.

3.2 Tensor energy-momentum, radial quantization, OPE

Under an arbitrary transformation of the coordinates $x^\mu \to x^\mu + \epsilon^\mu$, the action changes as follows:

$$\delta S = \int d^2x T^{\mu\nu}\partial_\mu \epsilon_\nu = \frac{1}{2}\int d^2x T^{\mu\nu}(\partial_\mu \epsilon_\nu + \partial_\nu \epsilon_\mu) \tag{3.22}$$

where $T^{\mu\nu}$ is the symmetric energy-momentum tensor. The infinitesimal conformal mapping brings the action to the following form

$$\delta S = \frac{1}{2}\int d^2x T^\mu_\mu \partial_\rho \epsilon^\rho \tag{3.23}$$

The trace of the energy-momentum tensor vanishes which means the invariance of the action under the conformal transformation. The current of conformal symmetry is

$$J_\mu = T_{\mu\nu}\epsilon^\nu \tag{3.24}$$

This current is conserved because

$$\partial^\mu J_\mu = \partial^\mu T_{\mu\nu}\epsilon^\nu + T_{\mu\nu}\partial^\mu \epsilon^\nu = 0 \tag{3.25}$$

the tensor energy-momentum is conserved and traceless. Euclidean metric $ds^2 = dx^2 + dy^2$ in the complex coordinates $z = x + iy$ has the form $ds^2 = dzd\bar{z}$ therefore

$$g_{zz} = g_{\bar{z}\bar{z}} = 0 \quad \text{and} \quad g_{z\bar{z}} = g_{\bar{z}z} = \frac{1}{2} \tag{3.26}$$

and

$$g^{zz} = g^{\bar{z}\bar{z}} = 0 \quad \text{and} \quad g^{z\bar{z}} = g^{\bar{z}z} = 2 \tag{3.27}$$

For the components of the energy-momentum tensor we have

$$\begin{aligned} T_{zz} &= \frac{1}{4}(T_{00} - 2iT_{10} - T_{11}) \\ T_{\bar{z}\bar{z}} &= \frac{1}{4}(T_{00} + 2iT_{10} - T_{11}) \\ T_{z\bar{z}} = T_{\bar{z}z} &= \frac{1}{4}(T_{00} + T_{11}) = \frac{1}{4}T^{\mu}_{\mu} \end{aligned} \tag{3.28}$$

Under tracelessness we understand

$$T_{z\bar{z}} = T_{\bar{z}z} = 0. \tag{3.29}$$

The conservation law $g^{\alpha\mu}\partial_\alpha T_{\mu\nu} = 0$ brings two equations

$$\partial_{\bar{z}} T_{zz} + \partial_z T_{\bar{z}z} = 0 \quad \text{and} \quad \partial_z T_{\bar{z}\bar{z}} + \partial_{\bar{z}} T_{z\bar{z}} = 0 \tag{3.30}$$

Using (3.29) we obtain

$$\partial_{\bar{z}} T_{zz} = 0 \qquad \text{and} \qquad \partial_z T_{\bar{z}\bar{z}} = 0 \tag{3.31}$$

The two non-vanishing components of the energy-momentum tensor will have the following form

$$T(z) \equiv T_{zz}(z) \qquad \text{and} \qquad \bar{T}(\bar{z}) \equiv T_{\bar{z}\bar{z}}(\bar{z}) \tag{3.32}$$

where there is only the holomorphic and anti-holomorphic dependence.

On a cylinder we can write $\Sigma = R \times S^1 = (t, x \mod 2\pi)$, where t is world-sheet time, and x is compactified space coordinate.

Suppose we have conformal map $w \to z = e^w = e^{t+ix}$, then infinite past and future on a cylinder, $t = \pm\infty$ are mapped to points $z = 0, \infty$ on a plane.What concerns to the equal time surfaces, $t =$ const it becomes circles of the constant radius on z-plane. Dilatation on the

plane e^a modifies time translation $t+a$ on the cylinder, and rotation on the plane $e^{i\alpha}$ is space translation $x+\alpha$ on the cylinder. In result the dilatation generator on the conformal plane can be considered as the Hamiltonian, and the rotation generator on the conformal plane can be considered as momentum.

The current of conformal transformations takes the form:

$$J_z = T(z)\epsilon(z) \quad \text{and} \quad J_{\bar{z}} = \bar{T}(\bar{z})\bar{\epsilon}(\bar{z}) \tag{3.33}$$

The conserved charge of the conformal transformations takes the form

$$Q = \frac{1}{2\pi i}\oint dz T(z)\epsilon(z) + \frac{1}{2\pi i}\oint d\bar{z}\bar{T}(\bar{z})\bar{\epsilon}(\bar{z}) \tag{3.34}$$

3.3 Boundary Liouville field theory

Recently the various semiclassical limits of the Liouville correlation functions appeared in different instances. For example we can mention study of conformal blocks in AdS/CFT correspondence, see *e.g.* [161–163], semiclassical limits of the Nekrasov partition functions, see *e.g* [164–169], minisuperspace limit of correlation functions in AdS_3/H_3^+ [170, 171], semiclassical limit of correlation functions in the presence of defects and boundaries [172, 173] and the most recently found application of the semiclasical limit of Liouville field theory to the SYK problem [174].

In this paper we study matrix elements of the boundary Liouville field theory in minisuperspace limit. In the minisuperspace limit one considers a limit where only the zero mode dynamics survives and the theory is reduced to the corresponding quantum mechanical problem. The mini-superspace limit of the Liouville field theory was considered in [175, 176]. In these papers the matrix elements of the Liouville quantum mechanics with exponential potential were computed. Later it was shown in [178] that the DOZZ structure constants [179, 204] in this limit coincide with the matrix elements found in [175, 176]. It was also demonstrated in [204] that the Liouville two-point function in the mini-superspace limit in agreement with the reflection function of the Liouville quantum mechanics wave functions

given by the modified Bessel function. In papers [181, 182] was studied the mini-super space limit of the boundary Liouville field theory (BLFT). It was found that BLFT in this limit reduced to the Morse potential quantum mechanics. It was shown in [181] that in the mini-super space limit the boundary two-point function, computed in [201], coincides with the reflection amplitude of the eigen-functions of the Morse potential Hamiltonian given by the Whittaker functions.

In this paper we study the mini-superspace limit of the boundary three-point function in the BLFT. The boundary three-point function in the BLFT was computed in [184] and expressed vie double Gamma and double Sine functions [185, 186]. Using known asymptotic properties of the double Gamma and Sine functions we have shown that in the mini-superspace limit the boundary three-point function can be expressed via the Meijer functions $G^{3,2}_{3,3}$ with the unit argument or equivalently via the generalized hypergeometric functions ${}_3F_2$ with the unit argument. We also computed matrix elements for the Morse potential and have shown that they can be expressed via the generalized hypergeometric functions ${}_3F_2$ with the unit argument as well. Using the identities, relating different generalized hypergeometric functions with the unit argument [187–189], and matching quantum and classical parameters, we established exact agreement between the mini-superspace limit of the boundary three-point function and the matrix elements for the Morse potential. It is important to note that in the BLFT relation of the boundary cosmological parameter to the corresponding quantum parameter appearing in the boundary one-point function is two-fold due to a sign ambiguity in the choice of the square-root branch. We found that to match the minisuperspace limit of the boundary three-point with the corresponding quantum mechanical matrix element we should use the branch with the negative sign. We also found that passing from one branch to another brings to additional factor in the normalization of the wave functions corresponding to the boundary condition changing operators. We would like also to mention that various consequences of the branching of the BLFT parameters earlier were considered in [190].

The paper is organized as follows. In section 2 we review the BLFT and compute the mini-superspace limit of the boundary three-point function. In section 3 we compute matrix elements for the Morse potential and establish precise agreement with the boundary three-

point function in the mini-superspace limit found in the previous section. In appendices A, B and C we review various properties of the special functions used in the paper.

Let us consider the Liouville field theory on a strip $\mathbb{R} \times [0, \pi]$, parameterized by the time τ and space σ coordinates, $0 \leq \sigma \leq \pi$. The conformal invariant action has the form:

$$S = \int_{-\infty}^{\infty} d\tau \int_0^{\pi} d\sigma \left(\frac{1}{4\pi} (\partial_a \phi)^2 + \mu e^{2b\phi} \right) + \int_{-\infty}^{\infty} d\tau M_1 e^{b\phi}|_{\sigma=0} + \int_{-\infty}^{\infty} d\tau M_2 e^{b\phi}|_{\sigma=\pi} \qquad (3.35)$$

where M_1 and M_2 are the corresponding boundary cosmological constants.

Let us review some facts on the boundary Liouville field theory [184,191,201]. The primary fields of the Liouville field theory are V_α, associated with the vertex operators $e^{2\alpha\phi}$. They have conformal dimension

$$\Delta_\alpha = \alpha(Q - \alpha), \quad Q = b + \frac{1}{b} \qquad (3.36)$$

In the presence of the boundary with the cosmological constant M the primary fields V_α have the one-point functions:

$$\langle 0|V_\alpha(z, \bar{z})|0\rangle = \frac{U_\sigma(\alpha)}{|z - \bar{z}|^{2\Delta_\alpha}} \qquad (3.37)$$

where

$$U_\sigma(\alpha) = \frac{2}{b} (\pi\mu\gamma(b^2))^{(Q-2\alpha)/2b} \Gamma(1 - b(Q - 2\alpha)) \Gamma(-b^{-1}(Q - 2\alpha)) \cos(\pi(2\sigma - Q)(2\alpha - Q)) \qquad (3.38)$$

where the parameter σ is related to the boundary cosmological constant M by the relation:

$$M = \sqrt{\frac{\mu}{\sin(\pi b^2)}} \cos \pi b \, (2\sigma - Q) \qquad (3.39)$$

Besides bulk primary fields in the boundary conformal field theory exist also boundary condition changing operators, parameterized by the types of the switched boundary conditions and conformal weight. In the case of the BLFT they are given by the fields $\Psi_\beta^{\sigma_1\sigma_2}$ with

conformal weight $\Delta_\beta = \beta(\beta - Q)$. They have the two-point function:

$$\langle 0|\Psi_{\beta_1}^{\sigma_1\sigma_2}(x)\Psi_{\beta_2}^{\sigma_2\sigma_1}(0)|0\rangle = \frac{\delta(\beta_2+\beta_1-Q)+S(\beta_1,\sigma_2,\sigma_1)\delta(\beta_2-\beta_1)}{|x|^{2\Delta_{\beta_1}}} \tag{3.40}$$

where

$$\begin{aligned} S(\beta,\sigma_2,\sigma_1) &= \left(\pi\mu\gamma(b^2)b^{2-2b^2}\right)^{\frac{Q-2\beta}{2b}} \times \\ &\times\frac{\Gamma_b(2\beta-Q)}{\Gamma_b(Q-2\beta)}\frac{S_b(\sigma_2+\sigma_1-\beta)S_b(2Q-\sigma_2-\sigma_1-\beta)}{S_b(\sigma_2-\sigma_1+\beta)S_b(\sigma_1-\sigma_2+\beta)} \end{aligned} \tag{3.41}$$

and three-point function

$$\begin{gathered} \langle 0|\Psi_{\beta_3}^{\sigma_1\sigma_3}(x_3)\Psi_{\beta_2}^{\sigma_3\sigma_2}(x_3)\Psi_{\beta_1}^{\sigma_2\sigma_1}(x_3)|0\rangle = \\ \frac{C_{\beta_3\beta_2\beta_1}^{\sigma_3\sigma_2\sigma_1}}{|x_{21}|^{\Delta_1+\Delta_2-\Delta_3}|x_{32}|^{\Delta_2+\Delta_3-\Delta_1}|x_{31}|^{\Delta_3+\Delta_1-\Delta_2}} \end{gathered} \tag{3.42}$$

$$C_{\beta_3|\beta_2\beta_1}^{\sigma_3\sigma_2\sigma_1} \equiv C_{Q-\beta_3,\beta_2,\beta_1}^{\sigma_3\sigma_2\sigma_1} \tag{3.43}$$

$$C_{\beta_3|\beta_2\beta_1}^{\sigma_3\sigma_2\sigma_1} = R_{\sigma_2,\beta_3}\begin{bmatrix}\beta_2 & \beta_1\\ \sigma_3 & \sigma_1\end{bmatrix}\int_{-i\infty}^{i\infty}\frac{d\tau}{i}J_{\sigma_2,\beta_3}\begin{bmatrix}\beta_2 & \beta_1\\ \sigma_3 & \sigma_1\end{bmatrix} \tag{3.44}$$

where

$$\begin{aligned} R_{\sigma_2,\beta_3}\begin{bmatrix}\beta_2 & \beta_1\\ \sigma_3 & \sigma_1\end{bmatrix} &= (\pi\mu\gamma(b^2)b^{2-2b^2})^{\frac{1}{2b}(\beta_3-\beta_2-\beta_1)} \\ \times\ &\frac{\Gamma_b(2Q-\beta_1-\beta_2-\beta_3)\Gamma_b(\beta_2+\beta_3-\beta_1)\Gamma_b(Q+\beta_2-\beta_1-\beta_3)\Gamma_b(Q+\beta_3-\beta_2-\beta_1)}{\Gamma_b(2\beta_3-Q)\Gamma_b(Q-2\beta_2)\Gamma_b(Q-2\beta_1)\Gamma_b(Q)} \\ \times\ &\frac{S_b(\beta_3+\sigma_1-\sigma_3)S_b(Q+\beta_3-\sigma_3-\sigma_1)}{S_b(\beta_2+\sigma_2-\sigma_3)S_b(Q+\beta_2-\sigma_3-\sigma_2)} \end{aligned} \tag{3.45}$$

and

$$J_{\sigma_2,\beta_3}\begin{bmatrix}\beta_2 & \beta_1\\ \sigma_3 & \sigma_1\end{bmatrix} = \frac{S_b(U_1+\tau)S_b(U_2+\tau)}{S_b(V_1+\tau)S_b(V_2+\tau)}\frac{S_b(U_3+\tau)S_b(U_4+\tau)}{S_b(V_3+\tau)S_b(V_4+\tau)} \tag{3.46}$$

$$\begin{aligned} U_1 &= \sigma_2+\sigma_1-\beta_1, & V_1 &= Q+\sigma_2+\beta_3-\beta_1-\sigma_3 \\ U_2 &= Q+\sigma_2-\beta_1-\sigma_1, & V_2 &= 2Q+\sigma_2-\beta_3-\sigma_3-\beta_1 \\ U_3 &= \sigma_2+\beta_2-\sigma_3, & V_3 &= 2\sigma_2 \\ U_4 &= Q+\sigma_2-\beta_2-\sigma_3, & V_4 &= Q \end{aligned} \tag{3.47}$$

$\Gamma_b(x)$ and $S_b(x)$ in the formulae above denote the double Gamma and Sine functions reviewed in appendix A.

The three-point function has the property, that setting one of the field to vacuum, one recovers the two-point function. For example it was checked in [184] that

$$\lim_{\beta_1\to 0} C^{\sigma_3\sigma_2\sigma_1}_{\beta_3|\beta_2\beta_1} = \delta(\beta_3-\beta_2)+S(\beta_2,\sigma_3,\sigma_2)\delta(\beta_3+\beta_2-Q) \tag{3.48}$$

Let us now consider the minisuperspace limit of three-point function.

As the warm-up exercise we review the minisuperspace limit of two-point function (3.41), computed in [181]. It is argued in [181] that one should take the limit $b\to 0$ and scale the parameters β and σ in the following way:

$$\beta = \frac{Q}{2}+ikb \tag{3.49}$$

and

$$\begin{aligned} \sigma_1 &= \frac{1}{4b}+\rho_1 b \\ \sigma_2 &= \frac{1}{4b}+\rho_2 b \end{aligned} \tag{3.50}$$

Using formulae (3.88, (3.89) and (3.91) in appendix A one can easily obtain:

$$S(\beta,\sigma_2,\sigma_1)\to\left(\frac{4\pi\mu}{b^2}\right)^{-ik}\frac{\Gamma(2ik)}{\Gamma(-2ik)}\frac{\Gamma\left(\rho_1+\rho_2-\frac{1}{2}-ik\right)}{\Gamma\left(\rho_1+\rho_2-\frac{1}{2}+ik\right)} \tag{3.51}$$

To compute the mini-superspace limit of the boundary three-point function we will use the ansatz (3.50) for all the three boundary condition parameters:

$$\begin{aligned}\sigma_1&=\frac{1}{4b}+\rho_1 b\\ \sigma_2&=\frac{1}{4b}+\rho_2 b\\ \sigma_3&=\frac{1}{4b}+\rho_3 b\end{aligned} \tag{3.52}$$

For the primary fields parameters we will use the ansatz suggested in [178] for calculation of the mini-superspace limit of the bulk three-point function [177]:

$$\begin{aligned}\beta_1&=\frac{Q}{2}+ik_1 b\\ \beta_2&=\eta b\\ \beta_3&=\frac{Q}{2}+ik_2 b\end{aligned} \tag{3.53}$$

It is convenient to denote

$$\rho_1+\rho_2=1-\lambda \tag{3.54}$$

$$\rho_2-\rho_3=\xi \tag{3.55}$$

implying also

$$\rho_1+\rho_3=1-\lambda-\xi \tag{3.56}$$

Inserting (3.52) and (3.53) in (3.46), using the formulas (3.88), (3.89),(3.90) in appendix A, and rescaling the integration variable $\tau\to b\tau$, one obtains in the limit $b\to 0$

$$\int_{-i\infty}^{i\infty}\frac{d\tau}{i}J_{\sigma_2,\beta_3}\begin{bmatrix}\beta_2 & \beta_1\\ \sigma_3 & \sigma_1\end{bmatrix}\to 2^{-7/2}(\pi b^2)^{-\lambda+ik_1}b^{-1}\pi^{-2}\times \tag{3.57}$$
$$\int_{-i\infty}^{i\infty}\frac{d\tau}{i}\frac{\Gamma(-\tau)\Gamma(\tau-ik_1+1/2-\lambda)\Gamma(\eta+\xi+\tau)\Gamma(ik_1-ik_2-\xi-\tau)\Gamma(ik_2+ik_1-\xi-\tau)}{\Gamma(\eta-\xi-\tau)}$$

Using the definition of the Meijer G-functions, reviewed in appendix B, one can write

$$\int_{-i\infty}^{i\infty}\frac{d\tau}{i}J_{\sigma_2,\beta_3}\begin{bmatrix}\beta_2 & \beta_1\\ \sigma_3 & \sigma_1\end{bmatrix}\to \tag{3.58}$$
$$2^{-5/2}(\pi b^2)^{-\lambda+ik_1}b^{-1}\pi^{-1}G^{3,2}_{3,3}\left(1\left|\begin{matrix}\frac{1}{2}+\lambda+ik_1, 1-\eta-\xi, \eta-\xi\\ 0, ik_1-ik_2-\xi, ik_1+ik_2-\xi\end{matrix}\right.\right)=$$
$$2^{-5/2}(\pi b^2)^{-\lambda+ik_1}b^{-1}\pi^{-1}G^{3,2}_{3,3}\left(1\left|\begin{matrix}\frac{1}{2}+\lambda+\xi+ik_1, 1-\eta, \eta\\ \xi, ik_1-ik_2, ik_1+ik_2\end{matrix}\right.\right)$$

In the second line we used the identity (3.96) in appendix B.

For further purposes, it is convenient to present the Meijer $G^{3,2}_{3,3}$-function (3.58) in a special way, use of which become clear in the next section. Namely, first we decompose the $G^{3,2}_{3,3}$-function as a sum of ${}_3F_2$ hypergeometric functions with the unit argument according to eq. (3.94) in appendix B. Afterwards we transform obtained in this way ${}_3F_2$ hypergeometric functions with the unit argument successively applying identities (3.97) and (3.98) in appendix

C. We end up with

$$G^{3,2}_{3,3}\left(1\left|\begin{array}{c}\frac{1}{2}+\lambda+ik_1+\xi,1-\eta,\eta\\ \xi,ik_1-ik_2,ik_1+ik_2\end{array}\right.\right)=\frac{\Gamma(\xi+\eta)\Gamma(\frac{1}{2}+\lambda-ik_1)}{\sin\pi(ik_1+\frac{1}{2}+\lambda)}\times \tag{3.59}$$
$$\left[\frac{\Gamma(2ik_2)\Gamma(ik_1-ik_2+\eta)\Gamma(\frac{1}{2}-ik_2-\lambda-\xi)}{\Gamma(-ik_1+ik_2+\eta)\Gamma(-ik_2+\frac{1}{2}+\lambda+\eta)\Gamma(-ik_2+\frac{1}{2}-\lambda+\eta)\Gamma(ik_2+\frac{1}{2}+\lambda-\eta)}\times\right.$$
$${}_3F_2\left(\begin{array}{c}-ik_1-ik_2+\eta,ik_1-ik_2+\eta,\frac{1}{2}+\lambda+\xi-ik_2;\\ 1-2ik_2,\frac{1}{2}+\lambda-ik_2+\eta:1\end{array}\right)+$$
$$\frac{\Gamma(-2ik_2)\Gamma(ik_1+ik_2+\eta)\Gamma(\frac{1}{2}+ik_2-\lambda-\xi)}{\Gamma(-ik_1-ik_2+\eta)\Gamma(ik_2+\frac{1}{2}+\lambda+\eta)\Gamma(ik_2+\frac{1}{2}-\lambda+\eta)\Gamma(-ik_2+\frac{1}{2}+\lambda-\eta)}\times$$
$$\left.{}_3F_2\left(\begin{array}{c}ik_1+ik_2+\eta,-ik_1+ik_2+\eta,\frac{1}{2}+\lambda+\xi+ik_2;\\ 1+2ik_2,\frac{1}{2}+\lambda+ik_2+\eta:1\end{array}\right)\right]$$

Now inserting (3.52) and (3.53) in (3.45), and using formulae (3.84)-(3.92) in appendix A, we obtain for the prefactor (3.45) in the limit $b\to 0$

$$R_{\sigma_2,\beta_3}\left[\begin{array}{cc}\beta_2 & \beta_1\\ \sigma_3 & \sigma_1\end{array}\right]\to\left(\frac{4\pi\mu}{b^2}\right)^{(ik_2-ik_1-\eta)/2}2^{5/2}(\pi b^2)^{-ik_1+\lambda}b\pi^2 \tag{3.60}$$
$$\frac{\Gamma(-ik_1+ik_2+\eta)\Gamma(-ik_1-ik_2+\eta)}{\Gamma(2ik_2)\Gamma(-2ik_1)\Gamma(\frac{1}{2}-ik_2-\lambda-\xi)\Gamma(\eta+\xi)}$$

Combining (3.60) and (3.59) finally we obtain:

$$
\begin{aligned}
&C^{\sigma_3\sigma_2\sigma_1}_{\beta_3|\beta_2\beta_1} \to C^{\lambda\xi}_{k_2|\eta k_1} = \\
&\left(\frac{4\pi\mu}{b^2}\right)^{(ik_2-ik_1-\eta)/2} \frac{\Gamma(\frac{1}{2}+\lambda-ik_1)}{\sin\pi(ik_1+\frac{1}{2}+\lambda)\Gamma(2ik_2)\Gamma(-2ik_1)\Gamma(\frac{1}{2}-ik_2-\lambda-\xi)} \times \\
&\left[\frac{\Gamma(2ik_2)\Gamma(ik_1-ik_2+\eta)\Gamma(-ik_1-ik_2+\eta)\Gamma(\frac{1}{2}-ik_2-\lambda-\xi)}{\Gamma(-ik_2+\frac{1}{2}+\lambda+\eta)\Gamma(-ik_2+\frac{1}{2}-\lambda+\eta)\Gamma(ik_2+\frac{1}{2}+\lambda-\eta)} \times \right. \\
&{}_3F_2\left(\begin{matrix} -ik_1-ik_2+\eta, ik_1-ik_2+\eta, \frac{1}{2}+\lambda+\xi-ik_2; \\ 1-2ik_2, \frac{1}{2}+\lambda-ik_2+\eta : 1 \end{matrix}\right) + \\
&\frac{\Gamma(-2ik_2)\Gamma(ik_1+ik_2+\eta)\Gamma(-ik_1+ik_2+\eta)\Gamma(\frac{1}{2}+ik_2-\lambda-\xi)}{\Gamma(ik_2+\frac{1}{2}+\lambda+\eta)\Gamma(ik_2+\frac{1}{2}-\lambda+\eta)\Gamma(-ik_2+\frac{1}{2}+\lambda-\eta)} \times \\
&\left.{}_3F_2\left(\begin{matrix} ik_1+ik_2+\eta, -ik_1+ik_2+\eta, \frac{1}{2}+\lambda+\xi+ik_2; \\ 1+2ik_2, \frac{1}{2}+\lambda+ik_2+\eta : 1 \end{matrix}\right)\right]
\end{aligned}
\tag{3.61}
$$

As we will see in the next section, especially important role plays the case when $\xi = -\eta$. For $\xi = -\eta$ (3.61) simplifies and takes the form:

$$
\begin{aligned}
&C^{\lambda(-\eta)}_{k_2|\eta k_1} = \\
&\left(\frac{4\pi\mu}{b^2}\right)^{(ik_2-ik_1-\eta)/2} \frac{\Gamma(\frac{1}{2}+\lambda-ik_1)}{\sin\pi(ik_1+\frac{1}{2}+\lambda)\Gamma(2ik_2)\Gamma(-2ik_1)\Gamma(\frac{1}{2}-ik_2-\lambda+\eta)} \times \\
&\left[\frac{\Gamma(2ik_2)\Gamma(ik_1-ik_2+\eta)\Gamma(-ik_1-ik_2+\eta)}{\Gamma(-ik_2+\frac{1}{2}+\lambda+\eta)\Gamma(ik_2+\frac{1}{2}+\lambda-\eta)} \times \right. \\
&{}_3F_2\left(\begin{matrix} -ik_1-ik_2+\eta, ik_1-ik_2+\eta, \frac{1}{2}+\lambda-\eta-ik_2; \\ 1-2ik_2, \frac{1}{2}+\lambda-ik_2+\eta : 1 \end{matrix}\right) + \\
&\frac{\Gamma(-2ik_2)\Gamma(ik_1+ik_2+\eta)\Gamma(-ik_1+ik_2+\eta)}{\Gamma(ik_2+\frac{1}{2}+\lambda+\eta)\Gamma(-ik_2+\frac{1}{2}+\lambda-\eta)} \times \\
&\left.{}_3F_2\left(\begin{matrix} ik_1+ik_2+\eta, -ik_1+ik_2+\eta, \frac{1}{2}+\lambda-\eta+ik_2; \\ 1+2ik_2, \frac{1}{2}+\lambda+ik_2+\eta : 1 \end{matrix}\right)\right]
\end{aligned}
\tag{3.62}
$$

Let us consider the limit $\beta_2 \to 0$ and correspondingly $\eta \to 0$.

Using, that as we explained in appendix C, in this limit ${}_3F_2$ reduces to ${}_2F_1$, which for the

unit argument is given by eq. (3.99), it is straightforward to show that:

$$\lim_{\eta\to 0} C^{\lambda(-\eta)}_{k_2|\eta k_1} = \delta(k_1-k_2) + \left(\frac{4\pi\mu}{b^2}\right)^{-ik_1} \frac{\Gamma(2ik_1)}{\Gamma(-2ik_1)} \frac{\Gamma\left(\frac{1}{2}-\lambda-ik_1\right)}{\Gamma\left(\frac{1}{2}-\lambda+ik_1\right)} \delta(k_1+k_2) \tag{3.63}$$

in agreement with (3.51).

3.4 Matrix elements in the Morse potential

In the mini-superspace limit the boundary Liouville field theory is described by the Hamiltonian with the Morse potential [181, 182]. The corresponding eigenfuntions satisfy the Schrödinger equation:

$$-\frac{\partial^2\psi}{\partial\phi_0^2} + \pi\mu e^{2b\phi_0}\psi + (M_1+M_2)e^{b\phi_0}\psi = k^2b^2\psi \tag{3.64}$$

The relation between parameters M_i appearing in the Schrödinger equation and parameters ρ_i used in the previous section can be found using (3.52) and (3.39) and taking the limit $b\to 0$:

$$M_i = \sqrt{\frac{\mu}{\sin(\pi b^2)}}\sin\pi b^2(2\rho_i-1) \to \pm(\mu\pi)^{1/2}b(2\rho_i-1) \tag{3.65}$$

The solution of the eq. (3.64) is given by the Whittaker function $W_{\mu,\nu}(y)$ [192, 193]:

$$\begin{aligned}\psi = \mathcal{N}\Bigg[& e^{-y/2}y^{ik}\frac{\Gamma(-2ik)}{\Gamma\left(\frac{1}{2}-ik+\frac{M_1+M_2}{2b\sqrt{\pi\mu}}\right)}{}_1F_1\left(\frac{1}{2}+ik+\frac{M_1+M_2}{2b\sqrt{\pi\mu}},1+2ik,y\right)+ \\ & e^{-y/2}y^{-ik}\frac{\Gamma(2ik)}{\Gamma\left(\frac{1}{2}+ik+\frac{M_1+M_2}{2b\sqrt{\pi\mu}}\right)}{}_1F_1\left(\frac{1}{2}-ik+\frac{M_1+M_2}{2b\sqrt{\pi\mu}},1-2ik,y\right)\Bigg] \equiv \\ & \mathcal{N}W_{-\frac{M_1+M_2}{2b\sqrt{\pi\mu}},ik}(y)y^{-\frac{1}{2}}\end{aligned} \tag{3.66}$$

where

$$y = \frac{2\sqrt{\pi\mu}}{b}e^{b\phi_0} \tag{3.67}$$

$\mathcal{N}$ is normalization and ${}_1F_1(a,c,z)$ is the confluent hypergeometric function:

$$ {}_1F_1(a,c,z) = \frac{\Gamma(c)}{\Gamma(a)} \sum_{n=0}^{\infty} \frac{\Gamma(a+n)}{\Gamma(c+n)} \frac{z^n}{n!} \tag{3.68} $$

Now we wish to compute matrix element of the "vertex operator" $e^{\eta b \phi_0}$, between the wave functions corresponding to the boundary condition changing operators. According to this solution to the operator $\Psi_{\beta_1}^{\sigma_2\sigma_1}$ corresponds the wave function $\mathcal{N}_1 W_{\chi_1,ik_1}(y) y^{-\frac{1}{2}}$ with

$$ \chi_1 = -\frac{M_1 + M_2}{2b\sqrt{\pi\mu}} = \pm\lambda \tag{3.69} $$

and to $\Psi_{\beta_3}^{\sigma_1\sigma_3}$ corresponds the wave function $\mathcal{N}_2 W_{\chi_2,ik_2}(y) y^{-\frac{1}{2}}$ with

$$ \chi_2 = -\frac{M_1 + M_3}{2b\sqrt{\pi\mu}} = \pm(\lambda + \xi) \tag{3.70} $$

The corresponding integral can be found in [192, 193]:

$$ \begin{aligned} &\mathcal{M}_{\eta k_1 k_2}^{\chi_1\chi_2} = \mathcal{N}_1\mathcal{N}_2^* \int_{-\infty}^{\infty} W_{\chi_1,ik_1}(y) y^{-\frac{1}{2}} W_{\chi_2,-ik_2}(y) y^{-\frac{1}{2}} e^{\eta b\phi_0} d\phi_0 = \\ &= \frac{\mathcal{N}_1\mathcal{N}_2^*}{b} \left(\frac{4\pi\mu}{b^2}\right)^{-\eta/2} \int_0^{\infty} W_{\chi_1,ik_1}(y) W_{\chi_2,-ik_2}(y) y^{\eta-2} dy = \mathcal{N}_1\mathcal{N}_2^* (4\pi\mu b^{-2})^{-\eta/2} b^{-1} \times \\ &\left[\frac{\Gamma(ik_1 - ik_2 + \eta)\Gamma(-ik_1 - ik_2 + \eta)\Gamma(2ik_2)}{\Gamma(\frac{1}{2} - \chi_2 + ik_2)\Gamma(\frac{1}{2} - \chi_1 - ik_2 + \eta)} \times \right. \\ &{}_3F_2\left(\begin{matrix} -ik_1 - ik_2 + \eta, ik_1 - ik_2 + \eta, \frac{1}{2} - \chi_2 - ik_2; \\ 1 - 2ik_2, \frac{1}{2} - \chi_1 - ik_2 + \eta : 1 \end{matrix} \right) + \\ &\frac{\Gamma(ik_1 + ik_2 + \eta)\Gamma(-ik_1 + ik_2 + \eta)\Gamma(-2ik_2)}{\Gamma(\frac{1}{2} - \chi_2 - ik_2)\Gamma(\frac{1}{2} - \chi_1 + ik_2 + \eta)} \times \\ &\left. {}_3F_2\left(\begin{matrix} ik_1 + ik_2 + \eta, -ik_1 + ik_2 + \eta, \frac{1}{2} - \chi_2 + ik_2; \\ 1 + 2ik_2, \frac{1}{2} - \chi_1 + ik_2 + \eta : 1 \end{matrix} \right) \right] \end{aligned} \tag{3.71} $$

Comparing (3.71) with (3.62) we see that they coincide if we set:

$$ \chi_1 = -\lambda \tag{3.72} $$

$$\chi_2 = -\lambda + \eta \tag{3.73}$$

$$\mathcal{N}_1 = \frac{(4\pi\mu b^{-2})^{-ik_1/2} b^{1/2}}{\sin\pi\left(\frac{1}{2} + ik_1 + \lambda\right)} \frac{\Gamma\left(\frac{1}{2} + \lambda - ik_1\right)}{\Gamma(-2ik_1)} \tag{3.74}$$

$$\mathcal{N}_2 = \frac{1}{\pi}(4\pi\mu b^{-2})^{-ik_2/2} b^{1/2} \sin\pi\left(\frac{1}{2} + ik_2 - \lambda + \eta\right) \frac{\Gamma\left(\frac{1}{2} + \lambda - \eta - ik_2\right)}{\Gamma(-2ik_2)} \tag{3.75}$$

This result leads us to the following conclusion on a role of the exponential operator $e^{\eta b\phi_0}$. Combining (3.69) and (3.70) with lower signes, as indicating in (3.72) and (3.73), and also remembering (3.52) and (3.55) one has

$$\frac{M_3 - M_2}{2\sqrt{\pi\mu}} = b\xi = -b\eta = \sigma_2 - \sigma_3 \tag{3.76}$$

Therefore recalling also that the exponential operator $e^{\eta b\phi_0}$ should correspond to a boundary condition changing operator $\Psi_{\beta_2}^{\sigma_3\sigma_2}$, this result implies that the operator $e^{\eta b\phi_0}$ in the semiclassical limit produces change of the boundary condition given by (3.76).

It is instructive to compare the normalization of the wave functions found here with those used in [181]. For this purpose let us compute the matrix element (3.71) for $\eta \to 0$ and $\chi_1 = \chi_2$. In this limit we obtain:

$$\mathcal{M}_{0k_1k_2}^{\chi_1\chi_1} = \frac{\mathcal{N}_1\mathcal{N}_2^* b^{-1}\Gamma(2ik_1)\Gamma(-2ik_1)}{\Gamma(\frac{1}{2} - \chi_1 + ik_1)\Gamma(\frac{1}{2} - \chi_1 - ik_1)}\delta(k_1 - k_2) + \frac{\mathcal{N}_1\mathcal{N}_2^* b^{-1}\Gamma(2ik_1)\Gamma(-2ik_1)}{\Gamma(\frac{1}{2} - \chi_1 - ik_1)\Gamma(\frac{1}{2} - \chi_1 + ik_1)}\delta(k_1 + k_2) \tag{3.77}$$

For $\chi_1, \chi_2, \mathcal{N}_1, \mathcal{N}_2$, chosen as in (3.72)-(3.75), with $\eta = 0$, expression (3.77) surely coincides with the two-point function (3.63). But note that for

$$\chi_1 = \lambda \tag{3.78}$$

$$\chi_2 = \lambda \tag{3.79}$$

$$\mathcal{N}_1 = (4\pi\mu b^{-2})^{-ik_1/2} b^{1/2} \frac{\Gamma\left(\frac{1}{2} - \lambda - ik_1\right)}{\Gamma(-2ik_1)} \tag{3.80}$$

$$\mathcal{N}_2 = (4\pi\mu b^{-2})^{-ik_2/2} b^{1/2} \frac{\Gamma\left(\frac{1}{2} - \lambda - ik_2\right)}{\Gamma(-2ik_2)} \tag{3.81}$$

expression (3.77) again coincides with the two-point function (3.63). This was established in [181].

This shows that passing from the one branch of the square root to another introduces additional sine factors in the normalization of the wave functions in a way to keep unchanged the two-point functions.

3.5 Conclusion

We discussed in this chapter semiclassical properties of the boundary three-point functions. We found perfect agreement with the corresponding quantum mechanical calculations. The matching of the calculations required to consider the negative branch in the branched correspondence of the classical and quantum parameters. We show that passing from one branch to another leads to the change in the normalization of the wave functions. We also found the flip of the boundary conditions induced by the exponential operators in the minisuperspace limit.

3.6 Double Gamma and double Sine functions

Here we review double Gamma $\Gamma_b(x)$ and double Sine $S_b(x)$ functions [185, 186].

$\Gamma_b(x)$ can be defined by means of the integral representation

$$\log \Gamma_b(x) = \int_0^\infty \frac{dt}{t}\left[\frac{e^{-xt} - e^{-Qt/2}}{(1-e^{-bt})(1-e^{-t/b})} - \frac{(Q-2x)^2}{8e^t} - \frac{Q-2x}{t}\right]. \tag{3.82}$$

It has the property:

$$\Gamma_b(x+b) = \sqrt{2\pi} b^{bx-\frac{1}{2}} \Gamma^{-1}(bx)\Gamma_b(x) \tag{3.83}$$

The double Sine function $S_b(x)$ may be defined in term of $\Gamma_b(x)$ as

$$S_b(x) = \frac{\Gamma_b(x)}{\Gamma_b(Q-x)}. \tag{3.84}$$

It has an integral representation:

$$\log S_b(x) = \int_0^\infty \frac{dt}{t}\left(\frac{\sinh t(Q-2x)}{2\sinh bt \sinh b^{-1}t} - \frac{Q-2x}{2t}\right). \tag{3.85}$$

and the properties:

$$S_b(x+b) = 2\sin(\pi b x) S_b(x) \tag{3.86}$$

$$S_b(x+1/b) = 2\sin(\pi x/b) S_b(x) \tag{3.87}$$

For $b \to 0$ the double Gamma $\Gamma_b(x)$ and double Sine $S_b(x)$ functions have the asymptotic behaviour [170]:

$$S_b(bx) \to (2\pi b^2)^{x-\frac{1}{2}}\Gamma(x) \tag{3.88}$$

$$S_b\left(\frac{1}{2b} + bx\right) \to 2^{x-\frac{1}{2}} \tag{3.89}$$

$$S_b\left(\frac{1}{b} + bx\right) \to \frac{2\pi(2\pi b^2)^{x-\frac{1}{2}}}{\Gamma(1-x)} \tag{3.90}$$

$$\Gamma_b(bx) \to (2\pi b^3)^{\frac{1}{2}(x-\frac{1}{2})}\Gamma(x) \tag{3.91}$$

$$\Gamma_b(Q-bx) \to \sqrt{2\pi}(2\pi b)^{\frac{1}{2}(\frac{1}{2}-x)} \tag{3.92}$$

3.7 Meijer G-function

The Meijer G-function can be defined via the integral [192]:

$$G_{p,q}^{m,n}\left(x\left|\begin{array}{c} a_1,\ldots,a_p \\ b_1,\ldots,b_q \end{array}\right.\right) = \frac{1}{2\pi i}\int \frac{\prod_{j=1}^{m}\Gamma(b_j-s)\prod_{j=1}^{n}\Gamma(1-a_j+s)}{\prod_{j=m+1}^{q}\Gamma(1-b_j+s)\prod_{j=n+1}^{p}\Gamma(a_j-s)}x^s ds \tag{3.93}$$

In this paper we will consider the $G_{3,3}^{3,2}$ function. It admits the decomposition [192]:

$$\begin{aligned} G_{3,3}^{3,2}\left(x\left|\begin{array}{c} a_1,a_2,a_3 \\ b_1,b_2,b_3 \end{array}\right.\right) = \\ \frac{\Gamma(a_1-a_2)\Gamma(1+b_1-a_1)\Gamma(1+b_2-a_1)\Gamma(1+b_3-a_1)}{\Gamma(1+a_3-a_1)}x^{a_1-1} \\ \times {}_3F_2\left(\begin{array}{c} 1+b_1-a_1,1+b_2-a_1,1+b_3-a_1 \\ 1+a_2-a_1,1+a_3-a_1;\, x^{-1} \end{array}\right) + \\ \frac{\Gamma(a_2-a_1)\Gamma(1+b_1-a_2)\Gamma(1+b_2-a_2)\Gamma(1+b_3-a_2)}{\Gamma(1+a_3-a_2)}x^{a_2-1} \\ \times {}_3F_2\left(\begin{array}{c} 1+b_1-a_2,1+b_2-a_2,1+b_3-a_2 \\ 1+a_1-a_2,1+a_3-a_2;\, x^{-1} \end{array}\right) \end{aligned} \tag{3.94}$$

Here ${}_3F_2$ is the generalized hypergeometric function:

$${}_3F_2\left(\begin{array}{c} a,b,c; \\ d,e:x \end{array}\right) = \sum_{n=0}^{\infty}\frac{(a)_n(b)_n(c)_n}{(d)_n(e)_n}\frac{x^n}{n!}$$

where

$$(a)_n = \frac{\Gamma(a+n)}{\Gamma(a)} \tag{3.95}$$

is the Pochhammer symbol. We will need also the following property of the Meijer G-function:

$$x^{\xi} G^{3,2}_{3,3}\left(x \left| \begin{array}{c} a_1, a_2, a_3 \\ b_1, b_2, b_3 \end{array} \right. \right) = G^{3,2}_{3,3}\left(x \left| \begin{array}{c} a_1+\xi, a_2+\xi, a_3+\xi \\ b_1+\xi, b_2+\xi, b_3+\xi \end{array} \right. \right) \tag{3.96}$$

3.8 ${}_3F_2$ and ${}_2F_1$ hypergeometric functions with unit argument

The ${}_3F_2$ function with the unit argument satisfies the identities [187–189]

$$\begin{aligned} {}_3F_2\left(\begin{array}{c} a, b, c; \\ d, e : 1 \end{array} \right) &= \frac{\Gamma(1-a)\Gamma(d)\Gamma(e)\Gamma(c-b)}{\Gamma(e-b)\Gamma(d-b)\Gamma(1+b-a)\Gamma(c)} {}_3F_2\left(\begin{array}{c} b, 1+b-d, 1+b-e; \\ 1+b-c, 1+b-a : 1 \end{array} \right) \\ &+ \frac{\Gamma(1-a)\Gamma(d)\Gamma(e)\Gamma(b-c)}{\Gamma(e-c)\Gamma(d-c)\Gamma(1+c-a)\Gamma(b)} {}_3F_2\left(\begin{array}{c} c, 1+c-e, 1+c-d; \\ 1+c-b, 1+c-a : 1 \end{array} \right) \end{aligned} \tag{3.97}$$

$${}_3F_2\left(\begin{array}{c} a, b, c; \\ d, e : 1 \end{array} \right) = \frac{\Gamma(d)\Gamma(d+e-a-b-c)}{\Gamma(d-a)\Gamma(d+e-b-c)} {}_3F_2\left(\begin{array}{c} e-c, e-b, a; \\ d+e-b-c, e : 1 \end{array} \right) \tag{3.98}$$

Note that if one of the “upper" arguments of the ${}_3F_2$ function coincide with one of the “lower" argument it reduces to ${}_2F_1$ function:

$${}_2F_1\left(\begin{array}{c} a, b; \\ c : x \end{array} \right) = \sum_{n=0}^{\infty} \frac{(a)_n (b)_n}{(c)_n} \frac{x^n}{n!}$$

${}_2F_1$ function with unit argument is equal to:

$${}_2F_1\left(\begin{array}{c} a, b; \\ c : 1 \end{array} \right) = \frac{\Gamma(c)\Gamma(c-a-b)}{\Gamma(c-a)\Gamma(c-b)} \tag{3.99}$$

In this chapter we also construct topological defects gluing 2D Liouville field theories with different cosmological constants [206].

Topological defects in the Louville field theory with the same cosmological constants on the both side were constructed almost ten years back in papers [194,195]. In that papers two-point functions in the presence of defects were computed using the Cardy-Lewellen equation for defects. It was derived that there exist two families of defects, discrete, with one-dimensional world-volume, and continuous, with two-dimensional world-volume. Later for the continuous family of defects also the Lagrangian description was suggested in [196]. It was shown in [173] that this Lagrangian description is in agreement with the found in [194,195] defect two-point function using various semiclassical limits.

Here we generalize above mentioned calculations to the case of the different cosmological constants. First we elaborate to this case the Cardy-Lewellen relation for defects. We find that in fact the two-point functions are given by the same functions as before but which get rescaled by the factor $\left(\frac{\mu_2}{\mu_1}\right)^{\frac{-iP}{b}}$, where μ_1 and μ_2 are the cosmological constants, and P is a momentum. Formulae (3.132) and (3.139) are our main result. For the continuous family of defect we also constructed the corresponding Lagrangian and checked via the heavy asymptotic limit that it is in agreement with the two-point function (3.139).

We would like to say that one of the motivations of this research was recently suggested in papers [198,199] the idea to describe the Fractional Quantum Hall effect (FQHE) by the Liuoville field theory, whose cosmological constant should play a role of a chemical potential. On the other hand it is known that in the FQHE one has jump of the chemical potential [200]. We have an impression that our construction which in fact connects two Liouville theories with the different cosmological constants may have an application to the FQHE.

The paper is organized as follows. In section 2 we collect several necessary for us facts on classical and quantum Liouville field theory. In section 3 we generalized and solved Cardy-Lewellen equation for defects to the case of the different cosmological constants. We showed also here that constructed defects indeed map FZZ [201] and ZZ [202] boundary states of the first theory to the linear combinations of the FZZ and ZZ boundary states of the second theory. In section 4 we have written down the Lagrangian for the continuous family of defects. In section 5 we checked, using the heavy asymptotic semiclassical limit, that the two-point function for the continuous family of defects computed in section 3, is in agreement with the

Lagrangian description of section 4.

3.9 Review of Liouville theory

Let us recall some basic facts on classical and quantum Liouville theory.

The action of the Liouville theory is

$$S = \frac{1}{2\pi i} \int \left(\partial\phi\bar{\partial}\phi + \mu\pi e^{2b\phi} \right) d^2z \,. \tag{3.100}$$

Here we use a complex coordinate $z = \tau + i\sigma$, and $d^2z \equiv dz \wedge d\bar{z}$ is the volume form.

The field $\phi(z, \bar{z})$ satisfies the Liouville equation:

$$\partial\bar{\partial}\phi = \pi\mu b e^{2b\phi} \,. \tag{3.101}$$

The general solution to (3.101) can be written in terms of two arbitrary functions $A(z)$ and $B(\bar{z})$:

$$\phi = \frac{1}{2b} \log \left(\frac{1}{\pi\mu b^2} \frac{\partial A(z)\bar{\partial}B(\bar{z})}{(A(z) + B(\bar{z}))^2} \right) \,. \tag{3.102}$$

The solution (3.102) is invariant if one transforms A and B simultaneously by the constant Möbius transformations:

$$A \to \frac{\zeta A + \beta}{\gamma A + \delta}, \qquad B \to \frac{\zeta B - \beta}{-\gamma B + \delta}, \qquad \zeta\delta - \beta\gamma = 1 \,. \tag{3.103}$$

Classical expressions for the holomorphic and anti-holomorphic components of the energy-momentum tensor are

$$T = -(\partial\phi)^2 + b^{-1}\partial^2\phi \,, \tag{3.104}$$

$$\bar{T} = -(\bar{\partial}\phi)^2 + b^{-1}\bar{\partial}^2\phi \,. \tag{3.105}$$

Inserting (3.102) in (3.104) and (3.105) we obtain, that components of the energy-momentum

tensor are given by the Schwarzian derivatives of $A(z)$ and $B(\bar{z})$:

$$T = \{A; z\} = \frac{1}{2b^2}\left[\frac{A'''}{A'} - \frac{3}{2}\frac{(A'')^2}{(A')^2}\right], \tag{3.106}$$

$$\bar{T} = \{B; \bar{z}\} = \frac{1}{2b^2}\left[\frac{B'''}{B'} - \frac{3}{2}\frac{(B'')^2}{(B')^2}\right]. \tag{3.107}$$

The Schwarzian derivative is invariant under a constant Möbius transformation:

$$\left\{\frac{\zeta F + \beta}{\gamma F + \delta}; z\right\} = \{F; z\}, \quad \zeta\delta - \beta\gamma = 1\,. \tag{3.108}$$

Quantum Liouville field theory is a conformal field theory enjoying the Virasoro algebra

$$[L_m, L_n] = (m-n)L_{m+n} + \frac{c_L}{12}(n^3 - n)\delta_{n,-m}\,, \tag{3.109}$$

with the central charge

$$c_L = 1 + 6Q^2\,. \tag{3.110}$$

Two-point functions of Liouville theory are given by the function $S(\alpha)$ (3.112):

$$\langle V_\alpha(z_1, \bar{z}_1) V_\alpha(z_2, \bar{z}_2)\rangle = \frac{S(\alpha)}{(z_1 - z_2)^{2\Delta_\alpha}(\bar{z}_1 - \bar{z}_2)^{2\Delta_\alpha}}\,, \tag{3.111}$$

$$S(\alpha) = \frac{(\pi\mu\gamma(b^2))^{b^{-1}(Q-2\alpha)}}{b^2}\frac{\Gamma(1 - b(Q-2\alpha))\Gamma(-b^{-1}(Q-2\alpha))}{\Gamma(b(Q-2\alpha))\Gamma(1 + b^{-1}(Q-2\alpha))}\,. \tag{3.112}$$

The spectrum of the Liouville theory has the form

$$\mathcal{H} = \int_0^\infty dP\; R_{\frac{Q}{2}+iP} \otimes R_{\frac{Q}{2}+iP}\,, \tag{3.113}$$

where R_α is the highest weight representation with respect to the Virasoro algebra.

3.10 Two-point function with Defect producing jump in cosmological constant

As we mentioned before the aim of this work is to construct topological defect gluing two Liouville theories with different cosmological constants. For this purpose we will use bootstrap programm. In fact the bootstrap programm for topological defects with the same theory on both sides was developed in [194, 195, 203]. Here we will reconsider it, taking into account the necessary changes caused by the presence of two different cosmological constants on the different sides of the defects.

We consider a topological defect mapping the Hilbert space of the first theory on the Hilbert space of the second theory $X : H_{(1)} \to H_{(2)}$ in the form:

$$X = \int_{\frac{Q}{2}+i\mathbb{R}} d\alpha \, \mathcal{D}(\alpha) \, \mathbb{P}^{\alpha} \,, \tag{3.114}$$

where $\mathbb{P}^{\alpha}$ are maps:

$$\mathbb{P}^{\alpha} = \sum_{N,M} (|\alpha, N\rangle_{(2)} \otimes \overline{|\alpha, M\rangle}_{(2)})(\langle_{(1)}\alpha, N| \otimes_{(1)} \overline{\langle\alpha, M|}) \,. \tag{3.115}$$

Here $|\alpha, N\rangle_{(i)}$ and $\overline{|\alpha, M\rangle}_{(i)}$, $i = 1, 2$ are vectors of orthonormal bases of left and right copy of R_{α} of the first and second theory respectively. Two-point functions with a defect X insertion can be written as

$$\langle V^{(2)}_{\alpha}(z_1, \bar{z}_1) X V^{(1)}_{\alpha}(z_2, \bar{z}_2)\rangle = \frac{D^{\alpha}}{(z_1 - z_2)^{2\Delta_{\alpha}} (\bar{z}_1 - \bar{z}_2)^{2\Delta_{\alpha}}} \,. \tag{3.116}$$

where

$$D^{\alpha} = \mathcal{D}(\alpha) S^{(1)}(\alpha) \tag{3.117}$$

Consider the following four-point function with the defects insertions:

$$\langle V^{(2)}_{-b/2}(z_1, \bar{z}_1) V^{(2)}_{\alpha}(z_2, \bar{z}_2) X V^{(1)}_{\alpha}(z_3, \bar{z}_3) V^{(1)}_{-b/2}(z_4, \bar{z}_4) X^{\dagger}\rangle \,. \tag{3.118}$$

One can compute (3.118) in two pictures. In the first picture at the beginning we use the OPE

$$V_{\alpha}^{(i)}V_{-b/2}^{(i)} \sim C_{-b/2,\alpha}^{(i)\,\alpha-b/2}V_{\alpha-b/2}^{(i)} + C_{-b/2,\alpha}^{(i)\,\alpha+b/2}V_{\alpha+b/2}^{(i)}\,. \quad i=1,2 \tag{3.119}$$

and then (3.116) for the fields produced in this process. This results in

$$\sum_{\pm} D^{\alpha\pm b/2}D^{0}C_{-b/2,\alpha}^{(1)\,\alpha\pm b/2}C_{-b/2,\alpha}^{(2)\,\alpha\pm b/2}\left(\mathcal{F}_{\alpha\pm b/2}\begin{bmatrix}\alpha & \alpha\\ -b/2 & -b/2\end{bmatrix}\right)^{2}, \tag{3.120}$$

where $\mathcal{F}_{\alpha\pm b/2}\begin{bmatrix}\alpha & \alpha\\ -b/2 & -b/2\end{bmatrix}$ is so called conformal block giving contribution of the descendant fields in the OPE (3.119). It appears squared since it is separately produced by the left and right modes.

In the second picture we move the field $V_{-b/2}^{(2)}(z_1,\bar{z}_1)$ to the most right position:

$$\langle V_{\alpha}^{(2)}(z_2,\bar{z}_2)XV_{\alpha}^{(1)}(z_3,\bar{z}_3)V_{-b/2}^{(1)}(z_4,\bar{z}_4)X^{\dagger}V_{-b/2}^{(2)}(z_1,\bar{z}_1)\rangle \tag{3.121}$$

and then use twice (3.116) resulting in

$$D^{\alpha}D^{-b/2}\left(\mathcal{F}_{0}\begin{bmatrix}\alpha & -b/2\\ \alpha & -b/2\end{bmatrix}\right)^{2} + \cdots\,. \tag{3.122}$$

Using the fusing matrix:

$$\mathcal{F}_{\alpha\pm b/2}\begin{bmatrix}\alpha & \alpha\\ -b/2 & -b/2\end{bmatrix} = F_{\alpha\pm b/20}\begin{bmatrix}-b/2 & -b/2\\ \alpha & \alpha\end{bmatrix}\mathcal{F}_{0}\begin{bmatrix}\alpha & -b/2\\ \alpha & -b/2\end{bmatrix} + \cdots\,, \tag{3.123}$$

we obtain

$$\sum_{\pm} D^{0}D^{\alpha\pm b/2}C_{-b/2,\alpha}^{\alpha\pm b/2(1)}C_{-b/2,\alpha}^{\alpha\pm b/2(2)}\left(F_{\alpha\pm b/20}\begin{bmatrix}-b/2 & -b/2\\ \alpha & \alpha\end{bmatrix}\right)^{2} = D^{\alpha}D^{-b/2}\,. \tag{3.124}$$

This is the Cardy-Lewellen cluster condition for defects.

Let us use the relation [195]:

$$C^{(i)\,\alpha_3}_{\alpha_1,\alpha_2} F_{\alpha_3,0}\left[\begin{array}{cc}\alpha_1 & \alpha_1\\ \alpha_2 & \alpha_2\end{array}\right] = W^{(i)}(0)\frac{W^{(i)}(\alpha_3)}{W^{(i)}(\alpha_1)W^{(i)}(\alpha_2)}\,, \quad i=1,2 \tag{3.125}$$

where $W^{(i)}(\alpha)$ is the ZZ function [202]:

$$W^{(i)}(\alpha) = -\frac{2^{3/4}e^{3i\pi/2}(\pi\mu_i\gamma(b^2))^{-\frac{(Q-2\alpha)}{2b}}\pi(Q-2\alpha)}{\Gamma(1-b(Q-2\alpha))\Gamma(1-b^{-1}(Q-2\alpha))}\,, \quad i=1,2 \tag{3.126}$$

Define $\Psi(\alpha)$ by the equation.

$$\frac{D^\alpha}{D^0} = \Psi(\alpha)\frac{W^{(1)}(0)W^{(2)}(0)}{W^{(1)}(\alpha)W^{(2)}(\alpha)}\,. \tag{3.127}$$

For $\Psi(\alpha)$ the equation (3.124) takes the form

$$\Psi(\alpha)\Psi(-b/2) = \Psi(\alpha-b/2)+\Psi(\alpha+b/2)\,, \tag{3.128}$$

The solution of the equation (3.128) is

$$\Psi_{m,n}(\alpha) = \frac{\sin(\pi m b^{-1}(2\alpha-Q))\sin(\pi n b(2\alpha-Q))}{\sin(\pi m b^{-1}Q)\sin(\pi n b Q)}\,, \tag{3.129}$$

Using (3.127) we obtain for the defect two-point function

$$D_{m,n}(\alpha) = \frac{\sin(\pi m b^{-1}(2\alpha-Q))\sin(\pi n b(2\alpha-Q))}{W^{(1)}(\alpha)W^{(2)}(\alpha)}\,. \tag{3.130}$$

And finally dividing on $S^{(1)}(\alpha)$:

$$S^{(1)}(\alpha) = \frac{(\pi\mu_1\gamma(b^2))^{b^{-1}(Q-2\alpha)}}{b^2}\frac{\Gamma(1-b(Q-2\alpha))\Gamma(-b^{-1}(Q-2\alpha))}{\Gamma(b(Q-2\alpha))\Gamma(1+b^{-1}(Q-2\alpha))}\,. \tag{3.131}$$

we get

$$\mathcal{D}_{m,n}(\alpha) = \left(\frac{\mu_2}{\mu_1}\right)^{\frac{Q-2\alpha}{2b}}\frac{\sin(\pi m b^{-1}(2\alpha-Q))\sin(\pi n b(2\alpha-Q))}{\sin\pi b^{-1}(2\alpha-Q)\sin\pi b(2\alpha-Q)}\,. \tag{3.132}$$

But this is not the end of the story.

Assume that we have a family of defects parameterized by κ. In this case $D^{-b/2}/D^0$, which is two-point function of the degenerate field $V_{-b/2}$ in the presence of defect, will be a function $A(\kappa, b)$ of κ and b. Substituting

$$A = \frac{D^{-b/2}}{D^0} \tag{3.133}$$

and

$$D^\alpha = \frac{\Lambda^\alpha}{W^{(1)}(\alpha)W^{(2)}(\alpha)}\,. \tag{3.134}$$

in (3.128) we obtain a linear equation for $\Lambda(\alpha)$:

$$\frac{W^{(1)}(-b/2)W^{(2)}(-b/2)}{W^{(1)}(0)W^{(2)}(0)}A\Lambda(\alpha) = \Lambda(\alpha - b/2) + \Lambda(\alpha + b/2) \tag{3.135}$$

The solution of (3.135) is indeed one-parametric family,

$$\Lambda_s(\alpha) = \cosh(2\pi s(2\alpha - Q))\,, \tag{3.136}$$

with parameter s related to A by

$$2\cosh 2\pi bs = A\frac{W^{(1)}(-b/2)W^{(2)}(-b/2)}{W^{(1)}(0)W^{(2)}(0)}\,. \tag{3.137}$$

Substituting (3.136) in (3.134) we obtain for $D_s(\alpha)$ and $\mathcal{D}_s(\alpha)$ respectively

$$D_s(\alpha) = -\frac{2^{1/2}i\cosh(2\pi s(2\alpha - Q))}{W^{(1)}(\alpha)W^{(2)}(\alpha)}\,. \tag{3.138}$$

$$\mathcal{D}_s(\alpha) = \left(\frac{\mu_2}{\mu_1}\right)^{\frac{Q-2\alpha}{2b}} \frac{\cosh(2\pi s(2\alpha - Q))}{2\sin\pi b^{-1}(2\alpha - Q)\sin\pi b(2\alpha - Q)}\,. \tag{3.139}$$

So we have two groups of topological defects:

$$X_s = \int_{\frac{Q}{2}+i\mathbb{R}} d\alpha\, \mathcal{D}_s(\alpha)\,\mathbb{P}^\alpha\,, \tag{3.140}$$

$$X_{m,n} = \int_{\frac{Q}{2}+i\mathbb{R}} d\alpha\, \mathcal{D}_{m,n}(\alpha)\, \mathbb{P}^{\alpha}\,, \tag{3.141}$$

Recall that in each copy of the Liouville field theory one has two groups of boundary states, FZZ states [201]:

$$|s\rangle^{(i)} = \int_{\frac{Q}{2}+i\mathbb{R}} B_s^{(i)}(\alpha)|\alpha\rangle\rangle_{(i)} d\alpha \tag{3.142}$$

and ZZ states [202]:

$$|m,n\rangle^{(i)} = \int_{\frac{Q}{2}+i\mathbb{R}} B_{m,n}^{(i)}(\alpha)|\alpha\rangle\rangle_{(i)} d\alpha \tag{3.143}$$

where $|\alpha\rangle\rangle_{(i)}$ are the Ishibashi states satisfying $L_n^{(i)} + \bar{L}_{-n}^{(i)} = 0$, and

$$B_s^{(i)}(\alpha) = -\frac{2^{1/2} i \cosh(2\pi s(2\alpha - Q))}{W^{(i)}(\alpha)}\,. \quad i = 1,2 \tag{3.144}$$

$$B_{m,n}^{(i)}(\alpha) = \frac{\sin(\pi m b^{-1}(2\alpha - Q))\sin(\pi n b(2\alpha - Q))}{W^{(i)}(\alpha)}\,. \quad i = 1,2 \tag{3.145}$$

Using the identities:

$$\sinh(2\pi n b P)\sinh(2\pi n' b P) = \sum_{l=0}^{\min(n,n')-1} \sinh(2\pi b P)\sinh(2\pi b(n+n'-2l-1)P) \tag{3.146}$$

and

$$\frac{\sinh(2\pi n b P)}{\sinh(2\pi b P)} = \sum_{l=1-n,2}^{n-1} \exp(2\pi l b P) \tag{3.147}$$

one obtains that fusion of the defects (3.140), (3.141) with boundary state of the first theory producing linear combination of the boundary states of the second theory:

$$X_{m,n}|m',n'\rangle^{(1)} = \sum_{l=0}^{\min(n,n')-1} \sum_{k=0}^{\min(m,m')-1} |m+m'-2k-1, n+n'-2l-1\rangle^{(2)} \tag{3.148}$$

$$X_{m,n}|s\rangle^{(1)} = \sum_{l=1-n,2}^{n-1} \sum_{k=1-m,2}^{m-1} |s + i(k/b + lb)/2\rangle^{(2)} \tag{3.149}$$

$$X_s|m,n\rangle^{(1)} = \sum_{l=1-n,2}^{n-1} \sum_{k=1-m,2}^{m-1} |s+i(k/b+lb)/2\rangle^{(2)} \tag{3.150}$$

as it is indeed expected.

3.11 Lagrangian of the Liouville theory with defect X_s

We propose the following action for the Liouville theories with the different cosmological constants connected by the topological defect:

$$\begin{aligned} S^{\text{top-def}} &= \frac{1}{2\pi i}\int_{\Sigma_1}\left(\partial\phi_1\bar\partial\phi_1+\mu_1\pi e^{2b\phi_1}\right)d^2z+\frac{1}{2\pi i}\int_{\Sigma_2}\left(\partial\phi_2\bar\partial\phi_2+\mu_2\pi e^{2b\phi_2}\right)d^2z \\ &+\int_{\partial\Sigma_1}\left[-\frac{1}{2\pi}\phi_2\partial_\tau\phi_1+\frac{1}{2\pi}\Lambda\partial_\tau(\phi_1-\phi_2)+\frac{\sqrt{\mu_1\mu_2}}{2}e^{(\phi_1+\phi_2-\Lambda)b}\right. \\ &\left.-\frac{1}{\pi b^2}e^{\Lambda b}\left(\frac{1}{2}\sqrt{\frac{\mu_1}{\mu_2}}e^{(\phi_1-\phi_2)b}+\frac{1}{2}\sqrt{\frac{\mu_2}{\mu_1}}e^{-(\phi_1-\phi_2)b}-\kappa\right)\right]\frac{d\tau}{i}\,. \end{aligned} \tag{3.151}$$

Here Σ_1 is the upper half-plane $\sigma = \text{Im}z \geq 0$ and Σ_2 is the lower half-plane $\sigma = \text{Im}z \leq 0$. The defect is located along their common boundary, which is the real axis $\sigma = 0$ parameterized by $\tau = \text{Re}z$. Note that $\Lambda(\tau)$ here is an additional field associated with the defect itself. In fact this is the Lagrangian proposed in [196] and considered in detail in [173], but which is modified in a way to take into account that now $\mu_1 \neq \mu_2$, and which becomes the old one for $\mu_1 = \mu_2$.

The action (3.151) yields the following defect equations of motion at $\sigma = 0$:

$$\begin{aligned} &\frac{1}{2\pi}(\partial-\bar\partial)\phi_1+\frac{1}{2\pi}\partial_\tau\phi_2-\frac{1}{2\pi}\partial_\tau\Lambda+\frac{\sqrt{\mu_1\mu_2}b}{2}e^{(\phi_1+\phi_2-\Lambda)b} \\ &-\frac{1}{\pi b}e^{\Lambda b}\left(\frac{1}{2}\sqrt{\frac{\mu_1}{\mu_2}}e^{(\phi_1-\phi_2)b}-\frac{1}{2}\sqrt{\frac{\mu_2}{\mu_1}}e^{-(\phi_1-\phi_2)b}\right)=0\,, \end{aligned} \tag{3.152}$$

$$\begin{aligned} &-\frac{1}{2\pi}(\partial-\bar\partial)\phi_2-\frac{1}{2\pi}\partial_\tau\phi_1+\frac{1}{2\pi}\partial_\tau\Lambda+\frac{\sqrt{\mu_1\mu_2}b}{2}e^{(\phi_1+\phi_2-\Lambda)b} \\ &+\frac{1}{\pi b}e^{\Lambda b}\left(\frac{1}{2}\sqrt{\frac{\mu_1}{\mu_2}}e^{(\phi_1-\phi_2)b}-\frac{1}{2}\sqrt{\frac{\mu_2}{\mu_1}}e^{-(\phi_1-\phi_2)b}\right)=0\,, \end{aligned} \tag{3.153}$$

$$\frac{1}{2\pi}\partial_\tau(\phi_1-\phi_2)-\frac{\sqrt{\mu_1\mu_2}b}{2}e^{(\phi_1+\phi_2-\Lambda)b}-\frac{1}{\pi b}e^{\Lambda b}\left(\frac{1}{2}\sqrt{\frac{\mu_1}{\mu_2}}e^{(\phi_1-\phi_2)b}+\frac{1}{2}\sqrt{\frac{\mu_2}{\mu_1}}e^{-(\phi_1-\phi_2)b}-\kappa\right)=0\,. \tag{3.154}$$

The last equation is derived calculating variation by the Λ.

Using that $\partial_\tau=\partial+\bar{\partial}$ and forming various linear combinations of equations (3.152)-(3.154) we can bring them to the form:

$$\bar{\partial}(\phi_1-\phi_2)=\pi\sqrt{\mu_1\mu_2}be^{b(\phi_1+\phi_2)}e^{-\Lambda b}\,, \tag{3.155}$$

$$\partial(\phi_1-\phi_2)=\frac{2}{b}e^{\Lambda b}\left(\frac{1}{2}\sqrt{\frac{\mu_1}{\mu_2}}e^{(\phi_1-\phi_2)b}+\frac{1}{2}\sqrt{\frac{\mu_2}{\mu_1}}e^{-(\phi_1-\phi_2)b}-\kappa\right)\,. \tag{3.156}$$

$$\partial(\phi_1+\phi_2)-\partial_\tau\Lambda=\frac{2}{b}e^{\Lambda b}\left(\frac{1}{2}\sqrt{\frac{\mu_1}{\mu_2}}e^{(\phi_1-\phi_2)b}-\frac{1}{2}\sqrt{\frac{\mu_2}{\mu_1}}e^{-(\phi_1-\phi_2)b}\right)\,. \tag{3.157}$$

Let us require, that Λ is restriction to the real axis of a holomorphic field

$$\bar{\partial}\Lambda=0\,. \tag{3.158}$$

This condition allows to rewrite (3.157) in the form

$$\partial(\phi_1+\phi_2-\Lambda)=\frac{2}{b}e^{\Lambda b}\left(\frac{1}{2}\sqrt{\frac{\mu_1}{\mu_2}}e^{(\phi_1-\phi_2)b}-\frac{1}{2}\sqrt{\frac{\mu_2}{\mu_1}}e^{-(\phi_1-\phi_2)b}\right)\,. \tag{3.159}$$

We can check that the system of the defect equations of motion (3.155)-(3.159) guarantees that both components of the energy-momentum tensor are continuous across the defects and therefore describes topological defects:

$$-(\partial\phi_1)^2+b^{-1}\partial^2\phi_1=-(\partial\phi_2)^2+b^{-1}\partial^2\phi_2\,, \tag{3.160}$$

$$-(\bar{\partial}\phi_1)^2+b^{-1}\bar{\partial}^2\phi_1=-(\bar{\partial}\phi_2)^2+b^{-1}\bar{\partial}^2\phi_2\,. \tag{3.161}$$

Therefore, remembering that the solution (3.102) is invariant under the transformation (3.103), and that the chiral components of the energy-momentum tensor are invariant under the

Möbius transformation (3.108), we can without loosing generality look for a solution in the form:

$$\phi_1 = \frac{1}{2b}\log\left(\frac{1}{\pi\mu_1 b^2}\frac{\partial A\bar{\partial}B}{(A+B)^2}\right), \tag{3.162}$$

$$\phi_2 = \frac{1}{2b}\log\left(\frac{1}{\pi\mu_2 b^2}\frac{\partial C\bar{\partial}B}{(C+B)^2}\right), \tag{3.163}$$

where

$$C = \frac{\zeta A+\beta}{\gamma A+\delta}. \tag{3.164}$$

Substituting (3.162) and (3.163) in (3.155) we find that it is satisfied with

$$e^{-\Lambda b} = \frac{A-C}{\sqrt{\partial A\partial C}}. \tag{3.165}$$

Since A and C are holomorphic functions, Λ is holomorphic as well, as it is stated in (3.158).

It is straightforward to check that (3.159) is satisfied as well with ϕ_1, ϕ_2 and Λ given by (3.162), (3.163) and (3.165) respectively. And finally inserting (3.162), (3.163) and (3.165) in (3.156) we see that it is also fulfilled with

$$\kappa = \frac{\zeta+\delta}{2}. \tag{3.166}$$

3.12 X_s defects in the heavy asymptotic limit

In this section we link the continuous family of defects constructed in section 3 with the Lagrangian constructed in the previous section. For this purpose we will use the heavy semiclassical asymptotic limit. Recall that in all semiclassical limits, one takes $b \to 0$ and the action blows to infinity like b^{-2}. It is known [204] that in the heavy asymptotic limit, when one additionally scales $\alpha = \frac{\eta}{b}$ and $\Delta_\alpha = \eta(1-\eta)/b^2$, correlation functions are given by the exponential of the regularized action with the inserted fields computed on solution with the logarithmic singularities around the insertion points. The regularization is necessary to keep the action finite, since singularities of the solution may render it divergent. So we should

compute the heavy asymptotic limit of the defect two-point function (3.144) and compare with the regularized defect action computed on the solutions with two singularities.

First we compute the heavy asymptotic limit of the defect two-point function (3.144). As we said before, in the heavy asymptotic limit we set $\alpha = \frac{\eta}{b}$, and also $s = \frac{\sigma}{b}$. Denote $\lambda_i = \pi\mu_i b^2$, $i = 1, 2$. Performing the same steps as in [173] we can write in the heavy asymptotic limit [1]

$$\langle V_\alpha(z_1, \bar{z}_1) X V_\alpha(z_2, \bar{z}_2)\rangle \sim \exp\left(-S^{\rm def}\right) , \tag{3.167}$$

where

$$b^2 S^{\rm def} = 4\eta(1-\eta)\log|z_1 - z_2| - \left(\frac{1}{2} - \eta\right)\log\lambda_1 - \left(\frac{1}{2} - \eta\right)\log\lambda_2 - \tag{3.168}$$
$$(4\eta - 2)\log(1 - 2\eta) + (4\eta - 2) - 2\pi|\sigma|(1 - 2\eta) .$$

Here we dropped all the terms in the exponential which blows slower then b^{-2}. As it is explained in [173] the required classical solution with two singular points can be built taking:

$$A(z) = e^{2\nu_1}(z - z_1)^{2\eta-1}(z - z_2)^{1-2\eta} . \tag{3.169}$$

$$B(\bar{z}) = -(\bar{z} - \bar{z}_1)^{1-2\eta}(\bar{z} - \bar{z}_2)^{2\eta-1} , \tag{3.170}$$

$$C(z) = e^{2\nu_2}(z - z_1)^{2\eta-1}(z - z_2)^{1-2\eta} = e^{2(\nu_2-\nu_1)}A(z) , \tag{3.171}$$

Eq. (3.166) implies

$$\kappa = \cosh(\nu_2 - \nu_1) . \tag{3.172}$$

Inserting (3.169)-(3.171) in (3.162 and (3.163) we obtain

$$\varphi_1 = -\log\lambda_1 + 2\log(1 - 2\eta) \tag{3.173}$$
$$-2\log\left(\frac{e^{\nu_1}|z - z_1|^{2\eta}|z - z_2|^{2-2\eta}}{|z_1 - z_2|} - \frac{e^{-\nu_1}|z - z_1|^{2-2\eta}|z - z_2|^{2\eta}}{|z_1 - z_2|}\right) ,$$

[1] Here we consider only the case of real η and real solutions of the Liouville equation. So we do not write here imaginary terms, which one has in [173].

$$\varphi_2 = -\log\lambda_2 + 2\log(1-2\eta) \qquad (3.174)$$
$$-2\log\left(-\frac{e^{\nu_2}|z-z_1|^{2\eta}|z-z_2|^{2-2\eta}}{|z_1-z_2|} + \frac{e^{-\nu_2}|z-z_1|^{2-2\eta}|z-z_2|^{2\eta}}{|z_1-z_2|}\right) .$$

Here $\varphi_i = 2b\phi_i$, $i = 1, 2$.

The leading terms of φ_1 around z_1 are

$$\varphi_1 \to -4\eta\log|z-z_1| + X_1 \,, \qquad (3.175)$$

where

$$X_1 = -\log\lambda_1 + 2\log(1-2\eta) - (2-4\eta)\log|z_1-z_2| - 2\nu_1 \,. \qquad (3.176)$$

The leading terms of φ_2 around z_2 similarly are

$$\varphi_2 \to -4\eta\log|z-z_2| + X_2 \,, \qquad (3.177)$$

where

$$X_2 = -\log\lambda_2 + 2\log(1-2\eta) - (2-4\eta)\log|z_1-z_2| + 2\nu_2 \,. \qquad (3.178)$$

Since we consider here only insertions of the bulk field, and do not consider insertions of the defect or boundary fields, following the same steps as in [204] the regularized action, with n fields inserted in the upper half-plane, and m fields inserted in the lower half-plane, takes

the form:

$$
\begin{aligned}
b^2 S^{\text{top}-\text{def}} &= \frac{1}{8\pi i}\int_{\Sigma_1^R - \cup_i d_i} \left(\partial\varphi_1\bar{\partial}\varphi_1 + 4\lambda_1 e^{\varphi_1}\right) d^2z \\
- &\sum_{i=1}^{n}\left(\frac{\eta_i}{2\pi}\oint_{\partial d_i}\varphi_1 d\theta_i + 2\eta_i^2\log\epsilon_i\right) + \frac{1}{2\pi}\int_{s_{R1}}\varphi_1 d\theta + \log R \\
+ &\frac{1}{8\pi i}\int_{\Sigma_2^R - \cup_j d_j} \left(\partial\varphi_2\bar{\partial}\varphi_2 + 4\lambda_2 e^{\varphi_2}\right) d^2z \\
- &\sum_{j=n+1}^{n+m}\left(\frac{\eta_j}{2\pi}\oint_{\partial d_j}\varphi_2 d\theta_j + 2\eta_j^2\log\epsilon_j\right) + \frac{1}{2\pi}\int_{s_{R2}}\varphi_2 d\theta + \log R \\
+ &\int_{-R}^{R}\left[-\frac{1}{8\pi}\varphi_2\partial_\tau\varphi_1 + \frac{1}{8\pi}\tilde{\Lambda}\partial_\tau(\varphi_1-\varphi_2) + \frac{\sqrt{\lambda_1\lambda_2}}{2\pi}e^{(\varphi_1+\varphi_2-\tilde{\Lambda})/2}\right. \\
&\left. -\frac{1}{\pi}e^{\tilde{\Lambda}/2}\left(\frac{1}{2}\sqrt{\frac{\lambda_1}{\lambda_2}}e^{(\varphi_1-\varphi_2)/2} + \frac{1}{2}\sqrt{\frac{\lambda_2}{\lambda_1}}e^{-(\varphi_1-\varphi_2)/2} - \kappa\right)\right]\frac{d\tau}{i}\,.
\end{aligned}
\tag{3.179}
$$

where $\tilde{\Lambda} = 2b\Lambda$, Σ_i^R is a half-disc of the radius R and s_{Ri} is a semicircle of the radius R in the half-plane Σ_i, $i = 1, 2$. The two-point function in question is given by the exponential of the regularized action with one field inserted in the upper half-plane, and with one field inserted in the lower half-plane, with $\eta_1 = \eta_2 = \eta$, calculated on solution (3.173) and (3.174). To calculate it, we will use, that it satisfies the equation [173, 204, 205]:

$$
b^2\frac{\partial S_{\text{cl}}^{\text{top}-\text{def}}}{\partial\eta} = -X_1 - X_2\,. \tag{3.180}
$$

Inserting (3.176) and (3.178) in (3.180) one obtains

$$
b^2\frac{\partial S_{\text{cl}}^{\text{top}-\text{def}}}{\partial\eta} = \log\lambda_1 + \log\lambda_2 - 4\log(1-2\eta) + (4-8\eta)\log|z_1-z_2| + 2(\nu_1-\nu_2)\,. \tag{3.181}
$$

Integrating equation (3.181) we obtain:

$$
\begin{aligned}
b^2 S^{\text{top}-\text{def}} &= 4\eta(1-\eta)\log|z_1-z_2| \\
&+\eta\log\lambda_1 + \eta\log\lambda_2 - (4\eta-2)\log(1-2\eta) + 4\eta + 2\eta(\nu_1-\nu_2) + C\,,
\end{aligned}
\tag{3.182}
$$

where C is a constant.

To fix the constant term we can directly compute the action (3.179) for the solution (3.173)-(3.174) with $\eta = 0$:

$$\varphi_1 = -\log\lambda_1 - \log\left(\frac{e^{\nu_1}}{|z_1 - z_2|}|z - z_2|^2 - \frac{e^{-\nu_1}}{|z_1 - z_2|}|z - z_1|^2\right)^2 , \tag{3.183}$$

$$\varphi_2 = -\log\lambda_2 - \log\left(\frac{e^{\nu_2}}{|z_1 - z_2|}|z - z_2|^2 - \frac{e^{-\nu_2}}{|z_1 - z_2|}|z - z_1|^2\right)^2 . \tag{3.184}$$

Evaluation of the action (3.179) on the solution (3.183), (3.184) can be carried out along the same steps as done in appendix C of [173]. The result is

$$b^2 S_0 = -\frac{1}{2}\log\lambda_1 - \frac{1}{2}\log\lambda_2 - 2 - (\nu_1 - \nu_2) . \tag{3.185}$$

Comparing (3.185) with (3.182) fixes the constant C:

$$C = -\frac{1}{2}\log\lambda_1 - \frac{1}{2}\log\lambda_2 - 2 - (\nu_1 - \nu_2) . \tag{3.186}$$

Inserting this value of C in (3.182) we indeed obtain (3.168) if we set

$$2\pi\sigma = \nu_1 - \nu_2 . \tag{3.187}$$

The main results of this chapter are published in [177, 206]

Conclusion

The main results of dissertation:

1.It has been obtained current-current correlation function in $3D$ massive Dirac theory with chemical potential.

2.It has been shown the behaviour of current-current correlation function in third order of Feynman diagrams in the presence of chemical potential and magnetic field .

3.It has been studied the moat spectra of topological insulator regarding cold atoms with spin-orbit interacting.

4.It has been obtained boundary three point function on mini-superspace in Liouville field theory and also has been computed matrix elements for the Morse potential quantum mechanics. An exact agreement between the former and latter has been found. We show that both of them are given by the generalized hypergeometric functions.

5.We construct topological defects in the Liouville filed theory producing jump in the value of cosmological constant. We construct them using the Cardy-Lewellen equation for the two-point function with defect.

6.We show that there are continuous and discrete families of such kind of defects. For the continuous family of defects we also find the Lagrangian description and check its agreement with the solution of the Cardy-Lewellen equation using the heavy asymptotic quasi-classical limit.

Bibliography

[1] F. D. M. Haldane (1988). "Model for a Quantum Hall Effect without Landau Levels: F. D. M. Haldane (1988). "Model for a Quantum Hall Effect without Landau Levels: Condensed-Matter Realization of the 'Parity Anomaly'". Physical Review Letters. 61 (18): 2015-2018.

[2] Ezawa, Zyun F. (2013). Quantum Hall Effects: Recent Theoretical and Experimental Developments (3rd ed.). World Scientific.

[3] Klitzing, K. V., Dorda, G.& Pepper, M. New method for high-accuracy determination of the fine-structure constant based on quantized hall resistance. Phys. Rev. Lett. 45, 494 (1980).

[4] Laughlin, R. B. Quantized Hall conductivity in two dimensions. Phys. Rev. B 23, 5632 (1981).

[5] Hasan, M. Z. & Kane, C. L. Topological insulators. Rev. Mod. Phys. 82, 3045 (2010).

[6] Qi, X. L. & Zhang, S. C. Topological insulators and superconductors. Rev. Mod. Phys. 83, 1057 (2011).

[7] C. L. Kane, E. J. Mele, Phys. Rev. Lett. 95, 226801 (2005).

[8] C. L. Kane, E. J. Mele, Phys. Rev. Lett. 95, 146802 (2005).

[9] K. Zigler, Phys. Rev. Lett. 80, 3113 (1998).

[10] R. B. Laughlin (1981). Quantized Hall conductivity in two dimensions. Phys. Rev. B. 23 (10): 5632-5633.

[11] Fei Lin, Erik S. Sorensen and D. M. Ceperley, Physical Review B 84, 094507 (2011) A. Tzalenchuk; S. Lara-Avila; A. Kalaboukhov; S. Paolillo; M. Syvajarvi; R. Yakimova; O. Kazakova; T. J. B. M. Janssen; V. Fal'ko; S. Kubatkin (2010). "Towards a quantum resistance standard based on epitaxial graphene". Nature Nanotechnology. 5 (3): 186-189.

[12] T. Ando; Y. Matsumoto; Y. Uemura (1975). Theory of Hall effect in a two-dimensional electron system. J. Phys. Soc. Jpn. 39 (2): 279-288.

[13] A.Cappelli,Guillermo R.Zembab Nuclear Physics B Volume 490, Issue 3, 21 April 1997, Pages 595-632

[14] S. Y. Muller, M. Pletyukhov, D.Schuricht and S. Andergassen, Magnetic field effects on the finite-frequency noise and ac conductance of a Kondo quantum dot out of equilibrium, Phys. Rev. B 87, 245115 (2013); arXiv:1211.7072.

[15] P. Cain, R. A. Romer, M. E. Raikh Phys. Rev. B 67, 075307-9 (2003).

[16] A.Cappelli,Guillermo R.Zembab, C. Trugenberger Physics Letters B 306(1-2):100-107

[17] R. B. Laughlin, Elementary Theory: the Incompressible Quantum Fluid.

[18] M. Baus and J.-P. Hansen, Phys. Rep. 59 (1980) 2.

[19] J. M. Caillol, D. Levesque, J. J. Weis and J. P. Hansen, Jour. Stat. Phys. 28 (1982) 325.

[20] R. B. Laughlin, Phys. Rev. Lett. 50 (1983) 1395.

[21] R. B. Laughlin, Fractional Statistics in the Quantum Hall effect, in F. Wilczek ed., Fractional Statistics and Anyon Superconductivity, World Scientific, Singapore, (1990).

[22] L. M. Metha, "Random Matrices", Academic Press, New York,(1967).

[23] D. J. Callaway, Phys. Rev. B43 (1991) 8641.

[24] E. Bratezin, C. Itzykson, G. Parisi and J. B. Zuber, Commun. Math. Phys. 59 (1978)35.

[25] I. Bakas, Phys. Lett. B 228 (1989) 57; C. N. Pope, X. Shen and L. J. Romans,Nucl. Phys. B 339 (1990) 191; for a review see, e.g.: X. Shen, W-Infinity and String Theory, preprint CERN-TH 6404/92.

[26] G. A. Goldin, R. Menikoff and D. H. Sharp, Phys. Rev. Lett. 58 (1987) 2162, ibid. 67 (1991) 3499.

[27] A. Dhar, G. Mandal and S. R. Wadia, "Classical Fermi fluid and geometrical action for c=1", IASSNS-HEP-91/89 preprint.

[28] S. Iso, D. Karabali and B. Sakita, Nucl. Phys. B 388 (1992) 700, Phys. Lett. B 296 (1992) 143.

[29] Y. Imai and Manfred Sigrist AIP Advances, vol. 8: no. 10, pp. 101324, College Park, MD: American Institute of Physics, 2018.

[30] R. Morf and B. I. Halperin, Phys. Rev. B33 (1986) 2221.

[31] N. Datta and R. Ferrari, Max-Planck Institute preprint MPI-Ph/92-16, March 1992.

[32] I. Kogan, A. M. Perelomov and G. W. Semenoff, Phys. Rev. B45 (1992) 12084.

[33] B. I. Halperin, Phys. Rev. B25 (1982) 2185; X. G. Wen, Gapless Boundary Excitations in the Quantum Hall States and the Chiral Spin States, preprint NSF-ITP-89-157, Phys. Rev. Lett. 64 (1990) 2206; M. Stone, Ann. Phys. (NY) 207 (1991) 38; J. FrÂĺohlich and T. Kerler, Nucl. Phys B 354 (1991) 369; for a review see: X. G. Wen,Int. Jour. Mod. Phys. B6 (1992) 1711.

[34] T.H. Hansson, M. Hermanns, S.H. Simon, S.F. Viefers, Quantum Hall hierarchies, preprint arXiv:1601.01697

[35] A. Kitaev, Periodic table for topological insulators and superconductors, AIP Conf. Proc. 1134 (2009) 22; A. P. Schnyder, S. Ryu, A. Furusaki, A. W. W. Ludwig, Classification of topological insulators and superconductors in three spatial dimensions, Phys. Rev. B 78 (2008) 195125; Topological insulators and superconductors: Tenfold way and dimensional hierarchy, New J. Phys. 12 (2010) 065010; A. LeClair, D. Bernard, Holographic classification of Topological Insulators and its 8-fold periodicity J. Phys. A 45 435202 (2012); C. K. Chiu, J. C. Y. Teo, A. P. Schnyder, S. Ryu, Classification of topological quantum matter with symmetries Rev. Mod. Phys. 88 (2016) 035005.

[36] X. G. Wen, Quantum Field Theory of Many-body Systems, Oxford University Press, Oxford (2007).

[37] G. Y. Cho, J. E. Moore,Topological BF field theory description of topological insulators, Annals Phys. 326 (2011) 1515.

[38] P. Di Francesco, P. Mathieu, D. Senechal, Conformal Field Theory, Springer-Verlag, New York (1997).

[39] M. Levin, A. Stern, Fractional Topological Insulators Phys. Rev. Lett., 103 (2009) 196803; Classification and analysis of two dimensional Abelian fractional topological insulators, Phys. Rev. B 86 (2012) 115131; T. Neupert, L. Santos, S. Ryu, C. Chamon, C. Mudry, Fractional topological liquids with time-reversal symmetry and their lattice realization, Phys. Rev. B, 84, (2011), 165107; Y. M. Lu, A. Vishwanath, âĂIJTheory and classification of interacting integer topological phases in two dimensions: A Chern-Simons approachâĂİ, Phys. Rev. B 86 (2012) 125119; Erratum Phys. Rev. B 89 (2014) 199903.

[40] T. H. Hansson, V. Oganesyan, S. L. Sondhi, Superconductors are topologically ordered, Annals Phys. 313 497 (2004).

[41] A. Amoretti, A. Blasi, N. Maggiore, N. Magnoli, Three-dimensional dynamics of four-dimensional topological BF theory with boundary,New J. Phys. 14 (2012) 113014.

[42] A. Chan, T. L. Hughes, S. Ryu, E. Fradkin, Effective field theories for topological insulators by functional bosonization,Phys. Rev. B 87 (2013) 085132; A. P. O. Chan,

T. Kvorning, S. Ryu, E. Fradkin, Effective hydrodynamic field theory and condensation picture of topological insulators, Phys. Rev. B 93 (2016) 155122.

[43] X. Wan, A. M. Turner, A. Vishwanath, and S. Y. Savrasov: Phys. Rev. B 83 (2011) 205101. Journal of High Energy Physics 2017(5)

[44] M. Z. Hasan and C. L. Kane: Rev. Mod. Phys. 82 (2010) 3045.

[45] J. E. Moore: Nature (London) 464 (2010) 194.

[46] X.-L. Qi and S.-C. Zhang: Rev. Mod. Phys. 83 (2011) 1057.

[47] A. P. Schnyder, S. Ryu, A. Furusaki, and A. W. W. Ludwig: Phys. Rev. B 78 (2008) 195125.

[48] F. Wilczek: Nat. Phys. 5 (2009) 614.

[49] L. Fu and C. L. Kane: Phys. Rev. Lett. 100 (2008) 096407.

[50] B. A. Bernevig, S.-C. Zhang, Phys. Rev. Lett. 96, 106802 (2006).

[51] B. I. Halperin: Phys. Rev. B 25 (1982) 2185.

[52] D. C. Tsui, H. L. Stormer, and A. C. Gossard: Phys. Rev. Lett. 48 (1982) 1559.

[53] X. G. Wen and Q. Niu: Phys. Rev. B 41 (1990) 9377.

[54] Bernevig, B. A., T. A. Hughes, and S. C. Zhang, 2006, Science 314, 1757.

[55] Berry, M. V., 1984, Proc. R. Soc. London, Ser. A 392, 45.

[56] Bolech, C. J., and E. Demler, 2007, Phys. Rev. Lett. 98, 237002.

[57] A. A. Taskin and Y. Ando: Phys. Rev. B 80 (2009) 085303.

[58] P. Roushan, J. Seo, C. V. Parker, Y. S. Hor, D. Hsieh, D. Qian, A. Richardella, M. Z. Hasan, R. J. Cava, and A. Yazdani: Nature 460 (2009) 1106.

[59] A.Cappelli, E. Randellini, J. Sisti

[60] D.Tong Quantum Hall Effect arXiv:1606.06687 [hep-th]

[61] S. Sasaki, M. Kriener, K. Segawa, K. Yada, Y. Tanaka, M. Sato, and Y. Ando: Phys. Rev. Lett. 107 (2011) 217001.

[62] Physics of Graphene, ed. H. Aoki and M. S. Dresselhaus (Springer, Cham, 2014).

[63] M. I. Katsnelson, Graphene: Carbon in Two Dimensions (Cambridge University Press, Cambridge,(2012).

[64] S. Das Sarma, S. Adam, E. H. Hwang, and E. Rossi, Rev. Mod. Phys. 83, 407 (2011).

[65] K. Ziegler, Phys. Rev. Lett. 97, 266802 (2006).

[66] K. Ziegler, Phys. Rev. B 75, 233407 (2007).

[67] M. Lewkowicz and B. Rosenstein, Phys. Rev. Lett. 102, 106802 (2009).

[68] A. W. W. Ludwig, M. P. A. Fisher, R. Shankar, and G. Grinstein, Phys. Rev. B 50, 7526 (1994).

[69] V. P. Gusynin and S. G. Sharapov, Phys. Rev. B 73, 245411 (2006).

[70] M. I. Katsnelson, Eur. Phys. J. B 51, 157 (2006).

[71] V. P. Gusynin, S. G. Sharapov, and J. P. Carbotte, Phys. Rev. Lett. 98, 157402 (2007).

[72] L. A. Falkovsky and S. S. Pershoguba, Phys. Rev. B 76, 153410 (2007).

[73] N. M. R. Peres and T. Stauber, Int. J. Mod. Phys. B 22, 2529.

[74] V. P. Gusynin, S. G. Sharapov, and J. P. Carbotte, New J. Phys. 11, 095013 (2009).

[75] S. A. Jafari, J. Phys.: Condens. Matter 24, 205802 (2012).

[76] T. G. Pedersen, A.-P. Jauho, and K. Pedersen, Phys. Rev. B 79, 113406 (2009).

[77] T. Louvet, P. Delplace, A. A. Fedorenko, and D. Carpentier, Phys. Rev. B 92, 155116 (2015).

[78] V. P. Gusynin and S. G. Sharapov, J. Phys.: Condens. Matter 19, 026222 (2007).

[79] V. P. Gusynin, S. G. Sharapov, and J. P. Carbotte, Int. J. Mod. Phys. B 21, 4611 (2007).

[80] A. Scholz and J. Schliemann, Phys. Rev. B 83, 235409 (2011).

[81] D. K. Patel, A. C. Sharma, and S. S. Z. Ashraf, Phys. Status Solidi 252, 282 (2015).

[82] T. Stauber, J. Phys.: Condens. Matter 26, 123201 (2014).

[83] M. Bordag, G. L. Klimchitskaya, V. M. Mostepanenko, and V. M. Petrov, Phys. Rev. D 91, 045037 (2015); 93, 089907(E) (2016).

[84] I. V. Fialkovsky, V. N. Marachevsky, and D. V. Vassilevich, Phys. Rev. B 84, 035446 (2011).

[85] M. Chaichian, G. L. Klimchitskaya, V. M. Mostepanenko, and A. Tureanu, Phys. Rev. A 86, 012515 (2012).

[86] A.H.Castro-Neto, F. Guinea, N.M.R.Peres et. all, Rev. Mod. Phys. **81**, 109 (2009).

[87] M.O.Goerbig, Rev.Mod.Phys. **83**, 1193 (20011).

[88] K. Novoselov, A. Geim-Nature, 2005.

[89] V.R. Khalilov and I.V. Mamsurov, Eur. Phys. J. C 75, 167 (2015).

[90] R.Jakiw-Phys. Rev. **D 29** , 2375 (1984) .

[91] E. H. Hwang and S. Das Sarma Phys. Rev. B 75, 205418 2007.

[92] M. J. CalderÃşn, L. Brey, and F. Guinea Phys. Rev. B 60, 6698

[93] D. T. Son, Phys. Rev. **B 75**, 235423 (2007).

[94] E. Gubankova, E. Mishchenko, F. Wilczek, Phys. Rev. B 74, 184516 (2006).

[95] A. H. Castro Neto, F. Guinea, N. M. R. Peres, K. S. Novoselov, and A. K. Geim Rev. Mod. Phys. 81, 109 (2009).

[96] K. Novoselov, A. Geim-Nature, 2005.

[97] J. Gonzalez, F. Guinea, M.A.H. Vozmediano. Mod. Phys. Lett. **B 7**, 1593 (1993); J. Gonzalez, F. Guinea, M.A.H. Vozmediano, Nucl.Phys. **B 424**, 596 (1994).

[98] G. Semenoff, Phys. Rev. Lett. 53, 2449 (1984).

[99] E.Apresyan Current-current correlation function in the presence of chemical potential and magnetic field, Journal of Contemporary Physics (Armenian Academy of sciences), Volume 5, Issue 2.

[100] E. Apresyan , Sh. Khachatryan and A. Sedrakyan- Mod. Phys. Lett. A 30, 1550035 (2015).

[101] J. E. Moore and L. Balents, Phys. Rev. B 75, 121306 R 2007. 14R. Roy, arXiv:cond-mat/0607531 unpublished.

[102] B. A. Bernevig with T. L. Hughes, Topological Insulators and Topological Superconductors-Princeton University press 2013, New Jersey, USA.

[103] B. A. Bernevig, T. A. Hughes and S. C. Zhang, Science 314, 1757 (2006).

[104] M.Z. Hasan, C.L. Kane, Rev. Mod. Phys. 82, 3045 (2010).

[105] Y. Ando Topological Insulator Materials arXiv.org > cond-mat > arXiv:1304.5693

[106] Y. Zheng and T. Ando, Physical Review B 65, 245420 (2002).

[107] L. Fu, C. L. Kane, and E. J. Mele, Phys. Rev. Lett. 98, 106803 2007.

[108] J. E. Moore and L. Balents, Physical Review B 75, 121306 (2007).

[109] Qi, X. L., Hughes, T. L. & Zhang, S. C. Topological field theory of time-reversal invariant insulators. Phys. Rev. B 78, 195424 (2008).

[110] Agergaard, S., C. Sondergaard, H. Li, M. B. Nielsen, S. V.Hoffmann, Z. Li and Ph. Hofmann, 2001, New J. Phys. 3,15.

[111] Akhmerov, A. R., J. Nilsson, and C. W. J. Beenakker, 2009, Phys. Rev. Lett. 102, 216404.

[112] Alpichshev, Z., J. G. Analytis, J. H. Chu, I. R. Fisher, Y. L.Chen, Z. X. Shen, A. Fang, and A. Kapitulnik, 2010, Phys. Rev. Lett. 104, 016401.

[113] Y. Zhang, Y.-W. Tan, H. L. Stormer, and P. Kim, Nature 438, 201 (2005), URL http://dx.doi.org/10.1038/nature04235.

[114] K. Ishikawa, Physical Review Letters 53, 1615 (1984).

[115] D. N. Sheng, L. Sheng, and Z. Y. Weng, Physical Review B 73, 233406 (2006).

[116] H. B. Nielsen and M. Ninomiya, Nuclear Physics B 185, 20 (1981), URL http://www.sciencedirect.com/science/article/pii/05503213819

[117] H. B. Nielsen and M. Ninomiya, Nuclear Physics B 193, 173 (1981).

[118] L. Fu, C. L. Kane, and E. J. Mele, Physical Review Letters 98, 106803 (2007), URL http://link.aps.org/doi/10.1103/PhysRevLett.98.106803.

[119] R. Yoshimi, A. Tsukazaki, Y. Kozuka, J. Falson, K. S. Takahashi, J. G. Checkelsky, N. Nagaosa, M. Kawasaki, and Y. Tokura, Nature Communications 6, 6627 EP (2015).

[120] W. Kohn, Phys. Rev. 133, A171 1964.

[121] X. G. Wen, Phys. Rev. B 44, 2664 1991.

[122] E. Demler, C. Nayak, H. Y. Kee, Y. B. Kim, and T. Senthil, Phys. Rev. B 65, 155103 2002, and references therein.

[123] D. J. Thouless, M. Kohmoto, M. P. Nightingale, and M. den Nijs, Phys. Rev. Lett. 49, 405 1982.

[124] M. Kohmoto, B. I. Halperin, and Y.-S. Wu, Phys. Rev. B 45, 13488 1992.

[125] B. I. Halperin, Phys. Rev. B 25, 2185 1982.

[126] Y. Hatsugai, Phys. Rev. Lett. 71, 3697 1993.

[127] C. L. Kane and E. J. Mele, Phys. Rev. Lett. 95, 226801 2005.

[128] L. Kane and E. J. Mele, Phys. Rev. Lett. 95, 146802 2005. 11B.

[129] A. Bernevig and S. C. Zhang, Phys. Rev. Lett. 96, 106802 2006.

[130] Roy, arXiv:cond-mat/0604211 unpublished.

[131] H. Suzuura and T. Ando, Phys. Rev. Lett. 89, 266603 2002.

[132] F. D. M. Haldane, Phys. Rev. Lett. 93, 206602 2004.

[133] H. Nielssen and N. Ninomiya, Phys. Lett. 130B, 389 1983.

[134] Fu, L. and C. L. Kane, 2006, Phys. Rev. B 74, 195312.

[135] E. I. Blount, Solid State Phys. 13, 305 1962.

[136] J. Zak, Phys. Rev. Lett. 62, 2747 1989.

[137] R. D. King-Smith and D. Vanderbilt, Phys. Rev. B 47, 1651 1993.

[138] R. Resta, Rev. Mod. Phys. 66, 899 1994.

[139] Fu, L. and C. L. Kane, 2007, Phys. Rev. B 76, 045302.

[140] Fu, L. and C. L. Kane, 2008, Phys. Rev. Lett. 100, 096407.

[141] Fu, L. and C. L. Kane, 2009, Phys. Rev. B 79, 161408(R).

[142] Fu, L. and C. L. Kane, 2009, Phys. Rev. Lett. 102, 216403.

[143] Fu, L., C. L. Kane and E. J. Mele, 2007, Phys. Rev. Lett. 98,106803.

[144] Golin, Phys. Rev. 166, 643,1968. 45Y. Liu and R. E.

[145] Allen, Phys. Rev. B 52, 1566 1995.

[146] L. M. Falicov and S. Golin, Phys. Rev. 137, A871 1965.

[147] S. Golin, Phys. Rev. 176, 830,1968.

[148] D. T. Morelli, D. L. Partin, and J. Heremans, Semicond. Sci.Technol. 5, S257 1990.

[149] S. Cho, A. DiVenere, G. K. Wong, J. B. Ketterson, and J. R. Meyer, Phys. Rev. B 59, 10691,1999.

[150] B. A. Bernevig with T. L. Hughes, Topological Insulators and Topological Superconductors-Princeton University press 2013, New Jersey, USA.

[151] B. A. Bernevig, T. A. Hughes and S. C. Zhang, Science 314, 1757 (2006).

[152] M.Z. Hasan, C.L. Kane, Rev. Mod. Phys. 82, 3045 (2010).

[153] Y. Ando, Journal of Phys. Soc. Jap. **82**, 102001(2013).

[154] N. Goldman, G. Juzeliunas, P. Ohberg, I. B. Spielman Rep. Prog. Phys. **77**, 126401 (2014).

[155] T. Sedrakyan, A. Kamenev, L. Glazman- Phys. Rev. **A 86**, 063639 (2012).

[156] T. Sedrakyan, V. Galitski, A. Kamenev. Phys.Rev.Lett. **115**, 195301 (2015).

[157] M. Pletyukhov and V. Gritsev, Phys. Rev. B 74, 045307 (2006).

[158] G.-H. Chen and M. E. Raikh, Phys. Rev. B 59, 5090 (1999).

[159] Y.-J. Lin, K. Jimenez-Garcia and I. B. Spielman, Nature 471, 83 (2011).

[160] 5. E.Apresyan, A.Sedrakyan,Transport properties of fermions with moat spectra Mod.Phys.Let. A, Vol.34 No. 05, (2019) 1950041 .

[161] E. Hijano, P. Kraus, E. Perlmutter and R. Snively, Semiclassical Virasoro Blocks from AdS_3 Gravity, JHEP **1512** (2015) 077 arXiv:1508.04987.

[162] K. B. Alkalaev and V. A. Belavin, Classical conformal blocks via AdS/CFT correspondence, JHEP **1508** (2015) 049 arXiv:1504.05943.

[163] A. L. Fitzpatrick, J. Kaplan and M. T. Walters, Virasoro Conformal Blocks and Thermality from Classical Background Fields, JHEP **1511** (2015) 200 arXiv:1501.05315.

[164] A. Mironov and A. Morozov, Proving AGT relations in the large-c limit, Phys. Lett. B **682** (2009) 118 arXiv:0909.3531.

[165] V. Fateev and S. Ribault, The Large central charge limit of conformal blocks, JHEP **1202** (2012) 001 arXiv:1109.6764.

[166] N. Hama and K. Hosomichi, AGT relation in the light asymptotic limit, JHEP **1310** (2013) 152 arXiv:1307.8174.

[167] M. Piatek, Classical torus conformal block, $N = 2^*$ twisted superpotential and the accessory parameter of LamAo equation, JHEP **1403** (2014) 124 arXiv:1309.7672.

[168] H. Poghosyan, The light asymptotic limit of conformal blocks in $\mathcal{N} = 1$ super Liouville field theory, JHEP **1709** (2017) 062, arXiv:1706.07474.

[169] H. Poghosyan, R. Poghossian and G. Sarkissian, The light asymptotic limit of conformal blocks in Toda field theory, JHEP **1605** (2016) 087 arXiv:1602.04829.

[170] S. Ribault, Boundary three-point function on AdS_2 D-branes, JHEP **0801** (2008) 004 arXiv:0708.3028.

[171] S. Ribault, Minisuperspace limit of the AdS_3 WZNW model, JHEP **1004** (2010) 096 arXiv:0912.4481.

[172] V. Fateev and S. Ribault, Conformal Toda theory with a boundary, JHEP **1012** (2010) 089 arXiv:1007.1293.

[173] H. Poghosyan and G. Sarkissian, On classical and semiclassical properties of the Liouville theory with defects, JHEP **1511** (2015) 005 arXiv:1505.00366.

[174] T. G. Mertens, G. J. Turiaci and H. L. Verlinde, Solving the Schwarzian via the Conformal Bootstrap, JHEP **1708** (2017) 136, arXiv:1705.08408.

[175] E. Braaten, T. Curtright, G. Ghandour and C. B. Thorn, Nonperturbative Weak Coupling Analysis of the Quantum Liouville Field Theory, Annals Phys. **153** (1984) 147.

[176] E. Braaten, T. Curtright and C. B. Thorn, An Exact Operator Solution of the Quantum Liouville Field Theory, Annals Phys. **147** (1983) 365.

[177] E.Apresyan, G.Sarkissian, On mini- superspace limit of boundary three point function in Liouville field theory JHEP 12 (2017) 058.

[178] C. B. Thorn, "Liouville perturbation theory," Phys. Rev. D **66** (2002) 027702 hep-th/0204142

[179] H. Dorn and H. J. Otto, "Two and three point functions in Liouville theory," Nucl. Phys. B **429** (1994) 375 arXiv:hep-th/9403141.

[180] A. B. Zamolodchikov and A. B. Zamolodchikov, Structure constants and conformal bootstrap in Liouville field theory, Nucl. Phys. B **477** (1996) 577 arXiv:hep-th/9506136.

[181] Z. Bajnok, C. Rim and A. Zamolodchikov, Sinh-Gordon boundary TBA and boundary Liouville reflection amplitude, Nucl. Phys. B **796** (2008) 622 arXiv:0710.4789.

[182] H. Dorn and G. Jorjadze, Operator Approach to Boundary Liouville Theory, Annals Phys. **323** (2008) 2799 arXiv:0801.3206.

[183] V. Fateev, A. B. Zamolodchikov and A. B. Zamolodchikov, Boundary Liouville field theory. 1. Boundary state and boundary two point function, hep-th/0001012.

[184] B. Ponsot and J. Teschner, Boundary Liouville field theory: Boundary three point function, Nucl. Phys. B **622** (2002) 309 hep-th/0110244.

[185] E. W. Barnes, "Theory of the double gamma function", Phil. Trans. Roy. Soc **A196** (1901) 265-388

[186] T. Shintani, "On a Kronecker limit formula for real quadratic fields", J. Fac. Sci. Univ. Tokyo Sect. 1A Math. **24** (1977) 167-199

[187] L. J. Slater, "Generalized Hypergeometric Functions", Cambridge, England: Cambridge University Press, (1966).

[188] W. N. Bailey, "Generalised Hypergeometric Series", New York and London: Stechert-Hafner Service Agency, (1964).

[189] F. J. W. Whipple, "A group of generalized hypergeometric series: relations betwecn 120 allied scries of the type $F[a, b, c; d, e]$", Proc. London Math. Soc. (2), 23 (1925), 104-114.

[190] J. Teschner, "On boundary perturbations in Liouville theory and brane dynamics in noncritical string theories," JHEP **0404** (2004) 023 hep-th/0308140.

[191] J. Teschner, "Remarks on Liouville theory with boundary," PoS tmr **2000** (2000) 041 hep-th/0009138.

[192] I. S. Gradshteyn, I. M. Ryzhik, "Table of Integrals, Series, and Products", Academic Press, (2015).

[193] H. Bateman, "Tables of integral Transforms" (A. Erdèlyi, Ed.), Vol. II, McGraw-Hill, New York, (1954).

[194] G. Sarkissian, "Defects and Permutation branes in the Liouville field theory," Nucl. Phys. B **821** (2009) 607 arXiv:0903.4422.

[195] G. Sarkissian, "Some remarks on D-branes and defects in Liouville and Toda field theories," Int. J. Mod. Phys. A **27** (2012) 1250181 arXiv:1108.0242.

[196] A. R. Aguirre, "Type-II defects in the super-Liouville theory," J. Phys. Conf. Ser. **474** (2013) 012001 arXiv:1312.3463.

[197] H. Poghosyan and G. Sarkissian, "On classical and semiclassical properties of the Liouville theory with defects," JHEP **1511** (2015) 005 arXiv:1505.00366.

[198] C. Vafa, "Fractional Quantum Hall Effect and M-Theory," arXiv:1511.03372.

[199] T. Can, M. Laskin and P. Wiegmann, "Collective Field Theory for Quantum Hall States," Phys. Rev. B **92** (2015) no.23, 235141 arXiv:1412.8716.

[200] S. M. Girvin, "The quantum Hall effect: Novel excitations and broken symmetries", Topological Aspects of Low Dimensional Systems, ed. A. Comtet, T. Jolicoeur, S. Ouvry, F. David (Springer-Verlag, Berlin and Les Editions de Physique, Les Ulis, 2000), cond-mat/9907002.

[201] V. Fateev, A. B. Zamolodchikov and A. B. Zamolodchikov, "Boundary Liouville field theory. I: Boundary state and boundary two-point arXiv:hep-th/0001012.

[202] A. B. Zamolodchikov and A. B. Zamolodchikov, "Liouville field theory on a pseudosphere," arXiv:hep-th/0101152.

[203] V. B. Petkova and J. B. Zuber, "The Many faces of Ocneanu cells," Nucl. Phys. B **603** (2001) 449 hep-th/0101151.

[204] A. B. Zamolodchikov and A. B. Zamolodchikov, "Structure constants and conformal bootstrap in Liouville field theory," Nucl. Phys. B **477** (1996) 577 hep-th/9506136.

[205] D. Harlow, J. Maltz and E. Witten, "Analytic Continuation of Liouville Theory," JHEP **1112** (2011) 071 arXiv:1108.4417. Lett. A6, 487, (1991). G. Moore and N. Read, Nucl. Phys. B360, 362, (1991).

[206] E.Apresyan G.Sarkissian, Topological defects in the Liouville field theories with different cosmological constants JHEP 05 (2018) 131.